DATA CAPTURING SYSTEM USING CELLULAR PHONE, VERIFIED AGAINST PROPAGATION MODELS

by

Schalk W.J. Visser

Thesis presented in partial fulfilment of the requirements for the degree of

Master of Science in Engineering

University of Stellenbosch
Supervisor: Professor Johan G. Lourens

November 2004

Declaration

I, the undersigned, hereby declare that the work contained in this thesis is my own original work, unless otherwise stated, and has not previously, in its entirety or in part, been submitted at any university for a degree.

Schalk W.J. Visser November 2004

University of Stellenbosch

Abstract

DATA CAPTURING SYSTEM USING CELLULAR PHONE, VERIFIED AGAINST PROPAGATION MODELS

by Schalk W.J. Visser

Data capturing equipment are an expensive part of testing the coverage of a deployed or planned wireless service. This thesis presents the development of such a data capturing system that make use of 1800MHz GSM base stations as transmitters and a mobile phone connected to a laptop as receiver. The measurements taken, are then verified against know propagation models.

Datavaslegging toerusting wat gebruik word om die dekking van draadlose stelsels te toets is baie duur en moeilik bekombaar. Hierdie tesis beskryf die ontwikkeling van so 'n datavaslegger wat baie goedkoper is en maklik gebruik kan word. Dit maak gebruik van 'n sellulêr foon en GPS gekoppel aan 'n skootrekenaar, wat die ontvanger is. Cell C basis staties word gebruik as die senders. Die data wat gemeet is word dan geverifieer deur gebruik te maak van bestaande radio frekwensie voortplanting modelle.

TABLE OF CONTENTS

LIST OF FIGURES

LIST OF TABLES

ACKNOWLEDGMENTS

The author wishes to express sincere appreciation to Professor Johan G. Lourens for his assistance in the preparation of this manuscript. In addition, special thanks to Clarence Smith from Cell C, Bennie Neethling from Telkom SA, Anton Meyer from Vodacom and Colleen de Villiers from the South African Weather Service. Thanks also to the members of the faculty for their valuable input.

Special thanks to
my Creator and family

GLOSSARY

FEKO. Software supplied by EMSS, used to simulate the effect of multipath propagation.

HerTZ Mapper. Software used to plot positions relative to each other on a digital terrain model.

Cell C. South African Cellular Service Provider.

WiMAX. Is a standards-based wireless technology that provides high-throughput broadband connections.

INTRODUCTION

With new technologies developed each day, customer satisfaction stays the number one factor that makes or breaks a product. The need for that product or service should firstly be customer orientated and if/when the product is accepted, the quality of service (QoS) need to be satisfactory towards the customers needs.

New systems and technologies such as voice over internet protocol (VoIP), WiMAX and many more are being used and rolled out all over the world at the moment. Although there are no guarantee for QoS on an IP network, the customer still need to find peace in the product or service he/she is paying for. Industry standards as set out by WiMAX are being implemented all over the world, making it possible for any user to go anywhere in the world and have wireless internet access available.

Access networks delivering some of these services to the customer are in place and new technologies are developed to take these services the last mile, from the known public switched telephone network (PSTN) to the customer at his/her house, office or even the car of the user. The copper infrastructure available in South Africa has been the main form of access the past few decades, but as technology progress, new means have been derived, such as high speed fiber optic connections and more recently wireless access in some of our airports.

Wireless access is unveiling new possibilities and also new challenges, but it is the dominant tool, delivering service to customers in future. The relative ease of deployment of the service providing components and the coverage gained from one such remote base station are forcing service providers to look into the development and deployment of such services. Mobile phones have been around for a few years now, but wireless communication using laptops, palmtops etcetera are becoming more and more prominent and are challenging communication as we know it.

To put this project into perspective, wireless communication and the importance of its reliability is a field in engineering where there is lots of room, and need, for the development of this technology. For development, the medium in which communication is done, need to be understood. For new designs to work at their optimum performance, the principals behind propagation need to be understood and even more so, the engineer need to apply these known theories in practical situations. Providing a service to a customer, once thought to be impossible, is now becoming a reality and customers don't take no as an answer anymore.

Data capturing equipment needed for planning these services are expensive and not easily accessible. This project provides an alternative to these problems as well as some new opportunities where this data capturing system can be used. The propagation data capturing system designed for this project, makes use of a Nokia mobile phone and a global position system (GPS) connected to a laptop computer, together functioning as the receiver. For the transmitters, Cell C (cellular service provider) base stations are used. The measured propagation data are then compared with predictions formulated using known propagation models. This is done to gain insight in how different surroundings influence the propagated electromagnetic wave. Reflections from surroundings, multipath propagation, diffraction over irregular terrain, attenuation due to vegetation etcetera are all taken into account when the measured signal level is compared with the prediction. The frequency band that will be used is the 1800MHz GSM band. All the propagation phenomenon and modeling that will be studied will be specifically for the 1800MHz frequency band.

This thesis take an in depth look at the development of the propagation measurement system. Then some of the propagation phenomenon are looked at and explained. These propagation phenomenons will then be used to calculate the predicted signal level and the predictions are then compared with the measured signal level. Some of the propagation mediums that will be looked at are informal settlements with metal shacks obstructing the line-of-sight view and also some with al clear line-of-sight in such areas. Vegetative obstructions are also considered as well as other diffraction examples.

From here conclusions are drawn and the author shares a few ideas for further work that can be done.

LITRITURE STUDY

Propagation mechanisms are very complex and diverse. The signal propagates by means of diffraction, scattering, reflection, transmission and refraction. To model these phenomenons, extensive work has been done by many academics and other parties. A few of these models will be looked at as well as how they can be applied in practical predictions

2.1. Propagation Models

A propagation model is a set of mathematical expressions, diagrams and algorithms used to represent the radio characteristics of a given environment. Propagation models can be separated into two main categories, namely empirical and theoretical.

Empirical models are based on measurements taken and from this then the model is derived. These models are also known as statistical. In these models, environmental influences are implicitly taken into account weather or not they can be separately recognised, this is the main advantage of these models. The shortcoming of these models on the other hand is that it is dependant on the quality of the measurements taken and the similarities between the environments analysed. Never the less, the computational effectiveness of these models is typically satisfying. An example of such a model is the Artificial Neural Network Model that will be looked at later.

Theoretical models deals with the fundamentals of radio wave propagation, based on physics. These models are also known as deterministic. Due to the fact that these models are based on physics, they can be applied to a wide variety of environments without affecting their accuracy. In practice though, their implementation requires an enormous database of environmental characteristics, which is sometimes not practical or impossible to obtain. For this reason, the implementation of such models is mostly restricted to smaller areas of microcell or indoor environments. Nevertheless, if these models are implemented correctly, greater accuracy can be expected than with the empirical models. This approach will be taken when measurements are compared with predicted signal levels later on.

First some of the most common propagation models will be looked at and also how they can be used in actual propagation predictions.

2.1.1. The Longley-Rice model, also known as the ITS irregular terrain model, can be used in line-of-sight links with carrier frequencies between 40MHz and 100GHz over any type of terrain [1]. The median transmission loss is predicted using the path geometry, terrain profile and 2-ray ground reflection model. Losses due to diffraction over obstacles are estimated using Fresnel-Kirchoff knife-edge models. For a given transmission path, the model take into account the transmission frequency, path length, polarization, antenna heights, surface refractivity, effective radius of the earth, ground conductivity, ground dielectric constant and the climate.

The Longley-Rice method operates in two modes, the first being when a detailed terrain path profile is available. From this the necessary path related parameters can be determined and such a prediction is known as a point-to-point mode prediction. When the terrain profile is not available the Longley-Rice method provides techniques to calculate these path related parameters and such predictions are known as area mode predictions [2].

Many modifications have been made to the Longley-Rice method and one such important modification deals with mobile phone propagation in urban areas [3]. This extra parameter allows excess attenuation due to urban clutter near the mobile receiver, called the urban factor (UF). This has been derived by comparing the original Longley-Rice predictions with obtained Okumura predictions.

A disadvantage for the Longley-Rice method is that it does not provide a correction due to environmental factors in the immediate vicinity of the mobile receiver, or consider correction factors that take into account the effects of buildings and foliage.

2.1.2. Durkin's model is a classical propagation prediction model, similar to that of the Longley-Rice model [4]. Durkin's path loss model consists of two parts. The first part is to access a topographic database for the proposed service area and reconstruct the ground profile between the transmitter and the receiver in the radial direction. The assumption is the receiver receives all its power along this radial direction and therefore no multipath propagation is taken into account. The result is that only the line-of-sight (LOS) and diffraction from obstructions along the radial is modelled, excluding reflections from surrounding objects and other scatters. The second part of the model is to calculate the expected path loss along that radial, thus resulting in the predicted loss between the transmitter and the receiver.

The first step is to determine if there is a LOS path available between the transmitter and the receiver. If no LOS path is present, the next step is to determine whether the first Fresnel zone clearance is achieved. If the first Fresnel zone of a radio path is unobstructed, then the loss is effectively the same as for a clear line-of-sight link. If however the obstruction just barely touches the line that connects the transmitter with the receiver, the signal strength at the receiver is 6dB less then the free space value due to energy diffracting off the obstruction and away from the receiver.

If there is insufficient first Fresnel clearance, the next step is to calculate the additional loss due to inadequate Fresnel zone clearance. This additional loss can be graded into four categories: single diffraction edge, two diffraction edges, three diffraction edges and more than three diffraction edges. The Epstein and Peterson method is used to calculate the shadow loss due to the obstacles. For cases where there are more than three diffraction edges, the outer two obstacles are approximated by a single virtual knife edge. After the approximation the problem is that of a three edge calculation.

The disadvantages of this method is that it does not take into account the attenuation due to buildings, foliage and other man made structures. It also does not account for multipath propagation which can be very important for urban areas.

2.1.3. Okumura's model is one of the most widely used models for predicting signal levels in urban areas [2]. This model is applicable for carrier frequencies ranging from 150MHz to 1920MHz. Okumura developed a set of curves giving the median attenuation relative to free space (A_{mu}), in an urban area over a quasi-smooth terrain with a base station antenna height (h_{te}) of 200m and a receiver height (h_{re}) of 3m. These curves were developed by taking extensive measurements using vertical omni-directional antennas at both the transmitter and the receiver and are plotted as a function of frequency, ranging from 100MHz to 1920MHz and distance between the transmitter and receiver ranging from 1km to 100km.

Using the method of Okumura, the free space propagation is first determined and then the value of $A_{mu}(f,d)$, as read from curves, is added to the free space propagation loss as well as the correction factors to account for the terrain.

$$L_{50}(dB) = L_F + A_{mu}(f,d) - G(h_{te}) - G(h_{re}) - G_{AREA} \qquad \text{Equation 2.1}$$

Where L_{50} is the 50th percentile (i.e. median value) of the propagation path loss, L_F is the free space propagation loss, A_{mu} is the median attenuation relative to free space, $G(h_{te})$ is the transmitter antenna height gain factor, $G(h_{re})$ is the receiver antenna height gain factor and G_{AREA} is the gain due to the type of environment.

Okumura's model is totally based on measured data and does not provide any analytical explanation for predictions made. The major disadvantage with the model is its slow response to rapid changes in terrain. Therefore the model works fairly well in urban and suburban areas, but not in rural areas. Standard deviations between measured and predicted signal level vary from 10dB to 14dB. In order to make the Okumura technique suitable for computer implementation, Hata has developed the analytic expressions for the median path loss for urban, suburban and open areas [5].

2.1.4. PCS Extension to Hata Model, is the next model that will be looked at. The Hata model in it self only cover the frequency range from150MHz to 1500MHz, but the PCS extension of the Hata model cover the frequency range from 1500MHz to 2000MHz [6]. The European Co-operative for Scientific and Technical research (EURO-COST) formed the COST-231 working group to develop the extension to the Hata model [7]. The COST extension to the Hata model is limited to the following range of parameters:

f : 1500MHz to 2000MHz

h_{te} : 30m to 200m

h_{re} : 1m to 10m

d : 1km to 20km

2.1.5. The Walfisch Bertoni model considers the impact of rooftops and building height by using diffraction to predict the average signal strength at street level. Another form of the model is the COST 231-Walfisch-Ikegami model [8] which is being used by designers of public mobile radio systems, such as global system for mobile communication (GSM), personal communication services (PCS), and digital enhanced cordless telecommunications (DECT) and digital cellular systems (DCS). This Walfisch-Ikegami model also takes into account free space propagation loss, loss due to diffraction down to the street and the street orientation factor.

Steep transitions of path loss occur when the base station antenna height is close to that of the surrounding rooftops of the buildings in the vicinity. The height accuracy of the base station is very important to avoid large prediction errors. The accuracy of the Walfisch-Ikegami model is $\pm 3dB$ standard deviation and about 4-8*dB* when the base station height is much higher than the surrounding rooftop levels.

2.1.6. The Ericsson model is specifically used by Ericsson engineers for designing cellular systems. The model is essentially based on the Okumura-Hata model and has few easy changeable parameters that are site specific. Obstacles in the line-of-sight view are modelled using single knife-edge diffraction. For the model to work at its best, clutter and terrain data for the area need to be collected before hand. The main advantage is that when test data has been collected such as clutter and terrain data, Ericsson model is computationally very fast.

2.1.7. The Lee model was proposed by W.C.Y. Lee in 1982 [5]. The parameters of this model can easily be adjusted to site specific needs by taking a few field measurements. By doing so, greater accuracy is achieved using this model. The computational efficiency of this model is also satisfactory. This model consists of two parts, one being the area-to-area prediction and the next being the point-to-point prediction. The short coming in the first is that it does not model hilly terrain very good, but the second part of the model takes this factor into account. Line-of-sight conditions are tested for and by doing this, obstacles are modelled

using single knife-edge diffraction. The application of this model between different cities also yield a difference in prediction accuracy, this can be explained by the fact that the city structure vary from city to city.

2.1.8. Using Artificial Neural Networks (ANN) for modelling is a relatively new effort in trying to maximise the accuracy of prediction models. The accuracy of this model exceeds that of some of the old models making use of a feed-forward neural network with sigmodial activation functions. Training data for this model can be collected from the area, making the model more accurate. Although training the model may take some time, the process of making predictions using the model after training, is fast. The proposed network [9] has three groups of inputs. The first being a normalised distance factor that take into account the distance between the base station transmitter and the mobile receiver. The second group of inputs consist of four variables according to the terrain profile analysis. The third group of inputs takes into account the land category analysis which is done in a straight line from the transmitter to the receiver. The output of the ANN is a single normalised electric field strength prediction. [10],[11]

When comparing the ANN model to other known models, the ANN demonstrates good performance. Urbanization is better modelled and more effectively taken into account. The ANN model has been used successfully in the 450MHz and 900MHz frequency bands for Terrestrial Trunked Radio (TETRA) and GSM planning purposes [5].

2.2. Other Influences

Most of the propagation models only take into account free space propagation loss and diffraction over obstacles and some reflections. But there are also other factors that sometimes influence the received signal level at a mobile receiver.

One such factor is the influence of sleet [12]. Sleet is defined in different terms all over the world. In Australia it is known as a combination of snow and rain, in the United States it is when rain or melting snow flakes passes through a shallow layer of cold air near the earth surface, re-freezing forming little ice pellets then forming a crust on the earth's surface. In South Africa it can be compared to frost on a cold morning in the Highveld. This causes outage in microwave links because more scattering is expected due to the change in the reflective properties of the ground cover. This will however not need to be taken into account for this project, because the measurements were taken on clear sunny days.

The next factor that also causes outage on radio links is rain. The rain rate and carrier frequency for a specific situation can lead to a prominent drop in signal strength due to attenuation caused by rain. There are two main methods to model the amount a signal loss namely the ITU terrestrial model [13] and the Crane model [14]. The ITU model makes use of rain maps, supplied by the ITU giving the rain rate for

99.99% availability. The Crane model is more popular in space-earth links but there are also terrestrial models. In general, the Crane model predicts higher rain attenuation than the ITU model. Because the rain rate in South Africa, more specifically Stellenbosch, is not expected to be that high, the ITU rain maps are used.

In general there are multiple actions that can be taken to improve the coverage gained by a transmitter. One such action that can be taken is to move the transmitter in a vertical direction, upwards or downwards [15]. The same can be done with the receiver antenna. This is because of multipath effects. The direct signal could interact positively with a good reflected signal or in some cases negatively. If the receiving antenna is moved upwards and the signal strength increases, it is known as positive height gain. If the signal strength increases when the receiver is lowered, it is known as negative height gain. The height gain factor relies on minimal clutter in the vicinity of the mobile receiver.

When using a directional antenna at the receiver, one should be very careful. The gain due to the directivity can be reduced because of scattering causing the effective gain to be less then the actual gain [16]. This can be characterized as Antenna Gain Reduction Factor (GRF) and should be considered when doing the link budget for a specific antenna configuration. For this reason the measurements taken for this project, will be taken using an omni-directional quarter wave monopole as an external antenna to the mobile phone.

2.3. Conclusions

From the known models it is found that these prediction models take mostly worst case scenarios into account. Therefore it is not possible to use these models to proof that the measurement system is accurate. In light of this, a more theoretical approach will be taken when comparing predicted signal levels with measured signal levels.

All the prediction methods that will be used, are discussed in detail in Chapter 4. These methods are then used in Chapter 5 to compare the measured signal level with a prediction.

DATA CAPTURING SYSTEM

The data capturing system developed for this project will be looked at in this chapter. It consists of two parts, the mobile phone and the global positioning system (GPS). Both these devices are connected to a laptop computer for logging the position of the mobile phone and the signal level it is measuring. The data that is logged is then used to compare the logged signal level with the predicted signal level and from this the conclusions are drawn. A diagram of the data capturing system is shown in Figure 3.1.

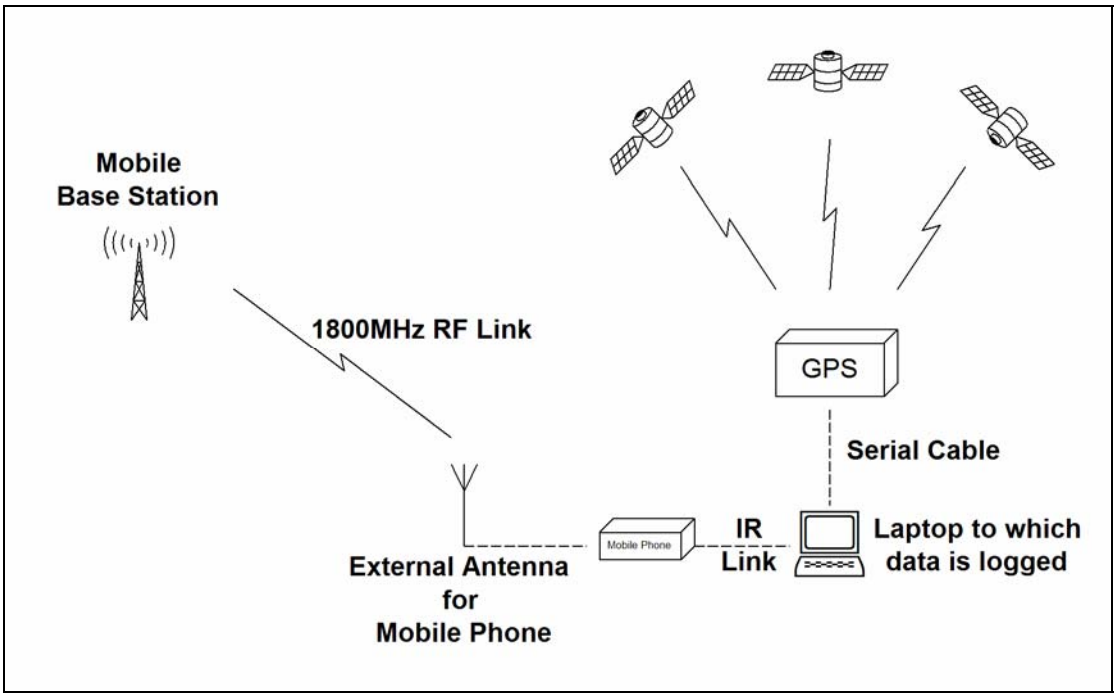

Figure 3.1: Diagram of Data Capturing System

The rest of the chapter will be split into two main parts; first the source of the logged signal, the transmitter, will be looked at. This is needed, because to make an accurate prediction it is necessary to know what to expect at the receiver. The last part of this chapter will then deal with the data capturing system that was developed.

3.1. The Transmitter

A Cell C Base Station is used as the transmitter for this data capturing system. The reason for this is because the base stations are already in place and available for use. The second and most important is that Cell C uses the 1800MHz GSM band. Although Vodacom also make use of this band, their base stations are not used. The reason being, for the mobile phone to log the received signal level, it needs to be idle on an 1800MHz tower. This is only the case for Vodacom subscribers if there is no 900MHz slots available, and then only if the subscriber is in a call. For this reason, Cell C is chosen.

All the information needed for the base stations, such as: Latitude, Longitude, Antenna Type, Azimuth, Tilt, Effective Isotropic Radiated Power (EIRP) and the antenna height, are supplied by Cell C. The radiation pattern for the base station antenna is supplied by Kathrein[1]. MATLAB and the data supplied by Kathrein are used to determine the loss in the link budget, due to the antenna radiation pattern, physical setup of the antenna at the base station and the position of the mobile phone receiver relative to the base station. The code used is shown in Appendix A1. In the next figure, the radiation pattern is shown.

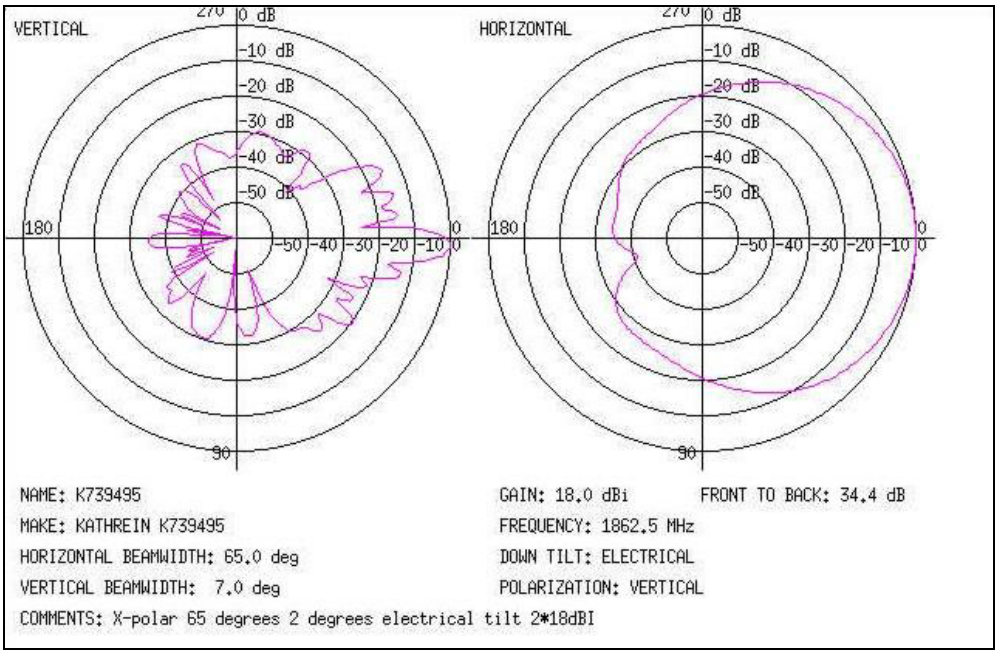

Figure 3.2: Radiation Pattern for a Cell C Base Station

[1] KATHREIN Werke, Suppliers of Mobile Base Stations

All the information supplied by Cell C regarding the base stations is given in the next table.

	Helshoogte Residence		Sentec	
Cell ID[2]	14408	34408	27761	37761
Antenna Type	K739495	K739495	K739495	K739495
Latitude (South)	33°55'53.22	33°55'53.22	33°54'56.02	33°54'56.02
Longitude (East)	18°52'14.52	18°52'14.52	18°52'10.99	18°52'10.99
Azimuth (degrees)	10	250	180	280
Tilt (degrees)	5	5	4	4
EIRP[3] (dB)	54.86	54.86	53.5	53.5
AGL[4] (m)	117	117	227	227
Antenna Height (m)	45.5	45.5	15	15

Table 3.1: Site Information for all Base Stations

The data as shown in the table above are all used during measurements. The cell ID is logged by the mobile phone and this is how the measured signal level is tracked. The AGL[4] and the antenna height are used during the prediction of multipath interference. The next section will deal with how all this related data are measured and it will explain how this data will be used.

[2] Cell Identification Number

[3] EIRP: Effective Isotropic Radiated Power

[4] AGL: Average Ground Level at the Site above Sea Level

3.2. The Receiver

The receiver can be split into two parts, GPS and the Nokia 6310i mobile phone. Both these devices are connected to a laptop computer. The GPS is connected to the laptop via a serial cable and the mobile phone is connected via an infra red connection. The data that are logged are saved in text format to the laptop computer from where it is used in the calculations for prediction purposes. First the GPS measurements will be looked at.

3.2.1. GPS Measurements:

The GPS measurements are used to calculate the distance between the Cell C base station and the remote mobile phone. Other methods for determining the distance can also be used, such as time of arrival (TOA) and time-difference of arrival (TDOA) [17]. TOA works by the handset bouncing a signal back to the base station, or vice-versa. Since radio waves travel at the speed of light (c), the distance (d) between the mobile phone and the base station can be estimated from the transmission delay. TDOA is a quite similar time-based technique. It works by measuring the relative arrival time at the mobile phone of the signals transmitted from three base stations at the same time. The difference of arrival time defines a hyperbola, with the loci at the two base stations. As three base stations are used, there are three sets of time differences, which create three hyperbolic equations that define a single solution. The position relative to the base station is therefore now known and from this the distance can be calculated. For location tracking purposes, TDOA are preferred to TOA because in most implementations, it requires less data to be exchanged over the wireless connection. For purposes of this project, the TOA method would have been best, because only the distance between the mobile phone and the base station is necessary and not the exact position of the mobile phone.

The GPS is chosen because it requires less programming and for purposes of prediction modelling, the distance calculated by the GPS coordinates is more accurate than the TOA method. The GPS coordinates are also used in a program called HerTZ Mapper from where it is possible to determine the elevation between the two points. This will then be used for the prediction of the received signal.

The GPS used, is a GARMIN GPSIII connected serially to the laptop computer via a serial cable. Microsoft Visual Basic programming is used to develop a graphical user interface (GUI), which enable the user to start and stop logging the GPS coordinates, by the click of a button. A screenshot of the GUI is shown in Figure 3.3.

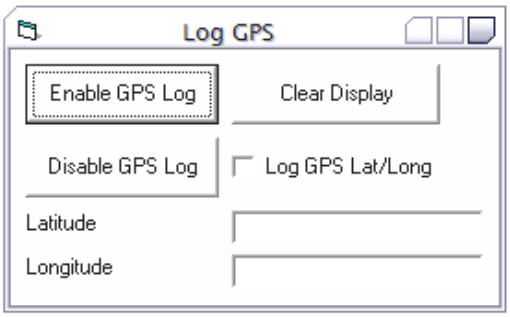

Figure 3.3: Screenshot of GUI used for logging GPS coordinates

The Visual Basic Program can be seen in Appendix A2. This now logs the latitude and the longitude of the mobile phone's position, by means off an averaging process.

3.2.2. Mobile Phone Measurements:

The mobile phone, a Nokia 6310i, is connected to the laptop via an infra red connection. An external antenna is connected to the mobile phone. This external antenna is an electrically small quarter wave monopole. The need for this external antenna is to eliminate the complex radiation pattern of the internal antenna of the mobile phone, hence simplifying the link budget that need to be done.

It is a single feed wire that has a uniform radiation pattern in all directions. The expression for these fields is given as [18]:

$$E_\theta \cong j\eta \frac{\mathrm{I}_0 e^{-jkr}}{2\pi r}\left[\frac{\cos\left(\frac{\pi}{2}\cos\theta\right)}{\sin\theta}\right] \qquad \text{Equation 3.1}$$

$$H_\phi \cong \frac{E_\theta}{\eta} \cong j\frac{\mathrm{I}_0 e^{-jkr}}{2\pi r}\left[\frac{\cos\left(\frac{\pi}{2}\cos\theta\right)}{\sin\theta}\right] \qquad \text{Equation 3.2}$$

This expression for the E-field is then simulated mathematically and the E-field is then plotted as:

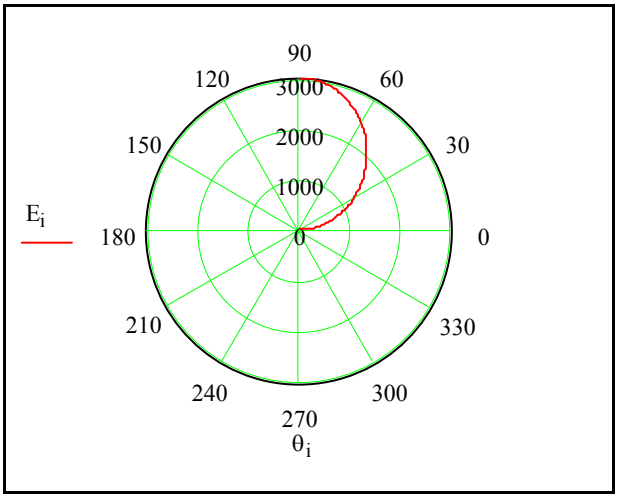

Figure 3.4: MathCAD Simulation

This is the E-field for a half-wave dipole, $0 \le \theta \le \pi/2$, above the ground plain. Through image theory, it is found that the field for the $\lambda/4$ monopole is exactly the same for $0 \le \theta \le \pi/2$. This can be visualised by placing a conducting ground plane at the centre feed point of the $\lambda/2$ dipole, resulting in:

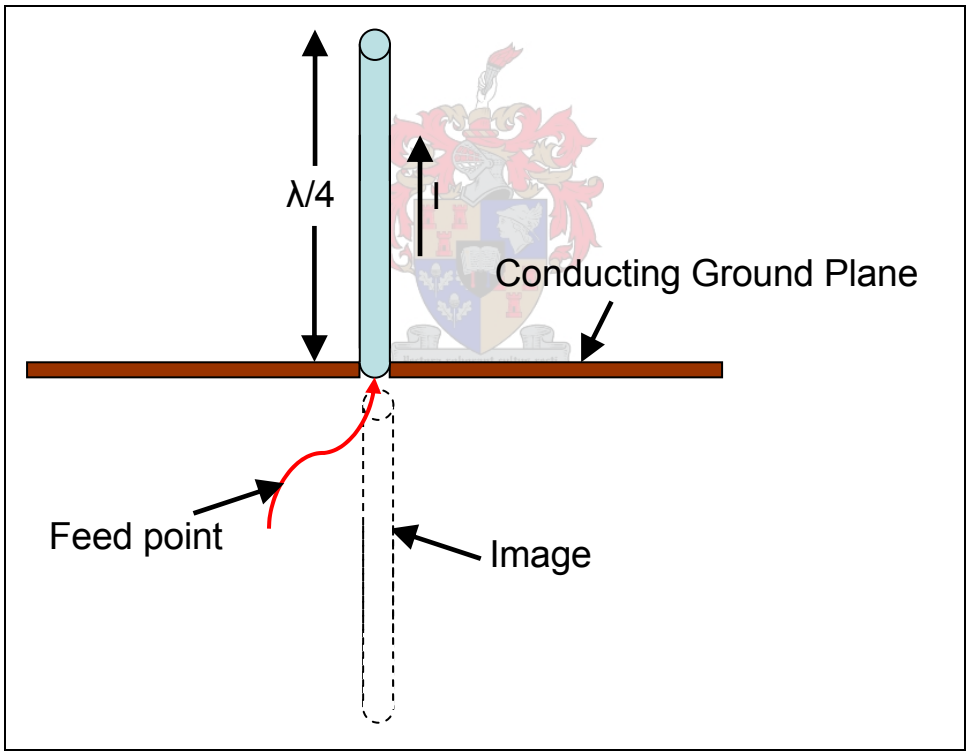

Figure 3.5: Monopole Visualisation

From this it is known that the radiated power will be half of that of the $\lambda/2$ dipole and the radiation resistance is also half of what the $\lambda/2$ dipole's radiation resistance was.

$$R_{rad} \cong 73\Omega$$

For the $\lambda/4$ monopole, the radiation resistance is therefore $R_{rad} = 36.5\Omega$. The radiation resistance for wire antennas are needed for matching purposes.

The $\lambda/4$ monopole is simulated using FEKO[5]. The output is given as:

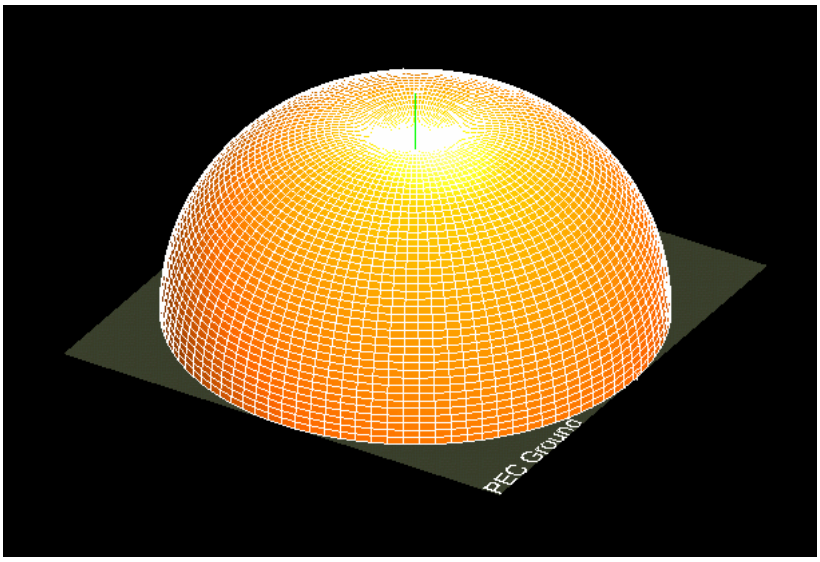

Figure 3.6: FEKO Simulation for External Mobile Antenna

From the schematic, it can be seen that a perfect conducting ground is used for the simulation of this model. This is done because, in practice, the external antenna is place on the roof of a car and the same radiation pattern is expected. The placement of the external antenna can be seen in the next figure.

Figure 3.7: External Antenna on Roof of the Vehicle

The gain of such an electrically small quarter wave monopole antenna is $1.73dB$ [19], [20]. The cable between the antenna and the mobile phone is a RG174 which has a loss of $1.5dB/m$ at 1800MHz. For the length of 2.24m, the cable will have a loss of $3.36dB$. The total loss due the external antenna is

[5] WinFEKO© Version 3.2.6m

therefore $1.63dB$ and must be taken into account in all the measurements and predictions that will be made. The far field gain and electric far field versus angle, as simulated using FEKO, can be seen in the next two figures.

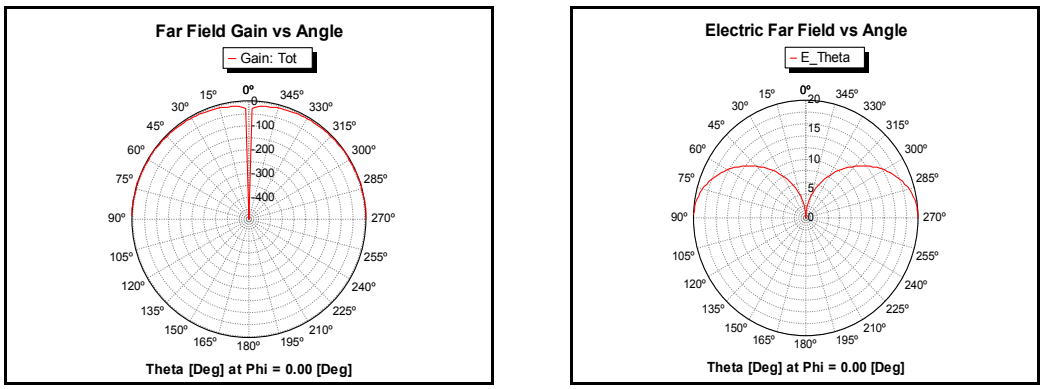

Figure 3.8: FEKO Simulation for Antenna Gain Plot and E-field Plot

Therefore, now the problem of the unknown radiation pattern for the internal antenna of the cellphone is solved. The only variable is the antenna radiation pattern of the mobile base station, which is known.

The external antenna, electrically small monopole, is connected to a vector network analyser (VNA) and S_{11} is measured. From this it can be seen that the element is resonant at about 1.8GHz. The next MATLAB plot shows this clearly.

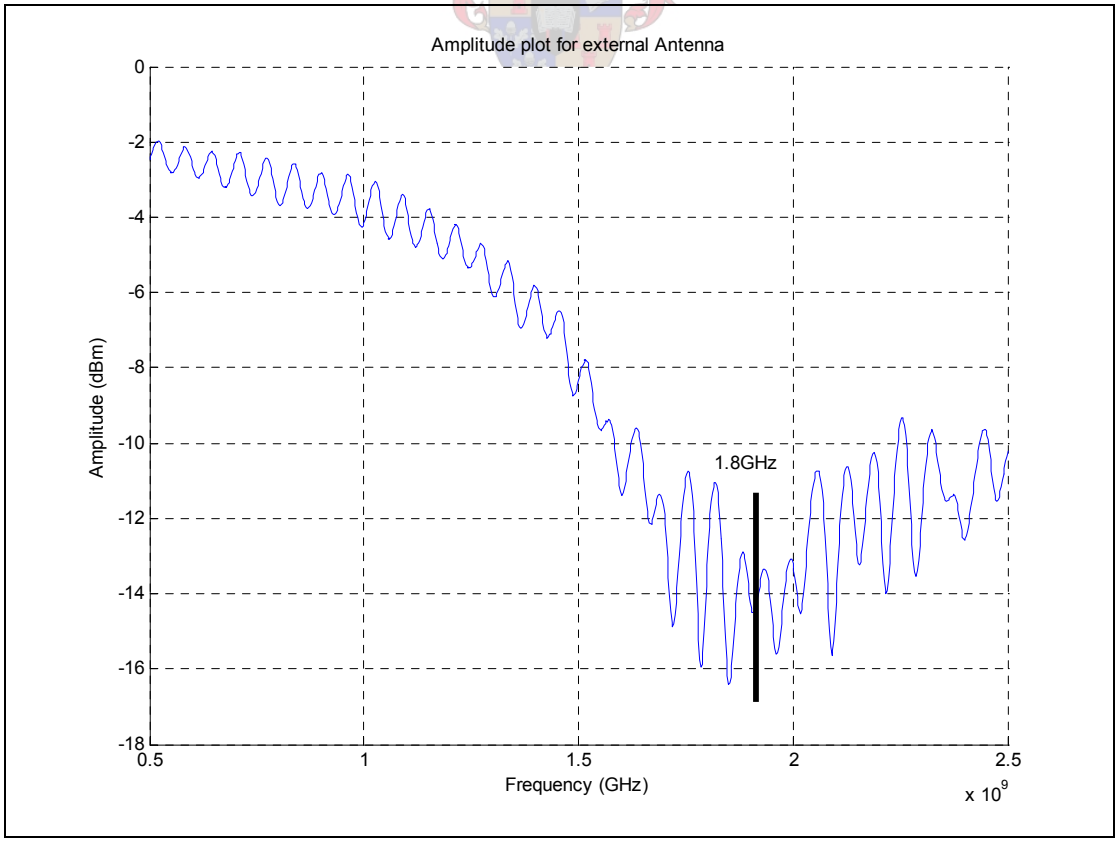

Figure 3.9: Amplitude Plot for External Antenna

From this figure it can also be seen that the antenna is resonant over a reasonable band of 250MHz. Thick monopoles are considered broadband, while thin monopoles are more narrowband [21]. For a monopole with length, ℓ, and diameter, d, the relationship between the bandwidth and physical properties can be given as follows. If the ℓ/d ratio is decreased, the bandwidth is enlarged. This can be accomplished by increasing the diameter of the wire. For example, an antenna with a $\ell/d \cong 5000$ has a bandwidth of about 3%, an antenna with that same length but with $\ell/d \cong 260$ has a bandwidth of about 30% of the centre frequency. This explains the relative bandwidth of the external antenna that can be seen in the above figure. For a broad band monopole, the physical length must be somewhat shorter than a free space quarter-wavelength, and as the antenna wire thickness is increased, the length must be reduced more to achieve resonance. This is clearly noticed when the external antenna is looked at. The physical length is measured as $32mm$ which is much less than $41.67mm$, the actual quarter wavelength length.

In Figure 3.9., small oscillations can be seen over the frequency band the antenna was tested for. This can be explained by looking at the cable that is connected to the antenna. For purposes of explaining these oscillations, the external antenna is disconnected and the end is terminated. Again S_{11} is measured and the plot is shown in Figure 3.10.

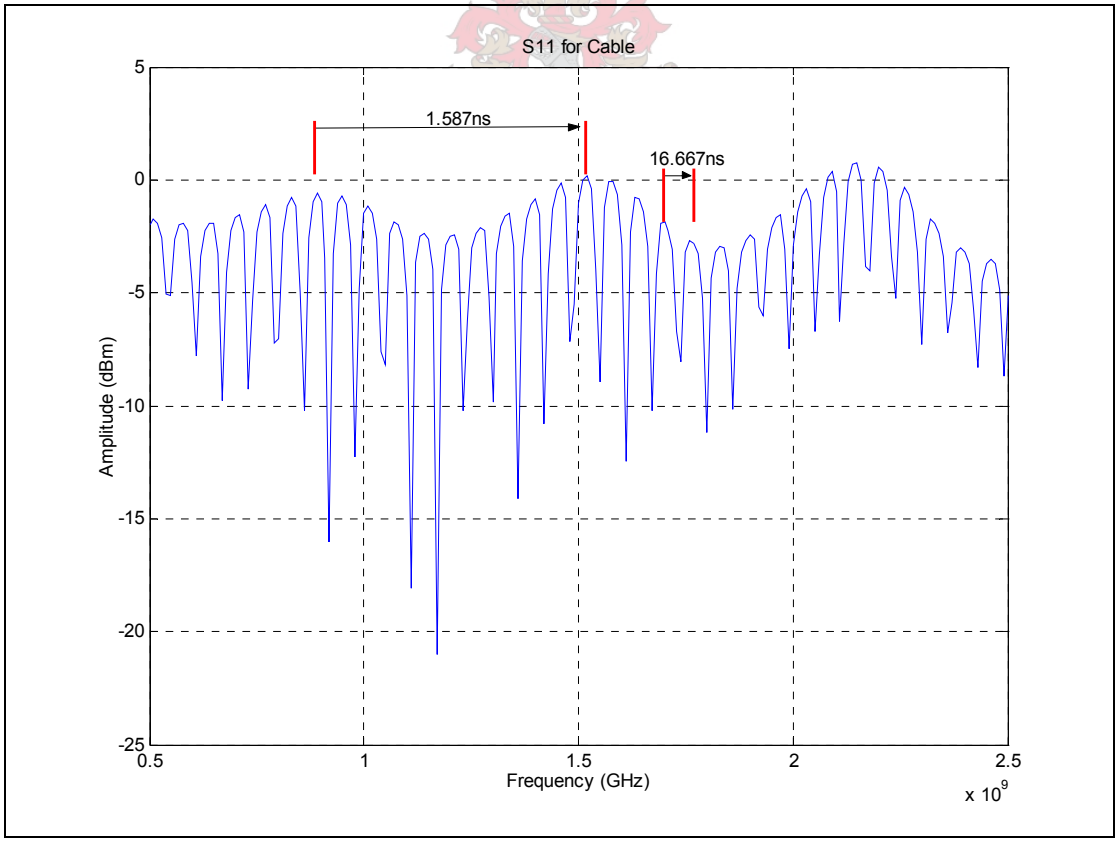

Figure 3.10: S_{11} measured for Antenna Cable

For this measurement, the length of the cable is 179cm and there is a joint in the cable at 17.4cm from the input. The speed of an electromagnetic (EM) wave in a coaxial cable is given as $2\times10^{8}\,m/s$. The period of the distance travelled by the electromagnetic wave can therefore be calculated as:

$$time(s)=\frac{dist(m)}{speed(m/s)} \qquad \text{Equation 3.3}$$

The length travelled by the EM wave is double, because it travels into the coaxial cable, reflects from the shorted end and the travel back to the input where S_{11} is measured. The periods for the total cable length as well as for the joint are calculated to be $17.9ns$ and $1.74ns$ respectively. These values compare well to those seen in Figure 3.10.

$$17.9ns \approx 16.667ns \text{ and } 1.74ns \approx 1.587ns$$

In a resonant antenna, almost the entire radio signal fed to the antenna is radiated [22]. From the above figures, it is clear that this external antenna will work well for the 1800MHz frequency band.

With the phone connected to the laptop computer, the signal level is logged. This is done using Microsoft Visual Basic programming. The code used for developing this GUI, is shown in Appendix A3. A screen shot of the GUI is shown in Figure 3.11.

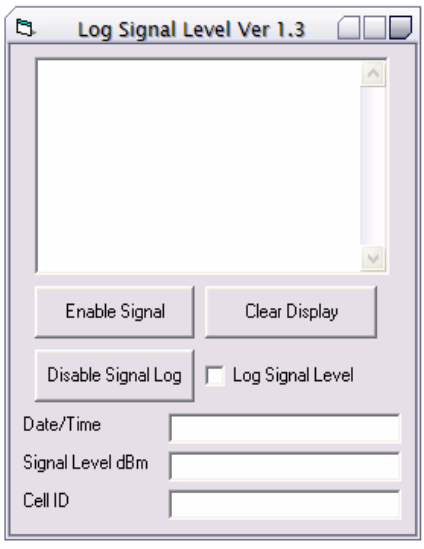

Figure 3.11: Screenshot of GUI used to log the Signal Level

The GUI is in a sense a sampler. The sampling rate can be changed to the needs of the user. The program, using Nokia Software Development Kit (SDK) software, monitors the measured signal level and log these values every $1.5\,\text{sec}$. The SDK software registers the signal level, each time the signal level changes, increments of 1dB.

3.3. Proof of Data Capturing System

To make sure that this measurement works, different Nokia 6310i phones are used and a measurement is taken over three days, to see how the signal level varies, if any.

First five different phones are used, each connected for half an hour, logging the measured signal level every $30\,\text{sec}$. The measurement setup used for this test, can be seen in Figure 3.12.

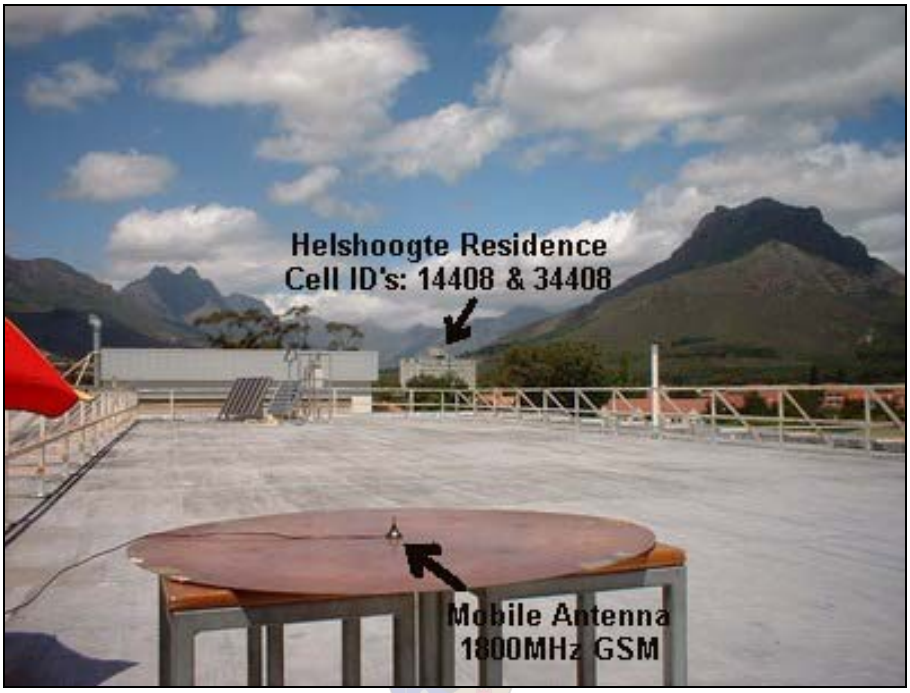

Figure 3.12: Setup on Roof of Electrical and Electronic Engineering Building

The signal logged for the phones, can be seen in the next two figures. From the figures, it can be seen that both the 14408 as well as the 34408 Cell ID, were picked up by the mobile phones, hence the two different plots. This happens if the signal picked up by the phone, is not strong enough. The phone sends out poling signals to the surrounding towers and then it becomes idle on the Cell ID or tower with the strongest down link. This is in a sense a battery saving feature that the phone use, less power transmitted, more battery power is saved for calls.

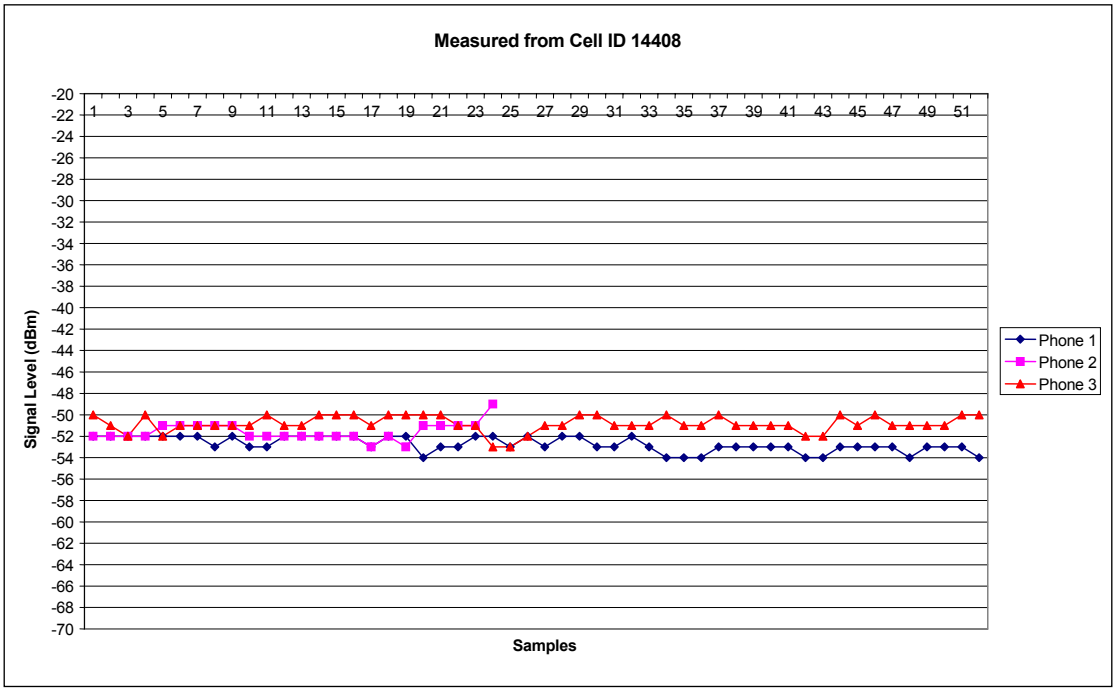

Figure 3.13: Signal logged from cell ID 14408

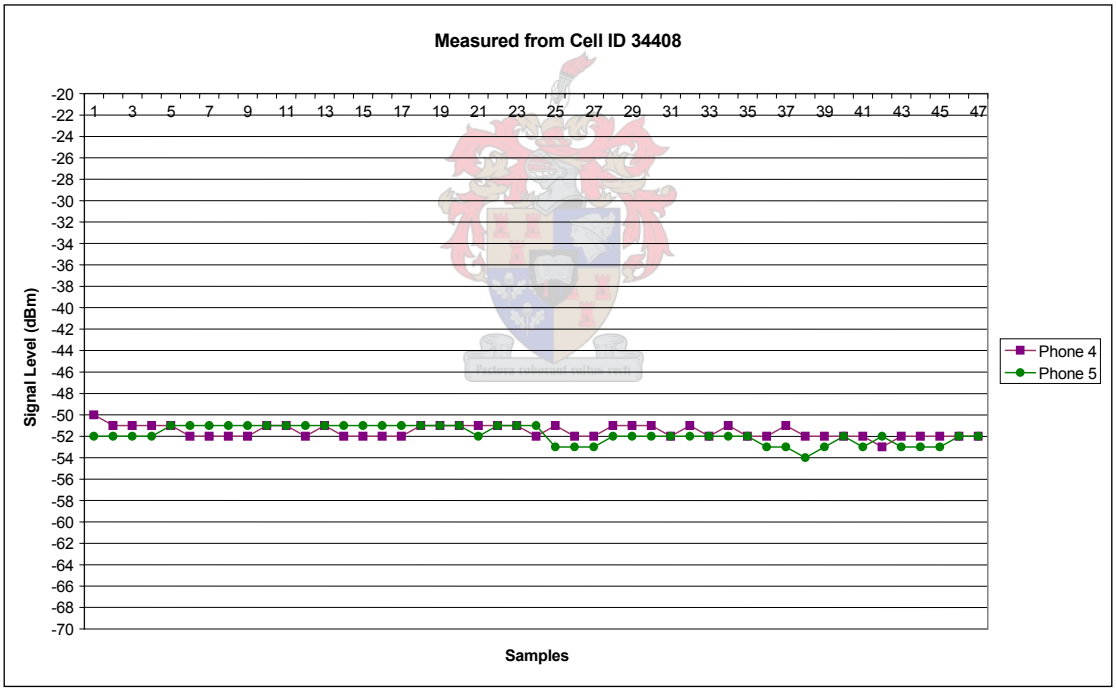

Figure 3.14: Signal logged from cell ID 34408

From the above two figures it can be seen that the signal logged by the measurement system is stable. Small scale fading can be seen, which is due to variations in the propagation medium, such as movement of cars, human beings and other reflector and absorbers. It is found from these results that the phone, Nokia 6310i, is suitable for the measurements, proposed to be taken.

The next setup, for the proof of the system, is done, by connecting the phone to a laptop computer for three days, logging the signal level every 30 seconds. This is to establish how the signal level logged by the measurement system, changes over time.

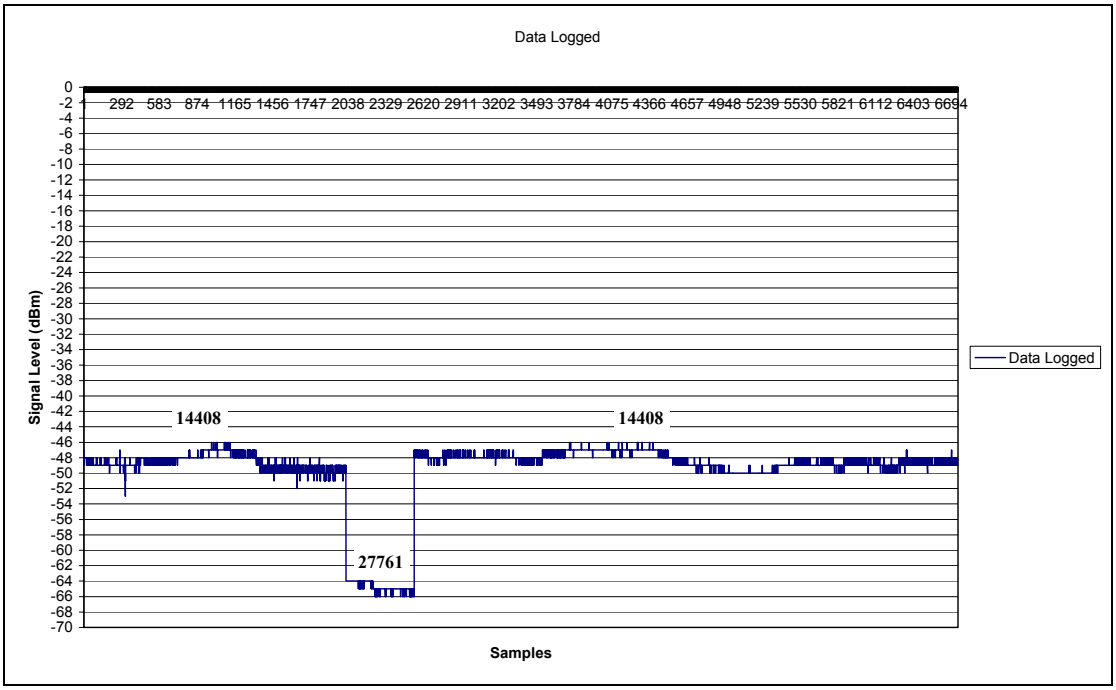

Figure 3.15: Data Logged over 3 Days

From the above figure it can be seen that the signal being logged stay stable. Small scale fading can be seen again, as expected. The drop in measured signal level, seen in the figure, is due to the fact that the mobile phone is locked onto another cell ID. The two cell sites can be seen in the next two figures.

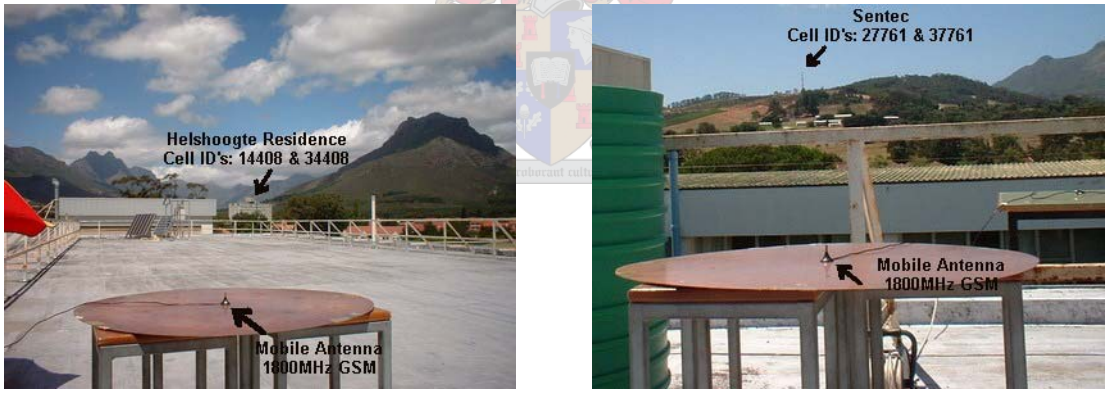

Figure 3.16: View towards cell ID 14408(left) and 27761(right)

The data presented is found to be conclusive that the measurements system work and that measurements taken, are accurate. The signal strength measured by the five different phones compares well. The signal level measured over three days is found to be satisfactory. The accuracy of the GPS is also found to be satisfactory. Alterations can be made to the device as needed, depending on the measurements needed.

PROPAGATION MODELING

In this chapter the phenomenon of radiowave propagation will be looked at. Some of the most important propagation phenomenon, some of which are used for predicting the received signal level in this project, will be acknowledged and explained in detail. It will be covered in the following order:

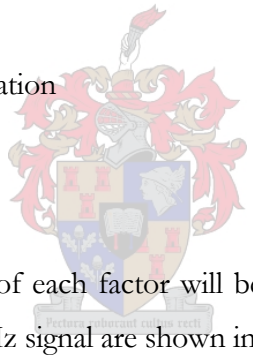

At the end of this chapter, the influence of each factor will be taken into account. A summery of these factors and there influence on the 1800MHz signal are shown in Table 4.4.

4.1. Common Propagation Phenomenon

Diffraction occurs when the radio path between the transmitter and the receiver is obstructed by an impenetrable body. According to Huygen's principle [23], secondary waves are formed behind the obstruction, even if there is no line of sight path. This phenomenon explains how radio frequency energy can travel in urban areas without any line-of-sight paths. This phenomenon is also known as "shadowing".

Scattering occurs when the radio channel contains objects with dimensions that are on the order of the wavelength or less. Scattering follows the same physical principles as diffraction and causes energy from the transmitter to be scattered in many different directions. Scattering has been proven to be the most difficult of the three propagation mechanisms and it also makes the theoretical prediction more complicated. However, scattering can be neglected in many cases because the contributions of reflections, diffraction, or a combination of these, are more significant.

Reflection occurs when a propagating electromagnetic wave impinges upon an obstacle with dimensions large compared to the wavelength of the radio wave. Reflections from buildings and surface of the earth can interfere constructively or destructively at the receiver, and is the main source of multipath propagation.

Refraction occurs when the propagating electromagnetic wave is bent due to the refractive index of the medium it is travelling through. Hence the phenomenon of trans horizon propagation is possible. Refraction can be neglected for micro- and pico-cellular mobile communications, due to the short distance between the mobile base station and the mobile receiver. However, if the distance between the transmitter and the receiver goes beyond tens of kilometres, the effect of the troposphere should be taken into account.

4.2. Free Space Propagation Loss

In this section, the formulation of free space loss will be considered and the end result will be used in calculating the link budget for each measurement taken in field measurements.

If an isotropic source radiates a total power of $P_t(W)$, then the power density F_0 at a distance d, will be given by [23]:

$$F_0 = \frac{P_t}{4\pi d^2} \qquad \text{Equation 4.1}$$

This model is useful for specifying a reference against which antenna gain can be defined. In practice any antenna poses a radiation pattern. Such a radiation pattern is a graphic representation of the radiated signal strength, in reference to the maximum delivered power as a function of position in reference to the radiating point. The gain of the antenna in the θ and ϕ direction, can be defined with respect to an isotropic power density, by taking the ratio of $F_d(\theta,\phi)$ with the flux density produced by an isotropic radiator at the same distance and fed with the same power P_t:

$$G(\theta,\phi) = \frac{F_d(\theta,\phi)}{F_0} \qquad \text{Equation 4.2}$$

This gain function will depend on what type of antenna is used. For this case, the radiation pattern of the mobile base station is known and the antenna pattern for the mobile phone is modelled as a quarter wave monopole antenna.

The power density at a distance d from the transmitting antenna, $F_d(\theta,\phi)$, is given by:

$$F_d(\theta,\phi) = \frac{P_t G_t(\theta,\phi)}{4\pi d^2} \qquad \text{Equation 4.3}$$

where G_t is the gain of the transmitting antenna. This gain of the antenna in different directions can be determined using the radiation pattern of the antenna. The radiation patterns for the base stations used in this project, are known.

To facilitate the calculation of P_r we may consider the antenna to be presenting an effective collecting-aperture area of A_e. Hence the received power becomes:

$$P_r = \frac{P_t G_t(\theta,\phi) A_e}{4\pi d^2} \qquad \text{Equation 4.4}$$

It should also be known that the effective aperture area is not necessary always the same, the aperture area can change as the direction of incident waves are changed. It is possible to relate the effective aperture to the antenna gain through the relation:

$$A_e(\theta,\phi) = G(\theta,\phi)\frac{\lambda^2}{4\pi} \qquad \text{Equation 4.5}$$

The ratio between the effective aperture and the physical area, in the direction of maximum gain, is a measure of the antenna efficiency η, for $\eta = \frac{A_e}{A}$. This now gives the expression for the maximum antenna gain as:

$$G = \left(\frac{\pi d}{\lambda}\right)^2 \eta \qquad \text{Equation 4.6}$$

If now combined, the received power at the receiving antenna is given by:

$$P_r = P_t G_t G_r \left(\frac{\lambda}{4\pi d}\right)^2 \qquad \text{Equation 4.7}$$

To evaluate this expression, the gain of both the receiving and transmitting antennas are made unity. From this it can be seen that the ratio of received power to transmitted power, P_r / P_t, depends on $(\lambda / 4\pi d)^2$, which is simply the free-space loss.

For engineering purposes, this expression can be written as a link budget:

$$P_r(dBw) = P_t(dBw) + G_t(dBi) + G_r(dBi) - L_{BF}(dB) \qquad \text{Equation 4.8}$$

where

$$L_{BF} = 20\{\log_{10}(4\pi d) - \log_{10}(\lambda)\} \qquad \text{Equation 4.9}$$

and dBi is the gain with respect to an isotropic antenna and dBw is with respect to $1W$. Noting that $\lambda = c/f$ (where c is the velocity of light in a vacuum $= 3\times10^8 ms^{-1}$) and take f to be in MHz and d in km, the following standard result can be obtained:

$$L_{BF} = 32.44 + 20\log_{10}(f) + 20\log_{10}(d) \qquad \text{Equation 4.10}$$

4.3. Multipath Propagation

Multipath propagation is a key issue faced in all wireless communications systems. It causes frequency selective fading and this degrades the reliability of the service supplied to the end user. The mechanics that govern radio propagation are complex and diverse, and they can generally be attributed to reflection, refraction, diffraction and scattering or a combination of these, according to the environment and the frequency band that is used. Such multipath propagation is particularly significant in urban environments, where the sides of buildings and paved road surfaces provide strong reflections. For these cases, where the sizes of the buildings and other reflectors are many wavelengths, high frequency approximations can be made. These high frequency approximations are known as: geometrical optics (GO), physical optics (PO), geometrical theory of diffraction (GTD) and uniform theory of diffraction (UTD). As a result, the received signal consists of the summation of several components having various amplitudes, phase angles and directions of arrival.

The resulting spatial variability of signal strength can be viewed as having two components [24]:

a) Rapid fading which varies over distances of the order of a wavelength due mainly to changes in phase angles of the different signal components.
b) Slow fading which varies over larger distances due mainly to changes in shadowing loss by surrounding objects.

In addition to this, the various signal components can be Doppler shifted by different amounts, due to the movement of the mobile phone or reflections coming from surrounding vehicles that are moving. For the purpose of this project, the mobile receiver was stationary at all times, therefore eliminating the Doppler

effect caused by the moving receiver. Movement in surrounding reflecting objects will still contribute a small amount of fading.

Fades of 30dB or more below the mean level are common. The instantaneous field strength when measured over distances of a few tens of wavelengths is approximately Rayleigh-distributed. The next table give an idea of the type off cell and the fading that can be expected [25]:

Item	Microcell	Small Macrocell
Cell Radius	0.1 to 1 km	1 to 3 km
Fading	Nakagami-Rice	Rayleigh
RMS delay spread	10 to 100 ns	0.1 to 10 μs

Table 4.1: Typical Parameters for Micro- and Macro Cells

The mean values of these small sector distributions vary widely from area to area, depending on the height, density and distribution of hills, trees, buildings and other structures. The root mean square (RMS) delay spread is the power weighted standard deviation of the excess delays. This provides a measure of the variability of the mean delay.

For the description of communication systems performance, it is often sufficient to observe the time series of signal fluctuation and characterize these fluctuations as a stochastic process. Stochastic, because the signal level at time, t, is the function of a random variable, and not deterministic. These random variables, as shown in Table 4.1, will now be looked at in more detail.

The first, is the Rayleigh distribution that applies to a non-limited positive continuous variable, linked to the Gaussian distribution as follows. Given a two-dimensional Gaussian distribution with two independent variables y and z of zero mean and the same standard deviation σ, the random variable

$$x = \sqrt{y^2 + z^2} \qquad \text{Equation 4.11}$$

has a Rayleigh distribution and the most probable value of x is equal to σ. Note that σ is the standard deviation of the Gaussian distribution, with which the Rayleigh distribution is linked.

The next distribution function is the Nakagami-Rice which is also derived from the Gaussian distribution, but generalizes the Rayleigh distribution. This distribution depends on two parameters, but for purposes of propagation problems, it is necessary to choose a relation between the amplitude, a, of the fixed vector and the root mean square amplitude, $\sigma\sqrt{2}$, of the random variable. This is done by taking the power in the fixed vector, line-of-sight component, as constant, but the total power in fixed and random components to vary. This is now used for studies on reflections from rough ground surfaces, or for the

consideration of multipath components in addition to the fixed component. The mean power is now given by

$$\left(a^2 + 2\sigma^2\right) \qquad \text{Equation 4.12}$$

The distribution is defined in terms of the parameter K, which is the ratio between the fixed line-of-sight components and the random reflected components. K is defined as:

$$K = 10\log\left(\frac{a^2}{2\sigma^2}\right) \quad (\mathbf{dB}) \qquad \text{Equation 4.13}$$

As seen in the following simulation, it is clear how the signal varies between 0.1 – 1km and then again from 1 – 3km, due to the effect of multipath propagation:

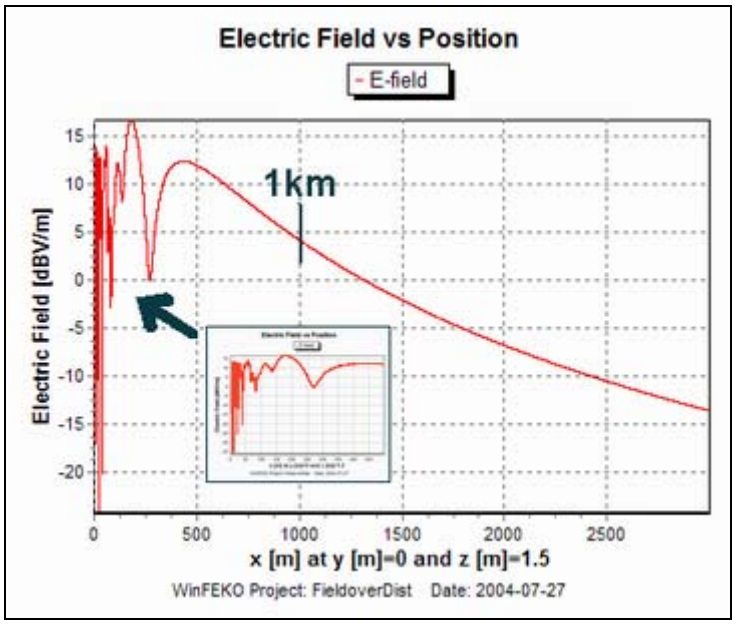

Figure 4.1: Electric Field vs. Distance from Base Station

This simulation was done with the base station antenna at a height of 15m and the mobile phone external antenna at a height of 1.5m. The height above ground level of both the transmitter and the receiver has an influence on the amount of multipath propagation that can be expected at the receiver.

The ground cover is the next important factor that needs to be taken into account when modelling the effect of multipath propagation. More reflection can be expected from certain ground cover than from other. Again, the recommendations of the ITU-R are taken into account and the reflection coefficient for the earth surface is calculated [26].

First and foremost, the complex permittivity, η, of the Earth surface in the vicinity of the reflections, need to be calculated. For this, the relative permittivity, ε_r, and conductivity, σ (S/m), need to be known. This is supplied by the ITU [27] and Von Hippel [28], as shown in the next figure as a function of carrier frequency.

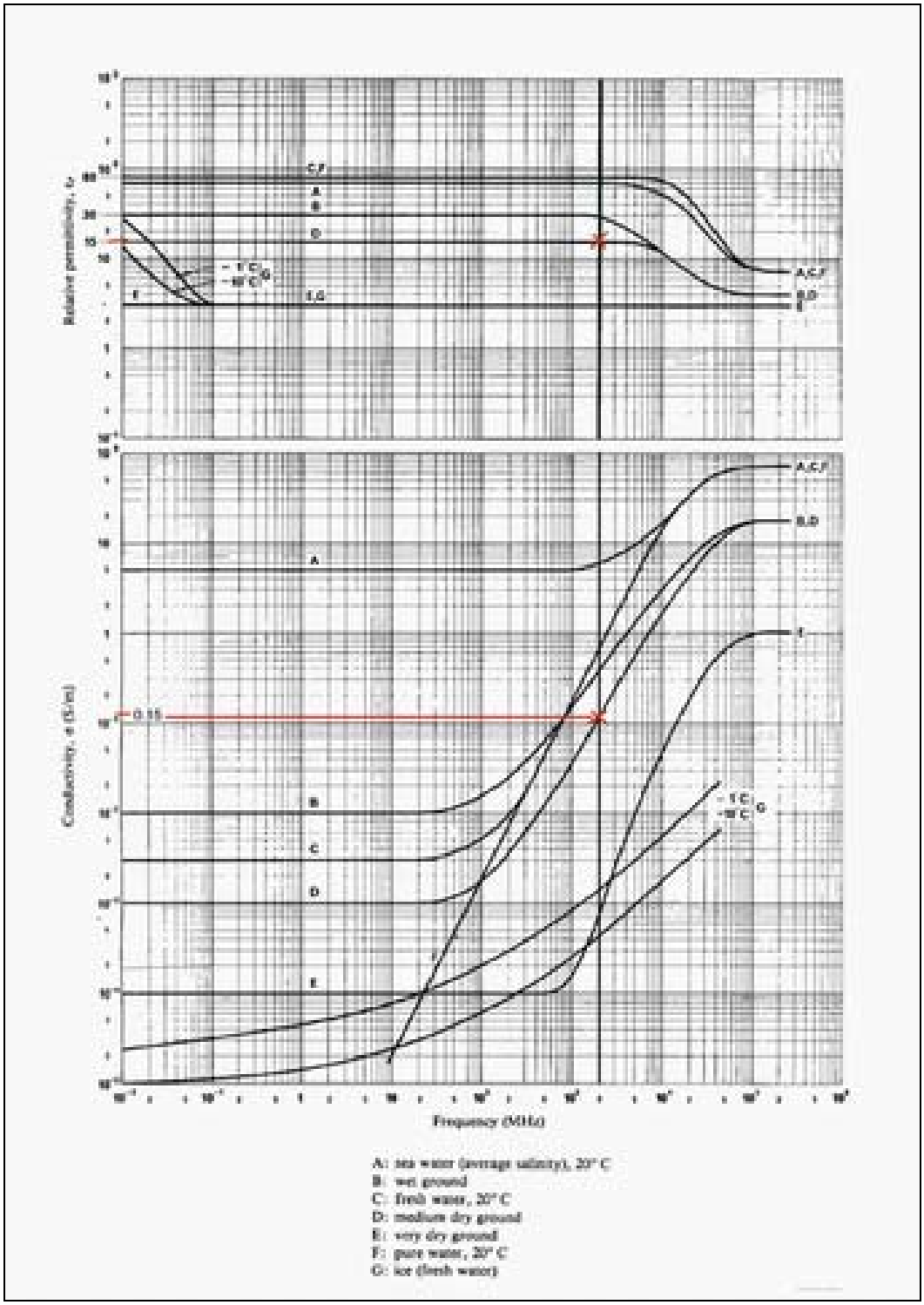

Figure 4.2: Relative Permittivity, ε_r, and conductivity, σ, as a function of frequency

$$\eta = \varepsilon_r - j18\frac{\sigma}{f}$$ Equation 4.14

Next, the grazing angle, the angle between the flat earth and the antenna, is calculated.

$$\varphi = \frac{h_1 + h_2}{d}\left[1 - m\left(1 + b^2\right)\right]$$ Equation 4.15

$$b = 2\sqrt{\frac{m+1}{3m}}\cos\left[\frac{\pi}{3} + \frac{1}{3}\arccos\left(\frac{3c}{2}\sqrt{\frac{3m}{(m+1)^3}}\right)\right]$$ Equation 4.16

$$m = \frac{d^2}{4a_e\left(h_1 + h_2\right)} \times 10^3$$ Equation 4.17

$$c = \frac{\left(h_1 - h_2\right)}{\left(h_1 + h_2\right)}$$ Equation 4.18

With $a_e = ka$ the effective radius of the Earth for a given k factor ($a = 6375km$ being the actual radius of the Earth), d is the distance between the base station and the mobile receiver in km and h_1 and h_2 the height of the base station and the mobile receiver antenna in m, respectively.

Now the reflection coefficient of the Earth surface can be calculated to be:

$$\rho = \left|\frac{\sin\varphi - \sqrt{C}}{\sin\varphi + \sqrt{C}}\right|$$ Equation 4.19

Where:

$C = \eta - \cos^2\varphi$ horizontal polarization

$C = \dfrac{\eta - \cos^2\varphi}{\eta^2}$ vertical polarization

Next, the divergence factor of the Earth's surface is calculated:

$$D = \sqrt{\frac{1 - m\left(1 + b^2\right)}{1 + m\left(1 - 3b^2\right)}}$$ Equation 4.20

Now calculate the length, L_1, of the first Fresnel zone ellipse on the Earth's surface along the path, using:

$$L_1 = d\sqrt{1+\frac{4fh_1h_2\times10^{-2}}{3d}}\left[1+\frac{f(h_1+h_2)^2\times10^{-2}}{3d}\right]^{-1} \qquad \text{Equation 4.21}$$

And the width, W_1, in the transverse direction from:

$$W_1 = \sqrt{\frac{3\times10^{-4}d}{f}} \qquad (km) \qquad \text{Equation 4.22}$$

For the purpose of these calculations, it has to be assumed that the centre of the first Fresnel ellipse is at the centre of the obvious surface reflection. If only portions of the Fresnel ellipse are reflected, the specular-reflection factor, R_s, need to be calculated:

$$R_s = \sqrt{\frac{f(h_1+h_2)^4(\Delta x)^2\times10^{-2}}{3h_1h_2d^3}} \qquad \text{Equation 4.23}$$

Where Δx is the length of the portion not reflected. If all is reflected, $R_s = 1$.

If the surface within the first Fresnel zone is rough, the surface roughness factor, R_r, need to be calculated from:

$$R_r = \sqrt{\frac{1+\left(\frac{g^2}{2}\right)}{1+2.35\left(\frac{g^2}{2}\right)+2\pi\left(\frac{g^2}{2}\right)^2}} \qquad \text{Equation 4.24}$$

Where:

$$g = \frac{40\pi f\sigma_h \sin\varphi}{3} \qquad \text{Equation 4.25}$$

with σ_h (m) the standard deviation of surface height for the part of the path profile within the first Fresnel ellipse. Again, if no roughness is present, such as water, the roughness factor should be taken as $R_r = 1$.

The effective reflection coefficient is then given by:

$$\rho_{eff} = \rho D R_s R_r \qquad \text{Equation 4.26}$$

On sufficiently inclined paths or paths with naturally large clearance, the angles between the direct and surface-reflected wave(s) become large enough to take advantage of the radiation pattern of one or both antennas to discriminate between the reflected wave(s).

All these calculations are done using software supplied by EMSS, a company based in Stellenbosch, South Africa. The software tool used is FEKO. The variables that are used in this software are given in the next table.

Input Variable	Unit
Carrier Frequency	Hz
Base Station Antenna Height	m
Mobile Antenna Height	m
Path Length	m
Relative Permittivity of Earth Surface	-
Conductivity of Earth Surface	S/m

Table 4.2: Variables used for Multipath Propagation Modelling

4.4. Diffraction over Obstacles and Irregular Terrain

Many of the propagation paths that were looked at during the course of this project encountered one or more obstacles and it is useful to estimate the losses caused by such impediments. To make such calculations, it is necessary to idealize these obstacles by assuming either a knife-edge of negligible thickness or a thick smooth obstacle with a well-defined radius of curvature at the top.

In this section, attention will be given to the single knife-edge obstacle and the single rounded obstacle; more examples of other obstacles are given in ITU Recommendation [29]. First the single knife-edge obstacle will be considered.

4.4.1. Single Knife-Edge Diffraction:

Single knife-edge obstacle is an extremely idealized case. All the geometrical parameters are combined together in a single dimensionless parameter, υ, given in terms of the geometrical data as follow:

$$\upsilon = h\sqrt{\frac{2}{\lambda}\left(\frac{1}{d_1}+\frac{1}{d_2}\right)} \qquad \text{Equation 4.27}$$

$$\upsilon = \theta\sqrt{\frac{2}{\lambda\left(\frac{1}{d_1}+\frac{1}{d_2}\right)}} \qquad \text{Equation 4.28}$$

$$\upsilon = \sqrt{\frac{2h\theta}{\lambda}} \qquad (\upsilon \text{ has the sign of } h \text{ and } \theta) \qquad \text{Equation 4.29}$$

$$\upsilon = \sqrt{\frac{2d}{\lambda}\alpha_1\alpha_2} \quad (\upsilon \text{ has the sign of } \alpha_1 \text{ and } \alpha_2) \qquad \text{Equation 4.30}$$

Where:

h: height of the top of the obstacle above the straight line joining the two ends of the path. If the height is below the line, h is negative.

d_1 and d_2: distance of the two ends of the path from the top of the obstacle.

d: length of the path

θ: angle of diffraction (rad); the sign must be the same as h, this angle is assumed to be less or equal to $0.2rad$ or $12°$.

α_1 and α_2: angles between the top of the obstacle and one end as seen from the other end. Again α_1 and α_2 have the same sign as h.

These variables are now illustrated in the next figure. Given (a) for when the obstacle is obstructing the line-of-sight path and (b) for when the obstacle is below the line-of-sight view.

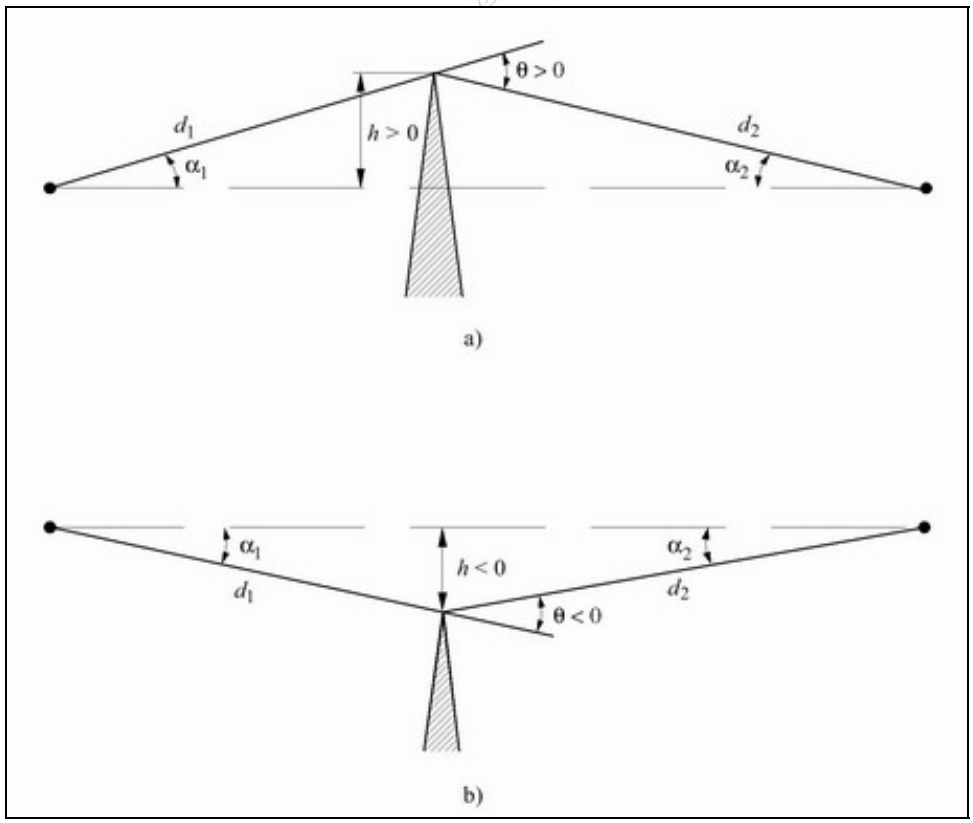

Figure 4.3: Geometrical elements used for Single Knife-Edge Diffraction

For υ greater than -0.7, the loss can be calculated using:

$$J(\upsilon) = 6.9 + 20\log\left(\sqrt{(\upsilon - 0.1)^2 + 1} + \upsilon - 0.1\right) \qquad \text{Equation 4.31}$$

4.4.2. Single Rounded Obstacle Diffraction:

Single rounded obstacle is the next obstacle that will be looked at. With radius, R, as illustrated in the next figure. Note that the distances and height from the baseline are all measured to the vertex where the projected rays intersect above the obstacle.

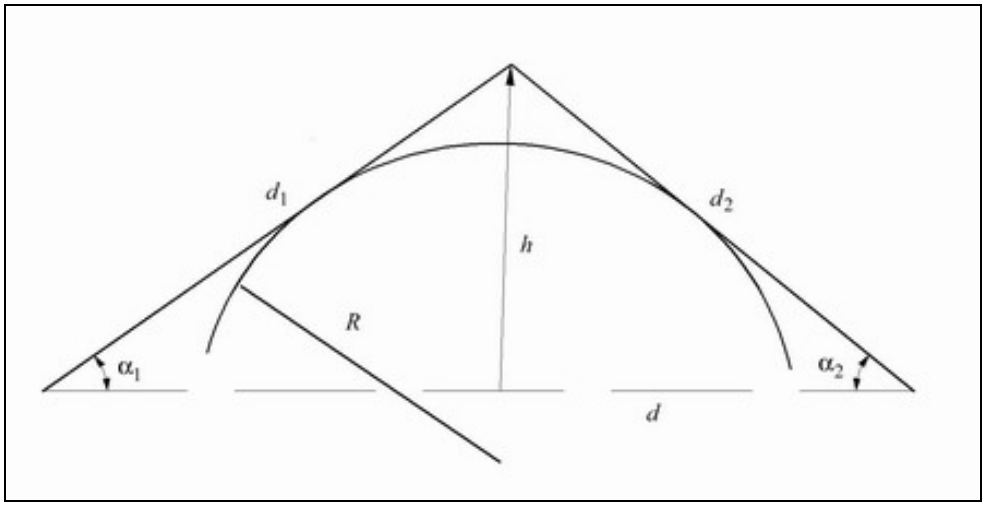

Figure 4.4: Geometrical elements used for Single Rounded Obstacle Diffraction

The loss due to diffraction for this geometry, can be calculated as follow:

$$A = J(\upsilon) + T(m,n) \quad (dB) \qquad \text{Equation 4.32}$$

Where:

i) $J(\upsilon)$ is the Fresnel-Kirchoff loss due to the equivalent knife-edged obstacle place in the propagation path, with its peak at the vertex point. The dimensionless parameter, υ, can now again be calculated, using:

$$\upsilon = 0.0316h\left[\frac{2(d_1 + d_2)}{\lambda d_1 d_2}\right]^{\frac{1}{2}} \qquad \text{Equation 4.33}$$

Where h and λ are in metres, and d_1 and d_2 are in kilometres. $J(\upsilon)$ can now again be calculated using the following:

$$J(\upsilon) = 6.9 + 20\log\left(\sqrt{(\upsilon - 0.1)^2 + 1} + \upsilon - 0.1\right) \qquad \text{Equation 4.34}$$

ii) $T(m,n)$ is the additional attenuation due to the curvature of the obstacle:

$$T(m,n) = km^b \qquad \text{Equation 4.35}$$

Where:

$$k = 8.2 + 12n$$ Equation 4.36

$$b = 0.73 + 0.27\left[1 - e^{-1.43n}\right]$$ Equation 4.37

$$m = R\frac{\left[\frac{d_1 + d_2}{d_1 d_2}\right]}{\left[\frac{\pi R}{\lambda}\right]^{\frac{1}{3}}}$$ Equation 4.38

$$n = h\frac{\left[\frac{\pi R}{\lambda}\right]^{-\frac{2}{3}}}{R}$$ Equation 4.39

The next figure can also be used to obtain $T(m,n)$ as given by the ITU.

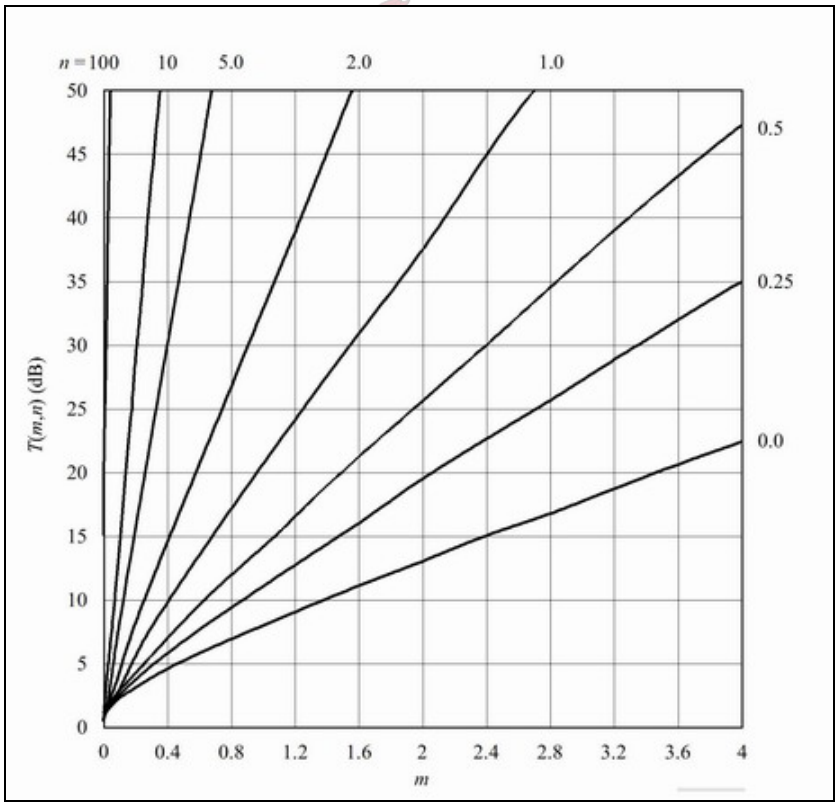

Figure 4.5: Value for $T(m,n)\ (dB)$ as a function of m and n

If the surface of the obstacle has irregularities not exceeding Δh:

$$\Delta h = 0.04^3\sqrt{R\lambda^2} \quad (m) \qquad \text{Equation 4.40}$$

Where:

R: the curvature of the obstacle (m)

λ: wavelength of the carrier frequency (m)

Then the obstacle may be considered to be smooth.

4.5. Gaseous Losses

These losses can be split into two contributions, namely dry air attenuation and attenuation due to water vapour. First the dry air attenuation will be considered.

4.5.1. Dry Air Attenuation:

In dry air, refractivity is proportional to air mass in the propagation path and is therefore predictable from atmospheric pressure. [30] *Dry air attenuation,* $\gamma_0(dB/km)$, is given by:

$$\gamma_0 = \left[\frac{7.34 r_p^2 r_t^3}{f^2 + 0.36 r_p^2 r_t^2} + \frac{0.3429 b \gamma_0'(54)}{(54-f)^a + b}\right] f^2 \times 10^{-3} \qquad \text{Equation 4.41}$$

for $f \le 54GHz$

where:

$$\gamma_0'(54) = 2.128 r_p^{1.4954} r_t^{-1.6032} e^{[-2.528(1-r_t)]} \qquad \text{Equation 4.42}$$

$$a = \frac{\ln\left(\frac{\eta_2}{\eta_1}\right)}{\ln(3.5)} \qquad \text{Equation 4.43}$$

$$b = \frac{4^a}{\eta_1} \qquad \text{Equation 4.44}$$

$$\eta_1 = 6.7665 r_p^{-0.505} r_t^{0.5106} e^{[1.5663(1-r_t)]-1} \qquad \text{Equation 4.45}$$

$$\eta_2 = 27.8843 r_p^{-0.4908} r_t^{0.8491} e^{[0.5496(1-r_t)]-1} \qquad \text{Equation 4.46}$$

where:

f : Frequency (GHz)

$r_p = \dfrac{p}{1013}$

$r_t = \dfrac{288}{273 + t}$

p : pressure (hPa)

t : temperature $(°C)$

If applied to the propagation channel used for the verification of this measurement system, it is found that the loss due to dry air attenuation is 0.0061 dB/km. This is illustrated in the next figure.

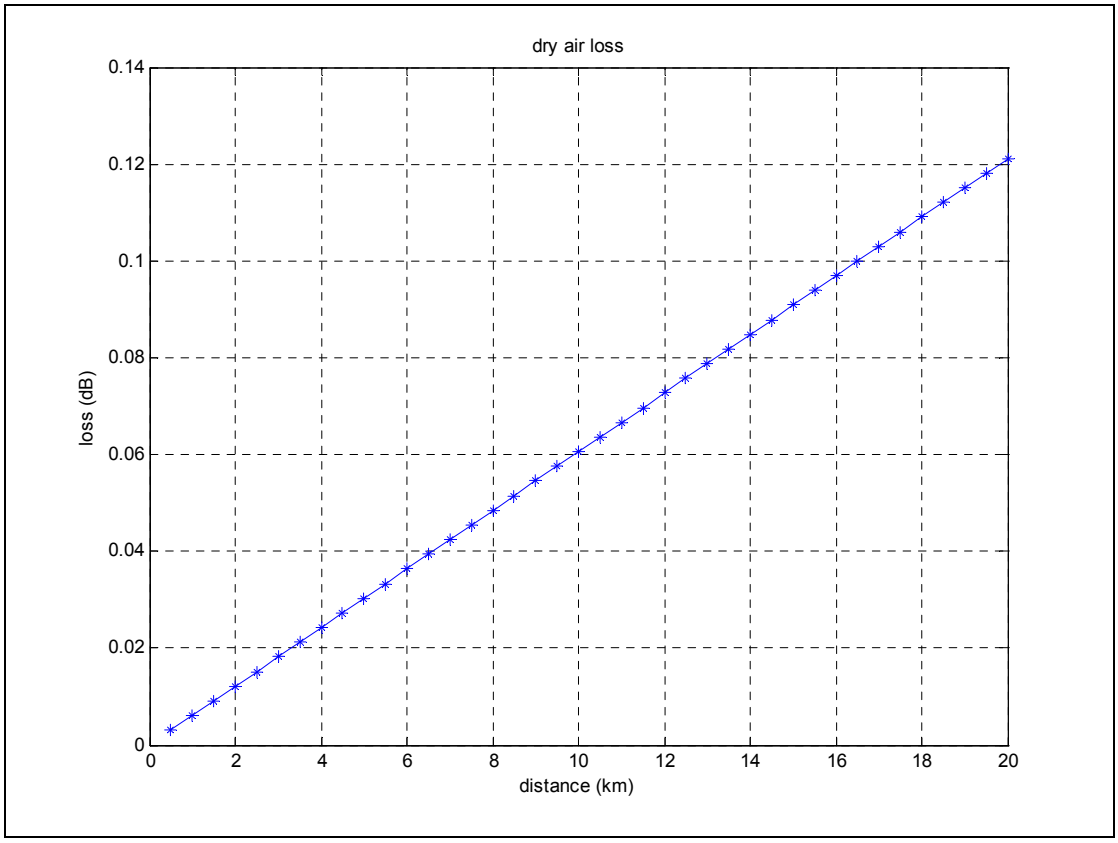

Figure 4.6: Dry Air Attenuation Loss vs. Distance

This is for pressure at 1017.8 hPa and temperature at $25.8\,°C$. This climatic data were supplied by South African Weather Service. From this, the conclusion is drawn that for purposes of measurements that will be taken; the effect of dry air attenuation can be neglected.

4.5.2. Water Vapour Attenuation:

Water vapour attenuation, $\gamma_w(dB/km)$, is given by:

$$\gamma_w = \left\{ 3.13\times10^{-2} r_p r_t^2 + 1.76\times10^{-3} \rho r_t^{8.5} + r_t^{2.5} \left[\frac{3.48\xi_{w1} g_{22} e^{(2.23(1.r_t))}}{(f-22.235)^2 + 9.42\xi_{w1}^2} \right.\right.$$
$$+ \frac{10.48\xi_{w2} e^{(0.7(1-r_t))}}{(f-183.31)^2 + 9.48\xi_{w2}^2} + \frac{0.078\xi_{w3} e^{(6.4385(1-r_t))}}{(f-321.226)^2 + 6.42\xi_{w1}^2}$$
$$+ \frac{3.76\xi_{w4} e^{(1.6(1-r_t))}}{(f-325.153)^2 + 9.22\xi_{w4}^2} + \frac{26.36\xi_{w5} e^{(1.09(1-r_t))}}{(f-380)^2}$$
$$+ \frac{17.87\xi_{w5} e^{(1.46(1-r_t))}}{(f-448)^2} + \frac{883.7\xi_{w5} g_{557} e^{(0.17(1-r_t))}}{(f-557)^2}$$
$$\left.\left. + \frac{302.6\xi_{w5} g_{752} e^{(0.41(1-r_t))}}{(f-752)^2} \right] \right\} f^2 \rho \times 10^{-4}$$

Equation 4.47

For $f \le 350GHz$

with:

$$\xi_{w1} = 0.9544 r_p r_t^{0.69} + 0.0061\rho$$ Equation 4.48

$$\xi_{w2} = 0.95 r_p r_t^{0.64} + 0.0067\rho$$ Equation 4.49

$$\xi_{w3} = 0.9561 r_p r_t^{0.67} + 0.0059\rho$$ Equation 4.50

$$\xi_{w4} = 0.9543 r_p r_t^{0.68} + 0.0061\rho$$ Equation 4.51

$$\xi_{w5} = 0.955 r_p r_t^{0.68} + 0.006\rho$$ Equation 4.52

$$g_{22} = 1 + \frac{(f-22.235)^2}{(f+22.235)^2}$$ Equation 4.53

$$g_{557} = 1 + \frac{(f-557)^2}{(f+557)^2}$$ Equation 4.54

$$g_{752} = 1 + \frac{(f-752)^2}{(f+752)^2}$$ Equation 4.55

where ρ is the water-vapour density (g/m^3). Take the water-vapour density as $7.5 g/m^3$. Again the linear relation between loss and distance can be seen as shown in the next figure.

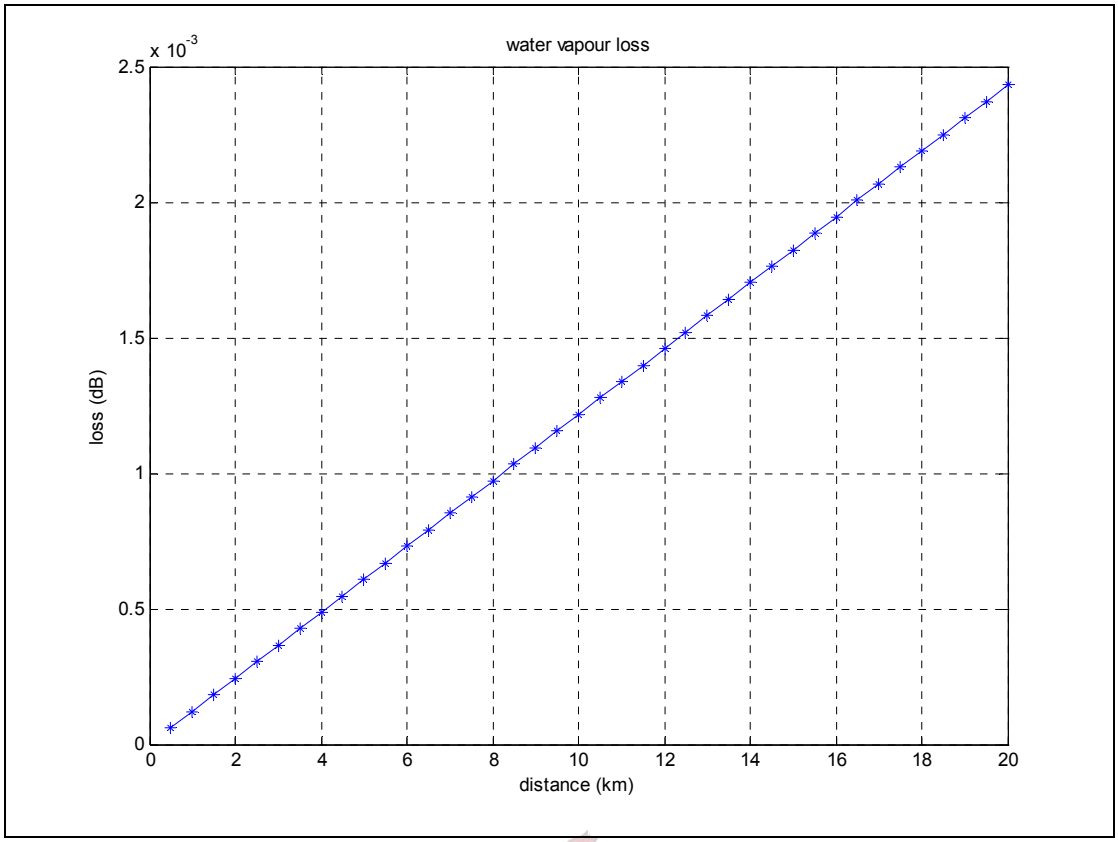

Figure 4.7: Water Vapour Attenuation Loss vs. Distance

Again the air pressure was taken as 1017.8 hPa and the temperature as $25.5\,°C$. From the figure it can be seen that the loss is 0.00012161 dB/km. Again, this loss will not be taken into account when comparing results.

In this section it is shown that water vapour and dry air attenuation does play a role in the propagation loss of a radio link. But for purposes of measurements that will be taken, these effects are small enough to not be taken into account.

4.6. Rain Attenuation

Attenuation of the propagated signal due to rain is another factor that needs to be taken into consideration. From the ITU Recommendations, ITU-R P.838-2, it is found that the specific attenuation γ_R (dB/km) is found using the rain rate R (mm/h):

$$\gamma_R = kR^{\alpha} \qquad \text{Equation 4.56}$$

The frequency dependant variables, k and α, is given in Table 4.3. They are split into vertical and horizontal polarization paths. For this project, both the Cell C base station antenna and the external antenna for the mobile phone are vertically polarized. The values in Table 4.3. have been tested, ITU-R

P838-2, and found to be sufficiently accurate for attenuation prediction up to 55GHz, therefore is adequate to use in this propagation channel.

Frequency (GHz)	k_H	k_V	α_H	α_V
1	0.0000387	0.0000352	0.9122	0.8801
1.5	0.0000868	0.0000784	0.9341	0.8905
2	0.0001543	0.0001388	0.9629	0.9230
2.5	0.0002416	0.0002169	0.9873	0.9594
3	0.0003504	0.0003145	1.0185	0.9927
4	0.0006479	0.0005807	1.1212	1.0749
5	0.001103	0.0009829	1.2338	1.1805
6	0.001813	0.001603	1.3068	1.2662
7	0.002915	0.002560	1.3334	1.3086
8	0.004567	0.003996	1.3275	1.3129
9	0.006916	0.006056	1.3044	1.2937
10	0.01006	0.008853	1.2747	1.2636
12	0.01882	0.01680	1.2168	1.1994
15	0.03689	0.03362	1.1549	1.1275
20	0.07504	0.06898	1.0995	1.0663
25	0.1237	0.1125	1.0604	1.0308
30	0.1864	0.1673	1.0202	0.9974
35	0.2632	0.2341	0.9789	0.9630
40	0.3504	0.3104	0.9394	0.9293
45	0.4426	0.3922	0.9040	0.8981
50	0.5346	0.4755	0.8735	0.8705
60	0.7039	0.6347	0.8266	0.8263
70	0.8440	0.7735	0.7943	0.7948
80	0.9552	0.8888	0.7719	0.7723
90	1.0432	0.9832	0.7557	0.7558
100	1.1142	1.0603	0.7434	0.7434
120	1.2218	1.1766	0.7255	0.7257
150	1.3293	1.2886	0.7080	0.7091
200	1.4126	1.3764	0.6930	0.6948
300	1.3737	1.3665	0.6862	0.6869
400	1.3163	1.3059	0.6840	0.6849

Table 4.3: Frequency dependant Coefficients for Estimating Specific Attenuation

The rain rate that is needed for calculating the attenuation can be found using the rainfall maps, supplied by the ITU, given in ITU-R P.837-4. For purposes of measurements taken during this project, the South African Weather Service (SAWS) was contacted to supply accurate data. But for planning purposes, the rainfall maps supplied by the ITU are satisfactory. When using the rainfall maps, it can be seen that the rain rate (mm/h) exceeded for 0.01% of the average year is given in the next figure. From this figure, it can be seen that for the Stellenbosch region peak rainfall are between 20 mm/h and 15 mm/h.

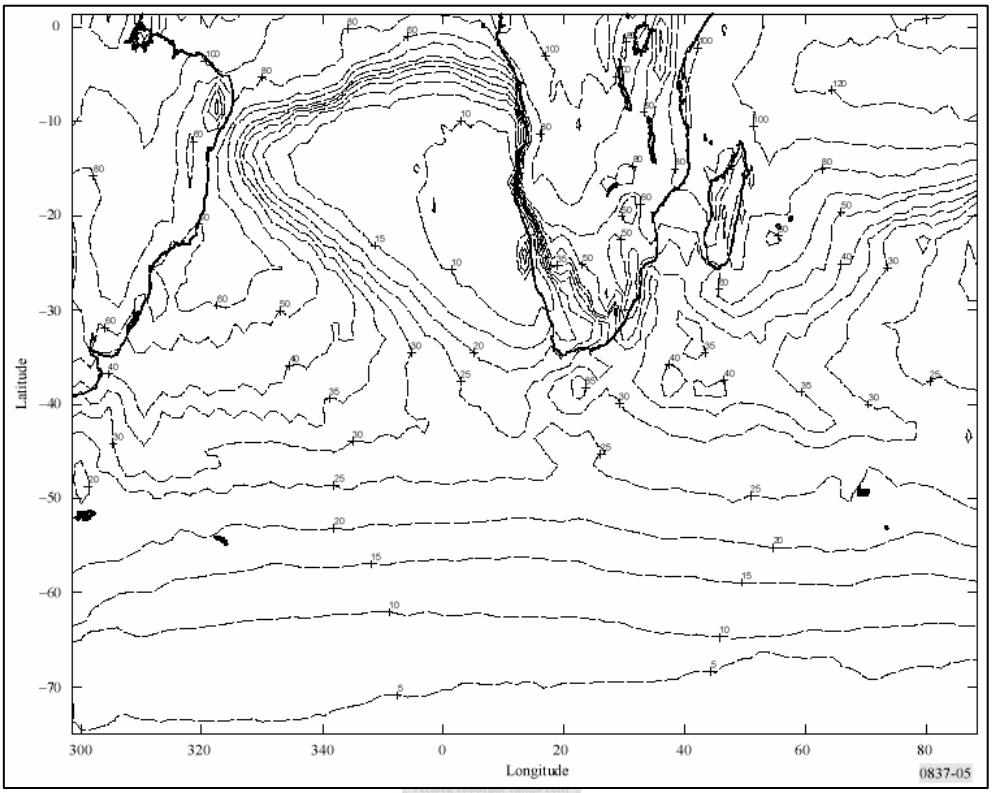

Figure 4.8: Rain rate (mm/h) exceeded for 0.01% of the Average year

For the month, June 2004, the data supplied by SAWS, show that the worst hour during the month was measured as 30 mm.

If all reason is now brought forth, it can be seen that even for the worst hour of the month, the rain rate is measured as 30mm/h. Using this, it is found for a radio path length of 3km, the total loss in signal strength due to rain fall is found to be 0.0096 dB. When using the ITU maps, this is found to be between 0.0051 dB and 0.0066 dB. Either way, it can be seen that this loss is negligibly small and that these variables can be eliminated by taking measurements on a clear day.

4.7. Attenuation due to Vegetation

It is difficult to develop a generalized prediction procedure for attenuation caused by vegetation. The reason for this is the wide range of conditions present and the spectrum of foliage. The lack of experimental data is also present then to model this attenuation; the recommendation of the ITU will be used [31].

For a radio path obstructed by a single vegetative obstruction, where both terminals, transmitter and receiver, are outside the vegetative medium, such as a path passing through the canopy of a single tree, the following can be used:

$$A_{et} = d\gamma \qquad \text{Equation 4.57}$$

Where:

d : length of the path within the tree canopy (m)

γ : specific attenuation for very short vegetative paths (dB/m)

And $A_{et} \leq$ lowest excess attenuation for other paths (dB)

If the specific attenuation is sufficiently high, a path with lower loss will exist around the vegetation. Therefore the restriction of a maximum value for A_{et} is necessary. The specific attenuation due to woodland as supplied by the ITU is given in the next figure.

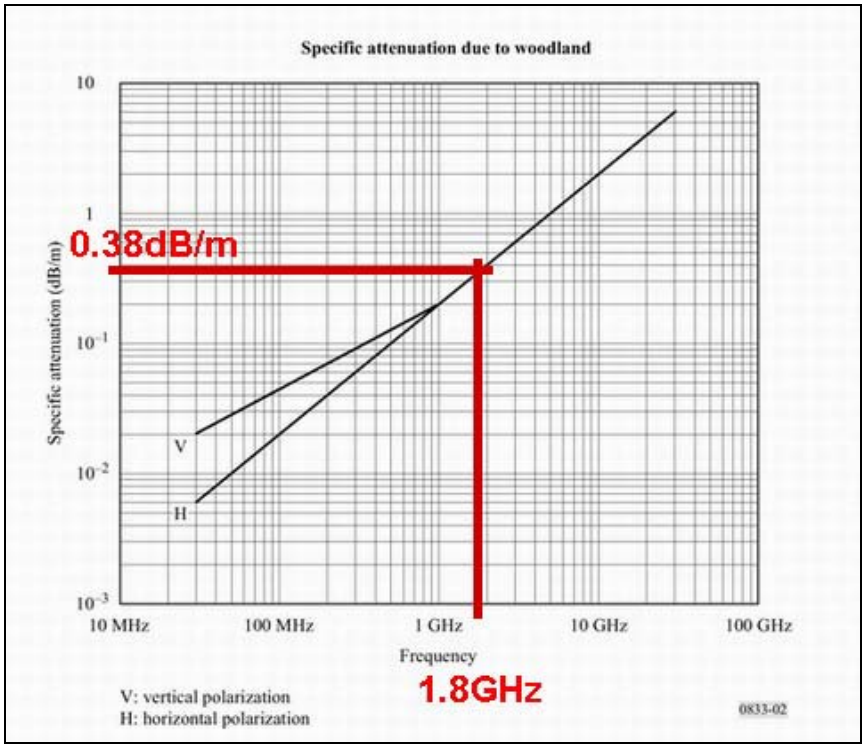

Figure 4.9: Specific Attenuation due to Woodland

This attenuation factor will now be used in the cases where there is a tree canopy obstructing the line-of-sight view between the transmitting base station and mobile receiver.

4.8. K-Factor

The K-factor is another important variable when looking at a fixed wireless access network. The path gain between the transmitter and the receiver in a wireless access network consist mainly of a fixed component and a fluctuating (scatter) component. The ratio of the average energy in the fixed component to that of the average energy is the scatter component is known as the K-factor [32].

When the base station antenna height is relative low, between 10-20m, and the mobile receiver antenna height is also low, between 0-3m, the K-factor is expected to be low. It is also found that as the distance between the transmitter and receiver increase, the K-factor decrease. For fixed wireless links, multipath echoes are possible, and the complex sum of these received waves will vary over space and frequency [33]. The result is that small slow temporal variations in received signal level will be seen, due to the fact of change in relative phase of the arriving echoes. Effects like wind blowing leaves and cars moving in vicinity of the propagation channel have an influence on the K-factor. Seasonal changes (leaves vs. no leaves), antenna heights, distance between transmitter and receiver, and also the antenna beam widths, all have an influence on the K-factor.

The Greenstein-Erceg model is used to model the median K-factor versus distance. This is done using a first order statistical model, meaning it gives the probability distribution of K over time, frequency, and location, given a set path and other system parameters. This is done as follow [34],[33]:

$$K \cong F_s F_h F_b K_0 d^{\gamma} \qquad \text{Equation 4.58}$$

d in km

Where:

F_s is the seasonal factor

$F_s = \begin{cases} 1.0 \\ 2.5 \end{cases}$, 1 in summer (leaves) and 2.5 in winter (no leaves)

F_h is the height factor

$$F_h = (h/3)^{0.46} \qquad \text{Equation 4.59}$$

h in meters

F_b is the beam width factor

$$F_b = (b/17)^{-0.62} \quad \text{Equation 4.60}$$

b in degrees

Using regression fitting, the values for K_0 and γ are determined to be:

$$K_0 \cong 10.0dB$$

$$\gamma \cong -0.5dB$$

Now for the first-order model, the K-factor is calculated to be given as:

$$K = K_1 d^{\gamma} u \quad \text{Equation 4.61}$$

Where K_1 is the 1-km intercept,

$$K_1 = F_s F_h F_b K_0 \quad \text{Equation 4.62}$$

with u the lognormal variate whose dB value is zero-mean with a standard deviation, σ, of 8.0dB.

From the above, it is found that the K-factor increase in the winter (no leaves) and the K-factor decrease as the beam width of the antenna increase. The lower the antenna is to the ground, the lower the K-factor will be. The K-factor is also highly dependable on the wind speed [34].

4.9. Fading

In this section a more detailed look will be taken at some of the statistics behind fading of the signal level, more specifically small-scale fading. As stated in the previous section, multipath propagation is the most important contributor to fading of the signal level. Small-scale fading is fluctuations of received power level due to small sub wavelength changes in the receiver position or movement of objects in the propagation medium [35].

As stated in the previous section, due to the random unpredictable nature, small-scale fading is studied as a stochastic process. Characterising the first-order statistics of these processes using a probability density function (PDF) [36] and the second-order statistics which include measures of a process such as power spectral density (PSD), level-crossing rate and average fade duration [37]. These second-order statistics are heavily dependant and the angles-of-arrival of the received multipath.

Multipath shape factors is a new method that allows the quantitative analysis of any distribution of nonomnidirectional multipath waves in a local area, with the signal strength assumed to be wide-sense stationary [38]. The three principal shape factors are: angular spread, the angular constriction and the azimuthal direction of maximum fading. From this, four of the basic second-order small-scale fading statistics: level-crossing rate, average fade duration, auto covariance, and coherence distance; are then derived using multipath shape factor theory.

Shape factors are derived from the angular distribution of multipath power, $p(\theta)$ and based on the complex Fourier coefficients of $p(\theta)$:

$$F_n = \int_0^{2\pi} p(\theta_x)\exp(jn\theta_x)d\theta_x \qquad \text{Equation 4.63}$$

First the angular spread, Λ, is calculated:

$$\Lambda = \sqrt{1 - \frac{|F_1|^2}{F_0^2}} \qquad \text{Equation 4.64}$$

Angular spread being a measure of how the multipath concentrates about a single azimuthal direction. Angular spread ranges from zero to one, with zero denoting the extreme case of a single multipath component and one denoting no clear bias in the angular distribution of the received power.

Second, the angular constriction, φ, is calculated:

$$\varphi = \frac{\left|F_0 F_2 - F_1^2\right|}{F_0^2 - |F_1|^2} \qquad \text{Equation 4.65}$$

Angular constriction is a measure of how multipath concentrates about two azimuthal directions. Values ranging again from zero to one, with zero denoting no clear bias in two arrival directions and one denoting the extreme case where there is exactly two multipath components arriving from two different directions.

The third shape factor, the azimuthal direction of maximum fading, $\theta_{\max}$, is the last shape factor that need to be calculated.

$$\theta_{\max} = \frac{1}{2}\arg\left\{F_0 F_2 - F_1^2\right\} \qquad \text{Equation 4.66}$$

From these three shape factors the second-order statistics can be determined. A Rayleigh fading signal is used because these types of channels are analytically tractable. The PDF is given by:

$$f_R(r) = r\sqrt{\frac{2}{P_T}}\exp\left(\frac{-r^2}{P_T}\right) \qquad (r \geq 0) \qquad \text{Equation 4.67}$$

Where P_T is the average total power received in a local area.

The level-crossing rate for a Rayleigh-fading signal is then given by:

$$N_R = \frac{\rho\sigma_{\dot{\tilde{V}}}}{\sqrt{\pi P_T}}\exp(-\rho) \qquad \text{Equation 4.68}$$

With ρ being the normalized threshold level such that $\rho = R^2 / P_T$. Also note that $\sigma_{\dot{\tilde{V}}}$ is simply the time-derivative of $\sigma_{\tilde{V}}$, which arises from a mobile receiver travelling through space at a constant velocity in an otherwise static channel[6]. $\sigma_{\tilde{V}}$ being the rate variance for the complex voltage of a receiver travelling along the azimuthal direction [38]. This gives rise to the fact that for purposes of this project, $N_R \approx 0$, because the mobile receiver is stationary at all times. But it can be assumed that this will not be the case for practical measurements, because movement will still be present in the propagation channel, such as cars and other scattering objects.

The next parameter that needs to be looked at, is the spatial autocovariance of the received voltage envelope. The autocovariance function determines the correlation of the received voltage envelope as a function of change in receiver position [39]. The approximation is:

$$\rho(r,\theta) \approx \exp\left[-23\Lambda^2\left(1+\varphi\cos[2(\theta-\theta_{\max})]\right)\left(\frac{r}{\lambda}\right)^2\right] \qquad \text{Equation 4.69}$$

Again, it can be assumed that this variable is insignificant, because the mobile receiver for the project is stationary during measurements.

The next variable, is the coherence distance, D_c. Coherence distance, is the separation distance in space over which a fading channel appears to be unchanged. This is important to know when spatial diversity is implemented at the receiver end. When using the generalised autocovariance function as given above, the coherence distance is given by:

$$D_c \approx \frac{\lambda\sqrt{\ln 2}}{\Lambda\sqrt{23\left(1+\varphi\cos[2(\theta-\theta_{\max})]\right)}} \qquad \text{Equation 4.70}$$

[6] Transmitter and Scatterers are Fixed

For an omnidirectional Rayleigh channel, the approximation for the coherence distance is given by:

$$D_c \approx \frac{9\lambda}{16\pi} \qquad \text{Equation 4.71}$$

From the above, it can be seen that in general, small-scale fading is expected to be negligible for measurements taken. The only factors that might contribute to some fading, will be the movement from other objects in the propagation medium.

4.10. Conclusions

It can be seen that some of the factors discussed, can be ignored for the 1800MHz frequency band. All the factors considered in Chapter 4 are summarised in Table 4.4.

	Influence	Attenuation Expected (dB)
Free Space Propagation Loss	Large	Site Specific
Multipath Propagation	Large	±10dB
Diffraction	Medium	Site Specific
Gaseous Losses	Negligible	Ignore
Rain Attenuation	Negligible	Ignore
Vegetative Attenuation	Medium	0.38dB/m
K-Factor	Small	±1dB
Fading	Small	Ignore

Table 4.4: Summary of Factors Influencing Propagated Signal Level

From Table 4.4. it is clear that the most dominant factors in the link budget, are free space propagation loss and multipath propagation loss/gain. Multipath propagation loss/gain is difficult to predict and model, therefore it is simulated using FEKO software. Free space propagation loss is easy to calculate and is different for each link.

Diffraction is site specific and terrain between the transmitter and receiver need to be considered for each specific link. Gaseous losses and rain attenuation can be ignored when the link budget is done. The measurements are taken on clear sunny days and there for these influences can be ignored.

Attenuation to the propagated signal level due to vegetation is taken into account. The amount of attenuation is a function of the path length travelled trough vegetation. The K-factor has an influence of ±1dB on the received signal level for these measurements. The K-factor is not directly taken into consideration when the link budgets are done, but it is taken note of.

Small scale fading can be seen in the measured signal level but it is not taken into account when the predictions are made. The reason being, it is very small for the measurements that were taken. The fading component is small because the mobile receiver is stationary at all times, while the signal level is being logged.

CASE STUDY

In this chapter, one of the line-of-sight measurements will be looked at in depth. Each calculation that was done will be explained and shown in detail. These calculations stay the same for all the measurements and predictions that is shown in Chapter 6.

The measurement that will be looked at in detail in this chapter is made between one of the Cell C base stations and the mobile phone. This measurement is chosen to be clear line-of-sight and the terrain between the transmitter and the receiver, as uniform as possible. The path between the transmitter and the receiver can be seen in the next picture.

Figure 5.1: View from Mobile phone to Base Station

First, the distance between the mobile phone and the base station need to be determined. The global positioning system (GPS) coordinates of the base station is known, supplied by Cell C. The coordinates of the mobile phone are obtained, using a GPS that is serially connected to a laptop. As said earlier, this is in effect an averaging process, because the position of the mobile phone stays the same, but the satellites move relative to the position of the mobile phone, therefore, each time the satellites move, the position of the mobile receiver is recalculated. Each time this calculated position changes, the graphical user interface

log the coordinates. Afterwards the average position is calculated, accurate to about five metres, which is sufficient for this project.

Using these GPS coordinates, the distance between the mobile phone and the base station can be determined. This is done by using an excel spreadsheet setup especially for these calculations. The calculations done in the spreadsheet will now be explained.

For purpose of the calculations, we will go back to the middle ages and assume that the earth is flat. On a flat earth, a line of longitude is parallel to the next line of longitude and lines of longitude are perpendicular to lines of latitude. As we know, this is not the case, but calculations have shown that for distances less then 1.6km, the error is less than 0.5m at 45° latitude. These errors get smaller as you go closer to the equator and bigger as you move towards the poles. Note that the measurements taken for this project were all at 33° latitude. Therefore we can assume that the distances calculated are accurate enough.

The constants used in these calculations are:

6378137m – equatorial earth radius
6356752m – polar earth radius

First, the GPS coordinates measured in DMS (Degrees, Minutes, and Seconds) need to be converted to decimal degrees. This is done as follow:

Point in DD°mm'ss.ss $= DD + (mm/60) + (ss.ss/(60*60))$ decimal degrees

The distance between two points is determined by converting the latitude/longitude values to values on an X/Y plane. Point 1 will be at the origin and Point 2 somewhere on the X/Y plane. The distance between the two points can then be calculated as follows:

$$\textbf{Distance} = \sqrt{(\Delta x)^2 + (\Delta y)^2} \quad \textbf{(m)} \qquad \text{Equation 5.4}$$

The excel table shown below, is for the specific situation under consideration:

	Latitude	Longitude
Point #1	-33.9275556	18.86563889
Point #2	-33.9155611	18.86971944
Determine true angle	-33.749552	
Determine true angle	-33.7375881	
Radius pt 1	6371513.582	
Radius pt 2	6371517.715	
X-Y earth coordinates	5297747.608	-3539781.858
X-Y earth coordinates	5298490.067	-3538677.86
X coordinates	1330.435409	
Y coordinates	-377.327413	6378137
		6356752.314
Distance in meter	1382.907934	

Table 5.1: Distance Calculation

From this, it can be seen that the distance has been calculated as 1.3829km. Therefore the free space propagation loss can now be calculated as:

$$\begin{aligned} L_{BF} &= 32.44 + 20\log_{10}(f) + 20\log_{10}(d) \\ &= 32.44 + 20\log_{10}(1862.5) + 20\log_{10}(1.3829) \\ &= 100.6259dB \end{aligned}$$ Equation 5.5

It is clear that there is a difference in distance between the direct line-of-sight and the actual distance along the ground, between the base station and the mobile phone. This can be ignored because the amount of free space propagation loss varies only by one-hundreds of decibels.

The next aspect to take into consideration, is the radiation pattern of the mobile base station. The radiation pattern was supplied by Cell C and gives the following information as shown in the figure below:

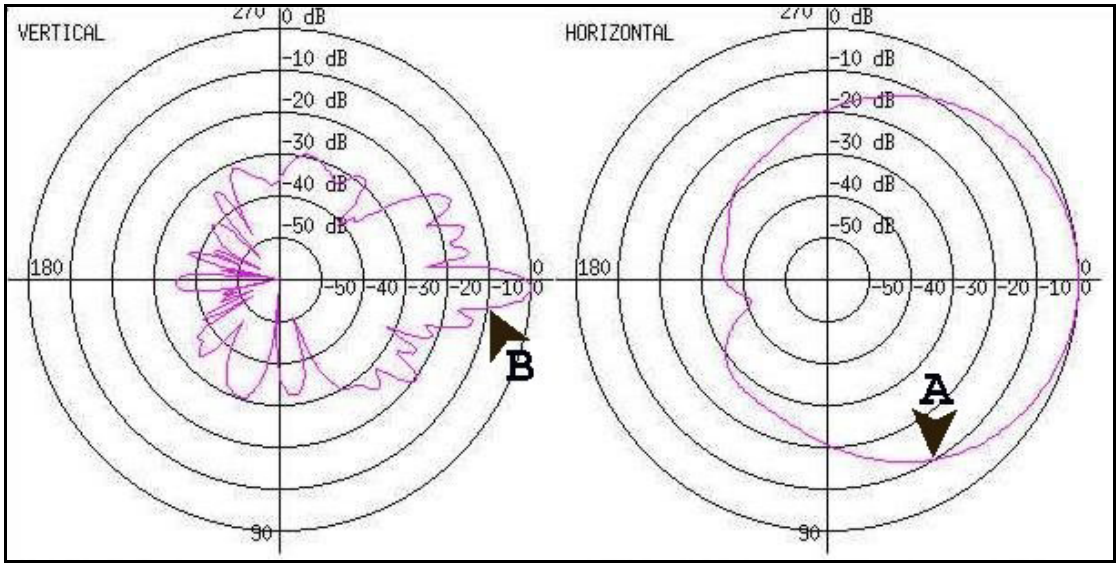

Figure 5.2: Radiation Pattern for Base Station Antenna

What is important here is the horizontal and vertical position that the mobile phone is in relation to the mobile base station. If the horizontal angle is 60°, the resulting loss due to this will be -10dBm (marked A). The same goes for the vertical angle. If the angle is 10°, the resulting loss will be 10dBm (marked B).

Using HerTZ Mapper, the base station antenna position and antenna height are entered. The position of the mobile phone as measured by the GPS and the antenna height is also entered. The HerTZ Mapper also make use of a digital terrain model (DTM) supplied by Telkom SA. Using this data, the elevation between the mobile phone and the base station is determined, as well as the position of the mobile phone relative to the base station. This can be seen in the next figure.

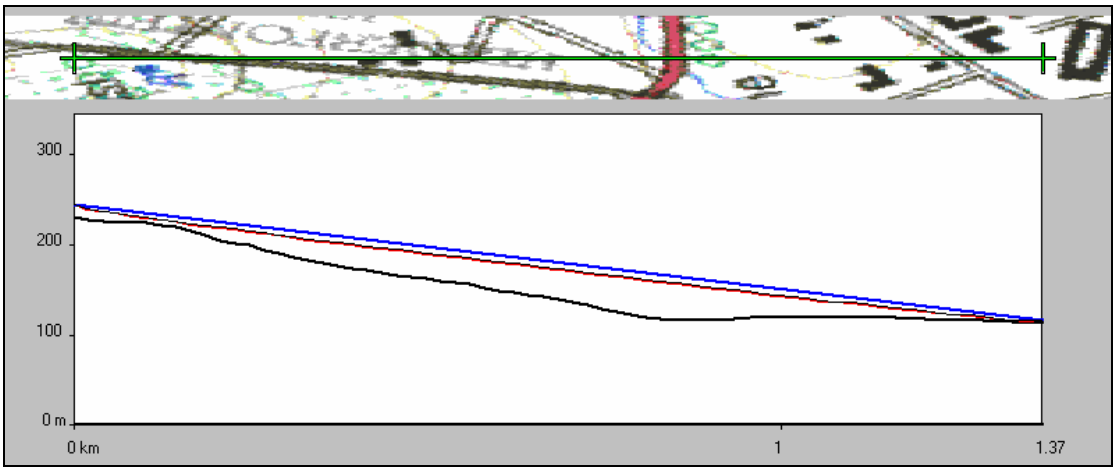

Figure 5.3: Path Elevation between Base Station and Mobile Phone

This information is then used in a MATLAB program, which is written to calculate the loss in propagated signal, due to the position of the mobile phone relative to the base station. The MATLAB code for the program can be seen in Appendix A1. Using this program, the losses are calculated to be:

Vertical Angle Loss = 2.7 dB

Horizontal Angle Loss = 0.6 dB

The next step is to calculate the loss or gain in received signal power due to multipath propagation. This is probably the most important part of the link budget that need to be done, but it is also the most difficult to determine. For this reason, FEKO software is used to simulate the amount of multipath loss/gain in a four square meter area in the vicinity of the mobile phone receiver. The FEKO code used for this simulation can be seen in Appendix B. The simulation shows the following.

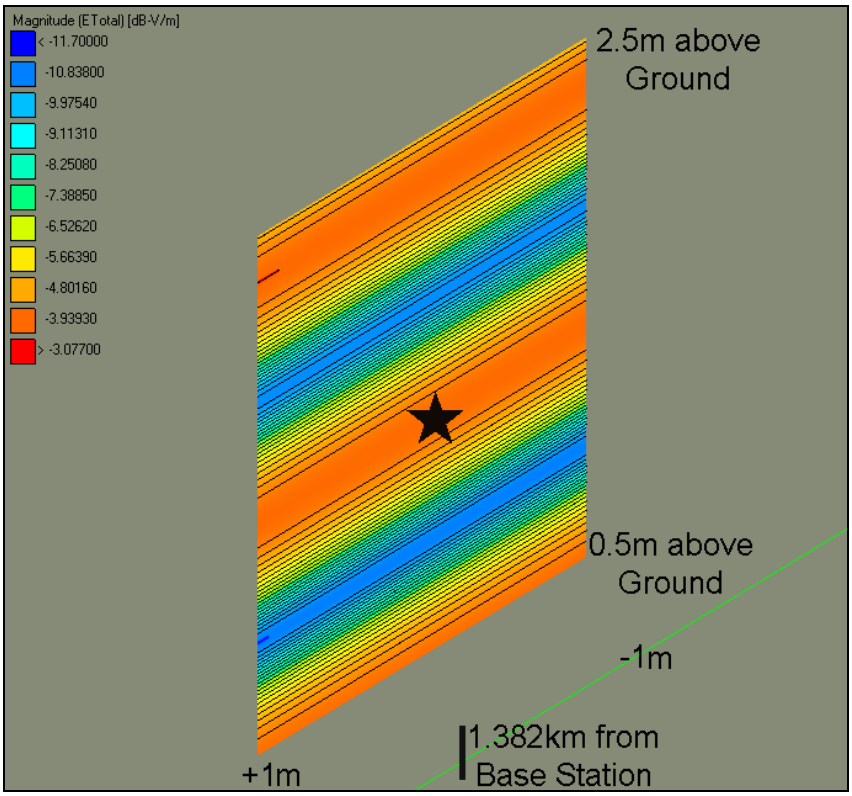

Figure 5.4: Multipath loss/gain at the Mobile Receiver

The position of the mobile phone antenna in this simulation is shown by the star. From the simulation it can be seen that the loss, in this case, due to multipath propagation, is found to be:

Multipath Loss = $3dB$

It is also found that the elevation of the receiver relative to ground in relation to the elevation of the base station antenna, plays a huge role in the amount of multipath propagation that can be expected at the mobile phone. This is illustrated in the next figure.

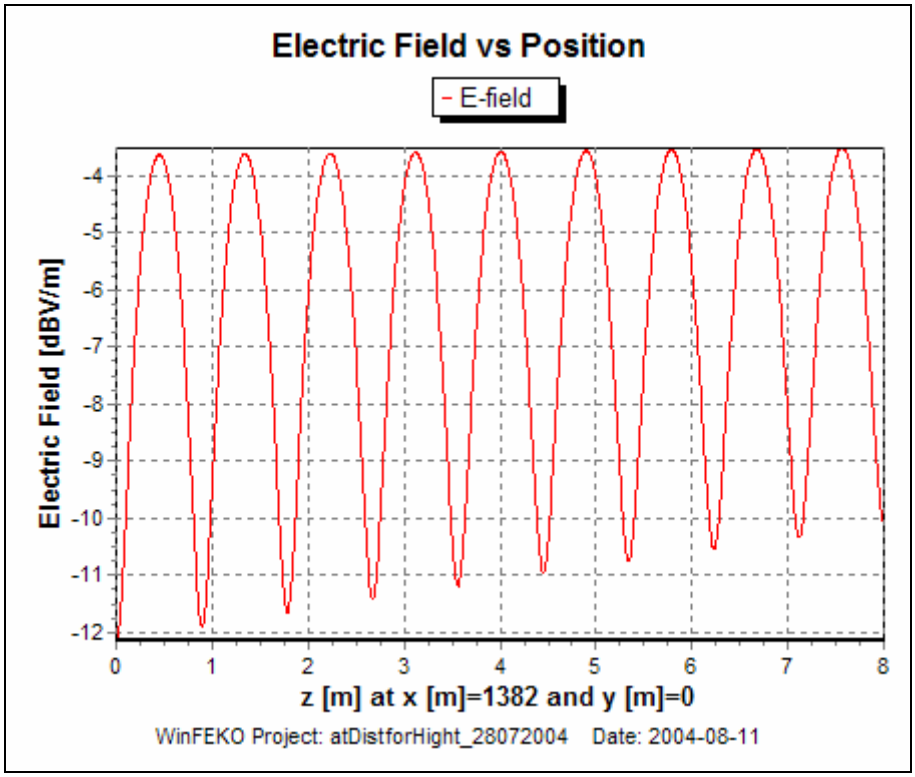

Figure 5.5: Multipath Error vs. Height above Ground Level

From the above figure it can be seen that the multipath component can vary from $-3dB$ to $-12dB$ over a change of 1m in height above ground. This will vary from measurement to measurement and will be taken into account. It is expected that the position from were this measurement was taken; the ground has not changed much, relative to what is used in the DTM. But at some of the other measurements, roads were built and this can have an influence on the real-time position of the mobile phone, relative to that what the DTM propose. The accuracy of the DTM is very important as large errors in multipath modelling can occur, especially when the ground elevation is significant. On flat surfaces, the error will not be significant.

The link budget for this specific case can now be done. All is shown in the next table.

	dB
Power Transmit	53.5
Free Space Propagation Loss	-100.614
Vertical Angle Loss	-2.7
Horizontal Angle Loss	-0.6
Multipath Loss/Gain	-3
Cable Loss	-1.63

Table 5.2: Link Budget

From the above table, it can be seen that the predicted received signal level is:

$$dBm_{prediction} = dB_{send} - dB_{FreeSpaceLoss} - dB_{RadPattern} - dB_{mobAnt} - dB_{Multipath}$$
$$= 53.5 - 100.614 - 2.7 - 0.6 - 3 - 1.63$$
$$= -55.04dBm$$

The signal logged using the data capturing system is shown in the next figure. In the figure, both the predicted signal level as well as the measured signal level is shown.

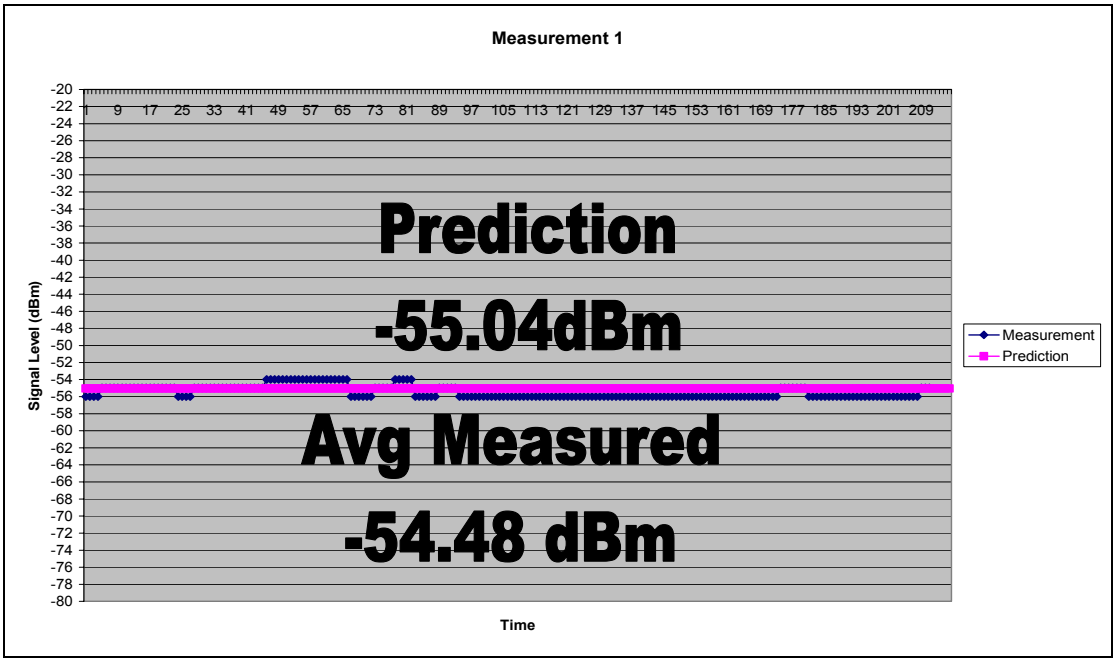

Figure 5.6: Prediction vs. Measurement

From the above figure it can be seen that the predicted signal level compares well with the measured signal level. Small scale fading can be seen, but this is minimal because the path between the mobile phone and the base station is clear and wide open. The average fading rate is small because multipath power becomes more concentrated about a single azimuthal direction, when an omni directional antenna is used.

An overview of this measurement will now be given. First the data logged from the Nokia 6310i phone and GPS were imported to Excel. From here the average measured signal level was determined and the distance between the transmitter and the mobile receiver was calculated.

The next step was to calculate the free space propagation loss, using Equation 5.2. Next the radiation pattern of the Cell C base station antenna was taken into account, calculating the loss at the mobile receiver due to its position relative to the base station transmitter.

Multipath propagation was the next factor taken into account and the result of the FEKO simulation was used in the link budget. For this link there were no line-of-sight obstructions. The link budget was done and the result was satisfactory.

OTHER MEASUREMENTS AND COMPARISONS

To proof the success of the measuring device more measurements are taken and presented in this chapter. A three dimensional (3D) digital terrain model (DTM) of the Stellenbosch area is shown in the next figure. On this, the positions at which these measurements are taken can be seen.

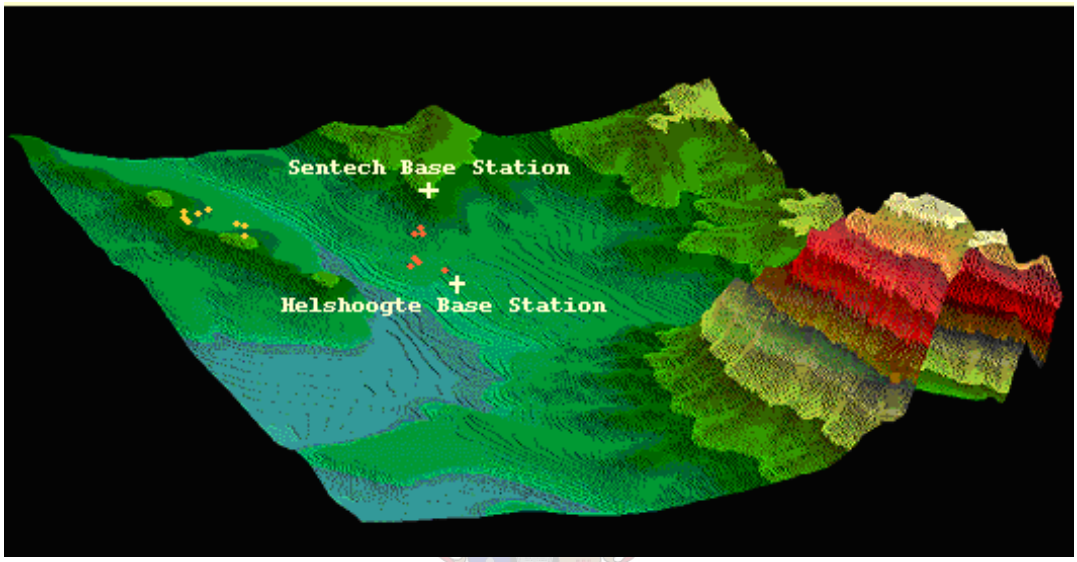

Figure 6.1: 3D DTM for Stellenbosch with Base Stations and Receiver Positions

It can be seen that two base stations are used, the first situated on the roof of Helshoogte residence and the second on Sentech hill just outside Stellenbosch. From Helshoogte, cell ID's 14408 and 34408 are used and from Sentech, cell ID's 27761 and 37761 are used.

The measurements taken can be split into mainly two groups. The first groups of measurements are taken in a residential area of University of Stellenbosch Campus. The second groups of measurements are taken in a rural area of Stellenbosch, Kayamandi. The first group that will be looked at is the measurements taken in residential area of Stellenbosch.

6.1. Measurements (Group 1)

In the next figure, the layout and positions of these measurements can be seen. These measurements are similar to the one in Chapter 5. These are done to illustrate the how well the data capturing device work and also the influence of different elements in the propagation medium on the received signal level.

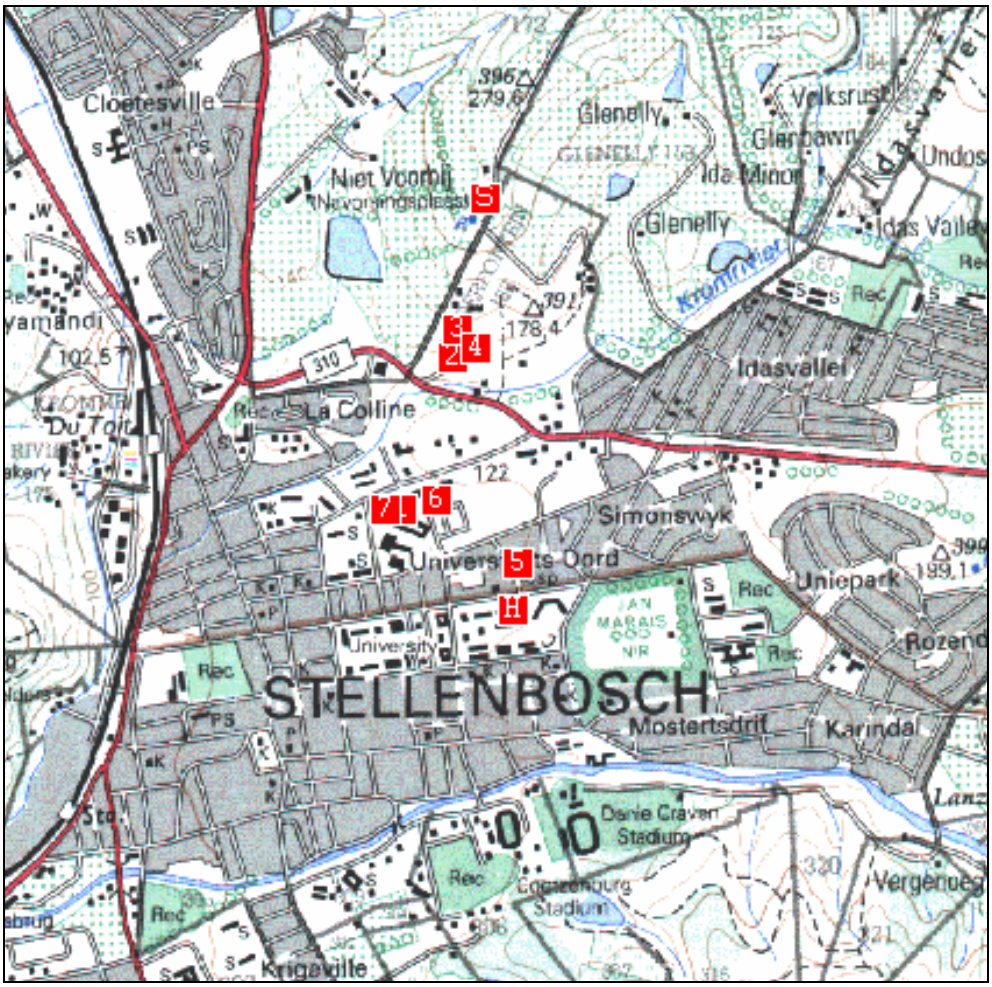

Figure 6.2: Setup for Measurements – Group 1

Helshoogte base station is marked (H) and Sentech Base Station is marked (S) as shown in the above figure. The distance, over which these measurements are taken, vary from 200m up to 2km. Most of which is clear line-of-sight, but some show the influence of vegetation and other obstacles.

6.1.1. Measurement 1.1:

This measurement is taken with clear line-of-sight. The propagation channel can be seen in the next figure. This measurement is the case study covered in Chapter 5, but is repeated here for comprehensiveness.

Figure 6.3: Measurement 1.1 – Clear line-of-sight

The distance between the base station and the mobile phone is calculated to be $1.38km$. Using this, now known variable, the free space propagation loss can be calculated.

$$L_{FSP} = 32.4 + 20\log_{10}(d_{km}) + 20\log_{10}(f_{MHz}) \qquad \text{Equation 6.1}$$

$$L_{FSP} = 100.614dB$$

The next step is to take into account the elevation difference between the mobile phone and the base station. The next figure shows the position of the mobile phone relative to that of the base station.

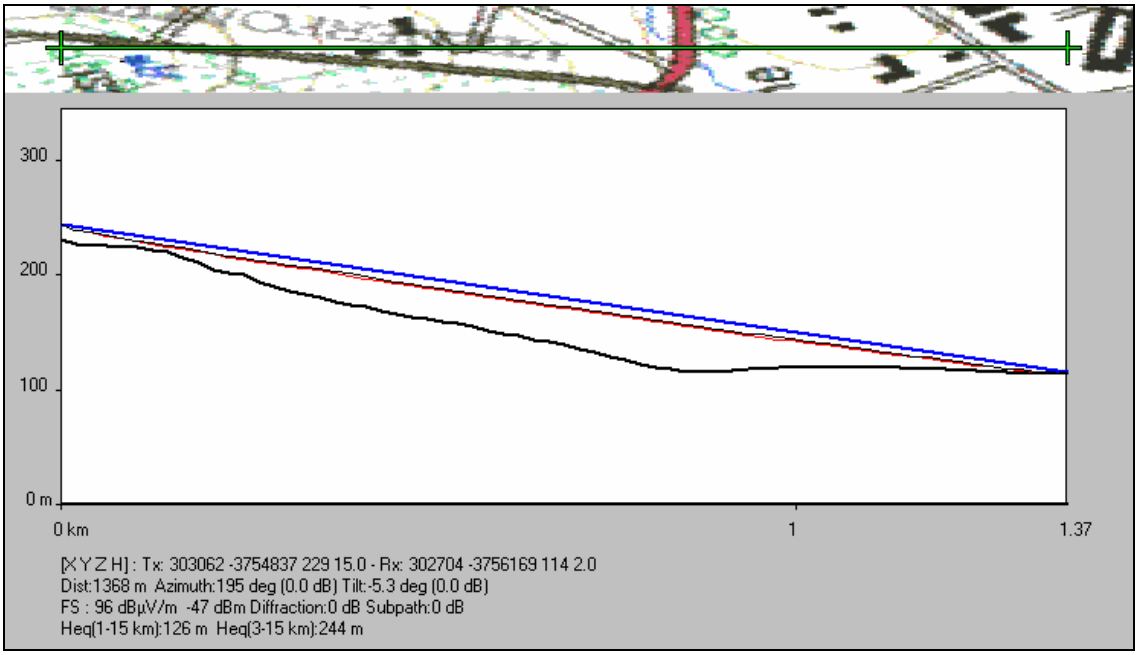

Figure 6.4: Path Elevation between Base Station and Mobile Phone

From Figure 6.4 it can be seen that the azimuth difference is $15°$ and the tilt is $5.3°$. From this, the loss due to the position of the mobile phone relative to the base station, is determined to be:

$$\text{Vertical Angle Loss} = 2.7dB$$

$$\text{Horizontal Angle Loss} = 0.6dB$$

The next step will be to simulate the influence of multipath propagation on this specific measurement. This is done using FEKO software and the result can be seen in the next figure.

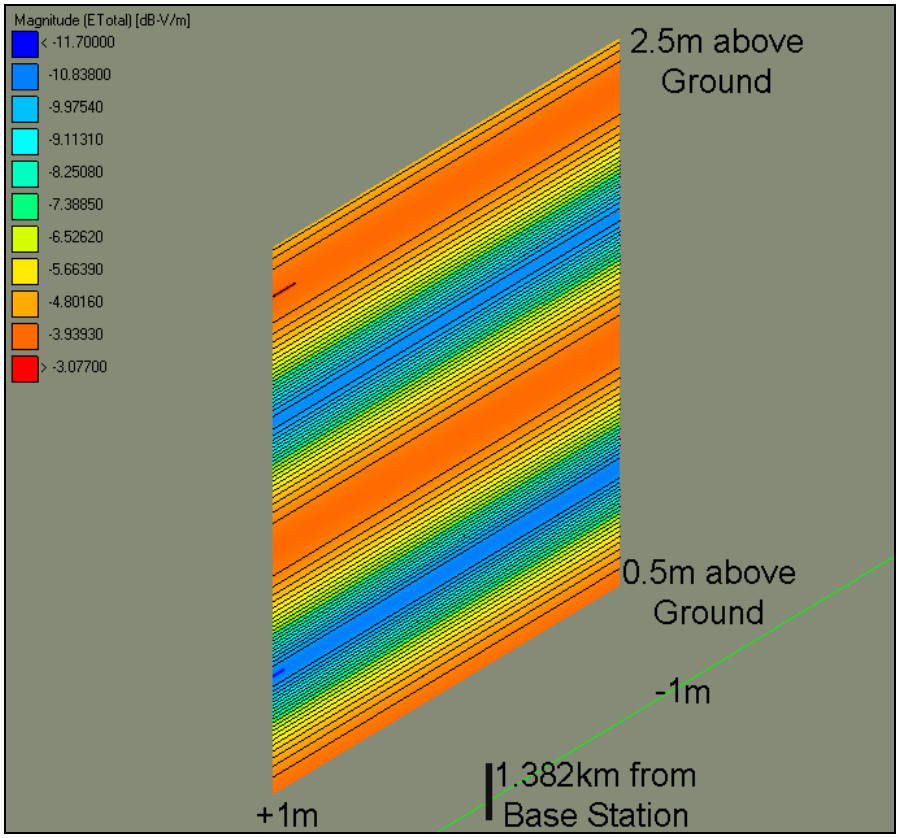

Figure 6.5: Multipath loss/gain at the Mobile Receiver

From Figure 6.5 it can be seen that the loss, in this case, due to multipath propagation through the propagation medium, at the mobile receiver is:

$$\text{Multipath Loss: } 3dB$$

From the known data, a link budget can be done and this is shown in the next table.

	dB
Power Transmit	53.5
Free Space Propagation Loss	-100.614
Vertical Angle Loss	-2.7
Horizontal Angle Loss	-0.6
Multipath Loss/Gain	-3
Cable Loss	-1.63

Table 6.1: Link Budget for Measurement 1.1.

For this specific measurement, the predicted signal level is calculated to be:

$$\begin{aligned} dBm_{prediction} &= dB_{send} - dB_{FreeSpaceLoss} - dB_{RadPattern} - dB_{mobAnt} - dB_{Multipath} \\ &= 53.5 - 100.614 - 2.7 - 0.6 - 3 - 1.63 \\ &= -55.04dBm \end{aligned}$$

In the next figure, the measured signal level is plotted with the predicted signal level and it can be seen that the two compares well.

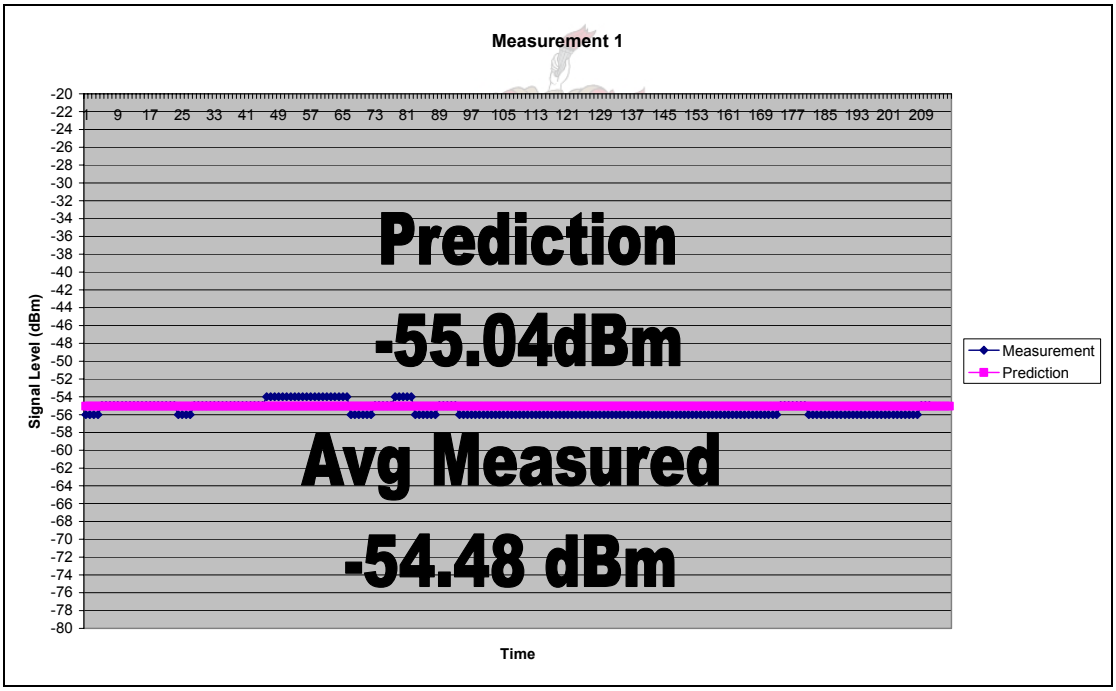

Figure 6.6: Prediction vs. Measurement

From Figure 6.6 it can be seen that the predicted signal level compares excellent to the measured signal level. Small-scale fading can be seen, but this is expected due to movement within the propagation medium.

6.1.2. Measurement 1.2:

This measurement is also taken with relative clear line-of-sight. This can be seen in the next figure.

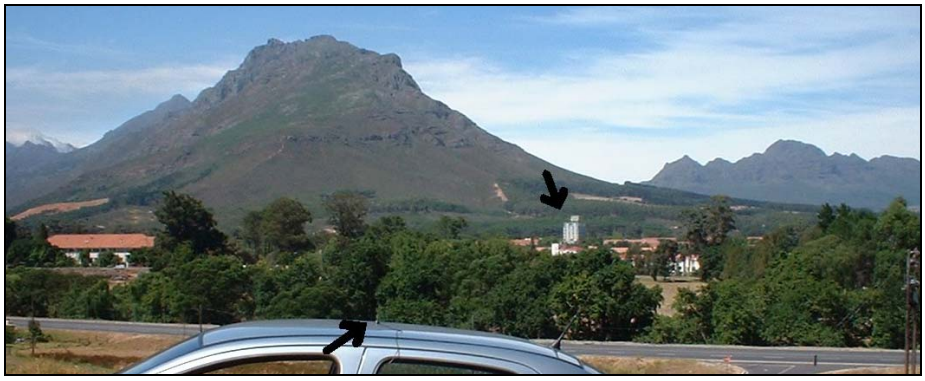

Figure 6.7: Propagation Channel for Measurement 1.2.

The distance between the mobile phone and the base station is calculated to be $1.112km$. From this, the free space propagation loss is calculated:

$$L_{FSP} = 32.4 + 20\log_{10}(d_{km}) + 20\log_{10}(f_{MHz})$$
$$L_{FSP} = 98.725dB$$

Next, the elevation between the mobile phone and the base station need to be taken into account, as well as the position of the mobile phone relative to the base station. This can be seen in the next figure.

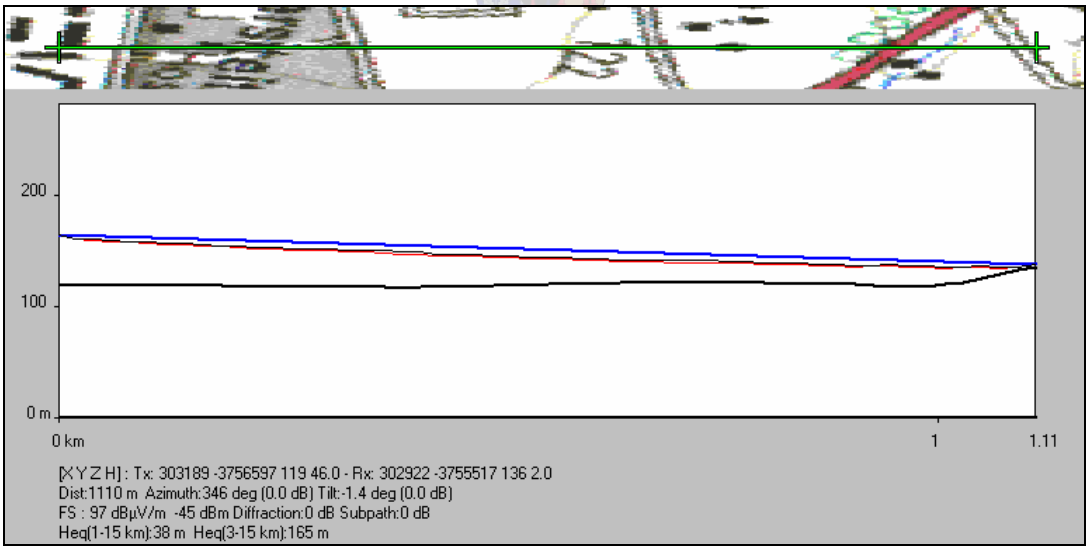

Figure 6.8: Path Elevation between Base Station and Mobile Phone

From Figure 6.8 it can be seen that the azimuth difference is $24°$ and the tilt is $1.4°$. From this, the vertical angle loss and horizontal angle loss are calculated to be $1.2dB$ and $1.7dB$ respectively. The next step is to simulate the multipath propagation component. This is done using FEKO software. The result can be seen in the next figure.

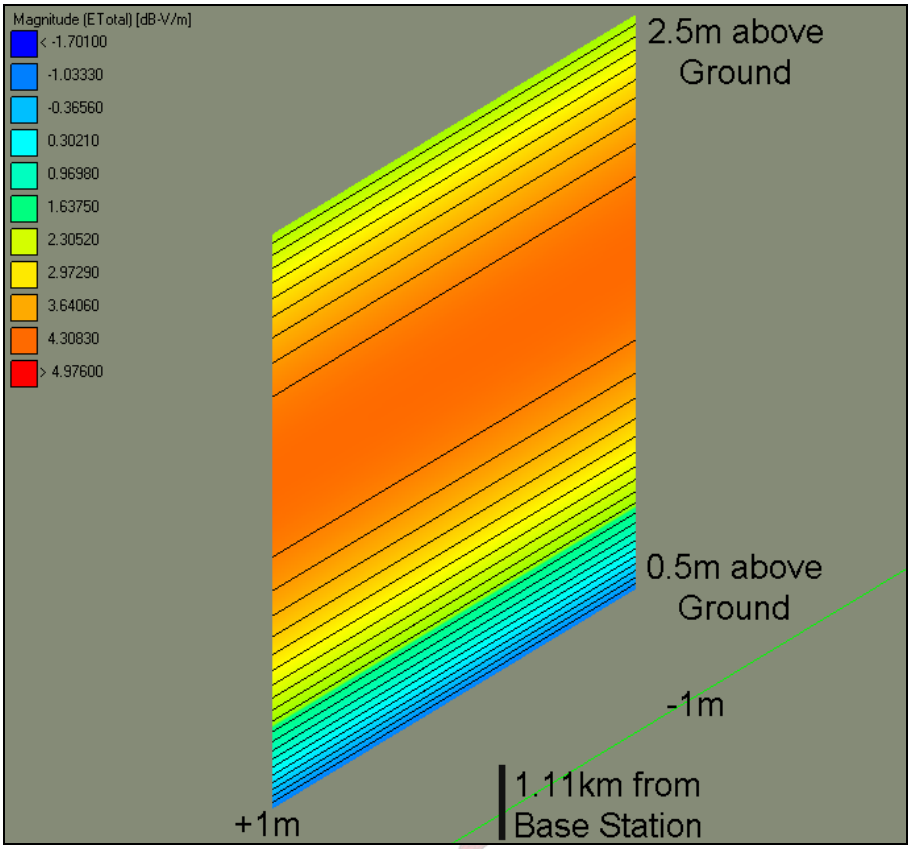

Figure 6.9: Multipath loss/gain at the Mobile Receiver

The position where this measurement is taken, is on an access road. It can be seen that the ground under foot needed to be moved and changed to accommodate the road built. Therefore it is safe to assume the height above ground and elevation of the mobile phone relative to the base station may not be as accurate as needed. Therefore a simulation is done to see how the signal level will change as a function of height above ground level, in affect taking into account the DTM errors and elevation errors there may be. The simulation can be seen in the next figure.

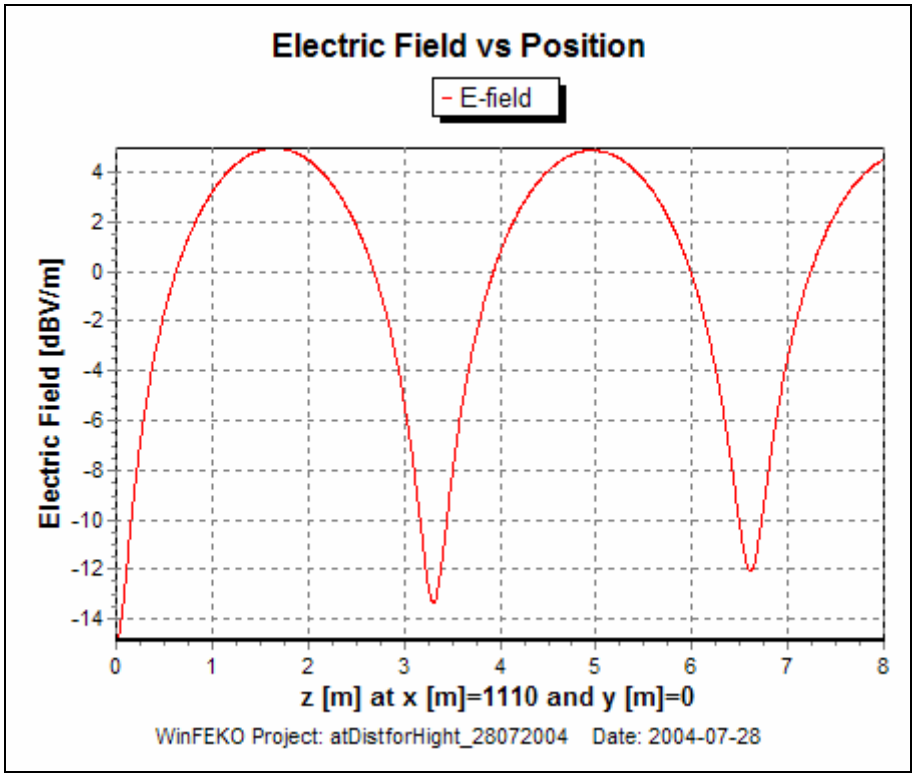

Figure 6.10: Multipath error as a function of Height above Ground Level

From Figure 6.10 it can be seen that for a height error of 1m, the multipath propagation loss is to be $5dB$. From this known data, the link budget can be done and is shown in the next table.

	dB
Power Transmit	54.86
Free Space Propagation Loss	-98.7255
Vertical Angle Loss	-1.2
Horizontal Angle Loss	-1.7
Multipath Loss/Gain	-5
Cable Loss	-1.63

Table 6.2: Link Budget for Measurement 1.2.

The predicted signal level is therefore given as:

$$\begin{aligned} dBm_{prediction} &= dB_{send} - dB_{FreeSpaceLoss} - dB_{RadPattern} - dB_{mobAnt} - dB_{Multipath} \\ &= 54.86 - 98.7255 - 1.2 - 1.7 - 5 - 1.63 \\ &= -53.4dBm \end{aligned}$$

The measured signal level and predicted signal level can be seen in the next figure.

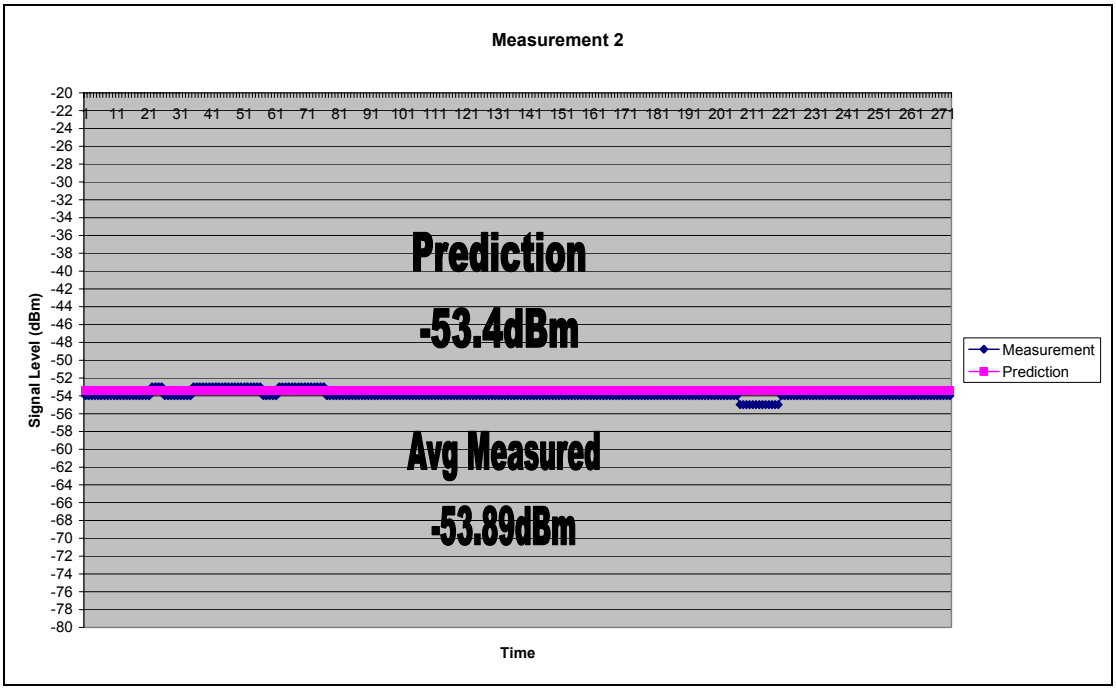

Figure 6.11: Prediction vs. Measurement

From Figure 6.11 it can be seen that the predicted signal level compares well with the measured signal level. In later measurements, the affect of the ground level and error in elevation will again be seen and noted. This error has a significant influence when measurements are taken with the receiver positioned in an area where the terrain is steep.

6.1.3. Measurement 1.3:

For this measurement, it can be seen that the logged signal alternates between two different cell ID's. These two cells can be seen in the next two figures.

Figure 6.12: Line-of-sight for cell ID 34408 (Helshoogte)

From Figure 6.12 it can be seen that there is a clear line-of sight for this part of the signal that is logged. But in Figure 6.13 it can be seen that there is no line-of-sight because it is obstructed by vegetation.

Figure 6.13: No Line-of-sight for cell ID 27761 (Sentec)

The distance between the two base stations are calculated and are found to be:

$$d_{(27761)} = 0.571km$$

$$d_{(34408)} = 1.228km$$

From this, the free space propagation loss for these two cell ID's are found to be:

$$L_{FSP(27761)} = 92.94dB$$

$$L_{FSP(34408)} = 99.58dB$$

The next step is to take into account the elevation of the mobile phone relative to the two base stations. This can be seen in the next two figures.

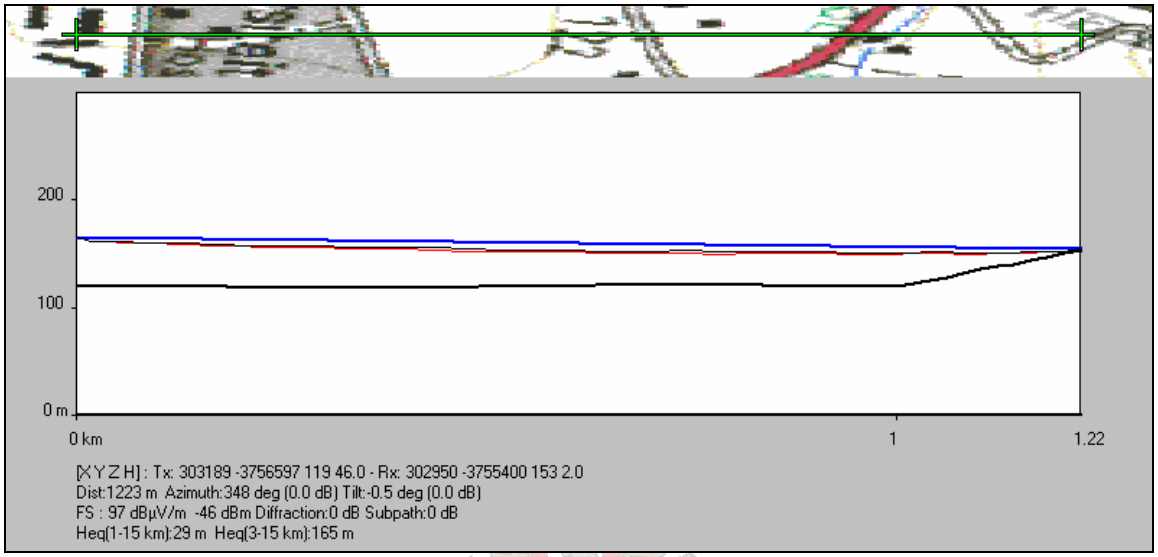

Figure 6.14: Path Elevation for Cell ID 34408

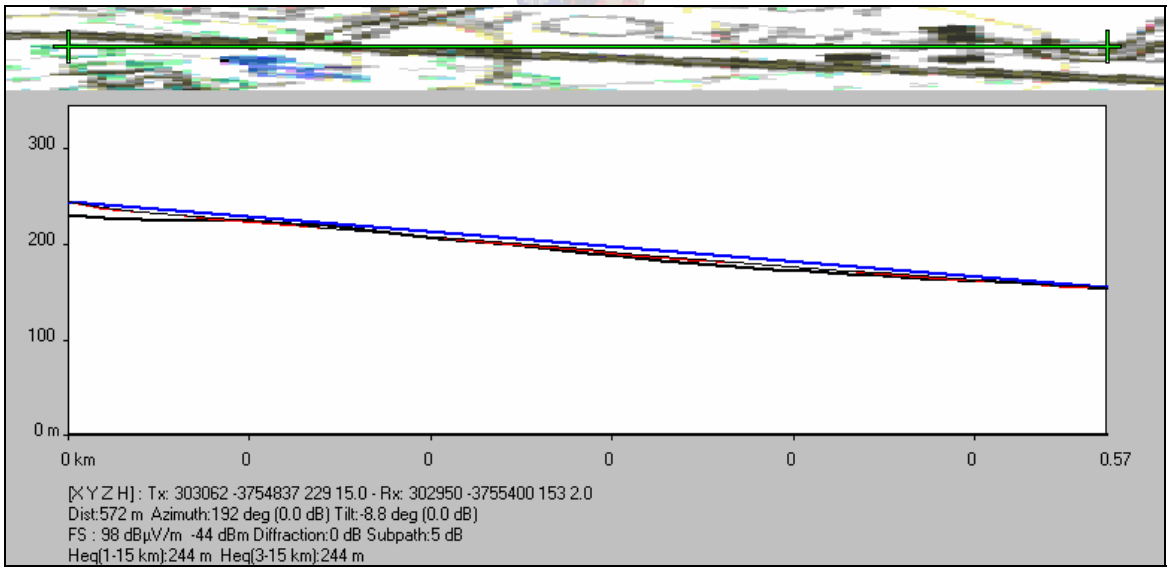

Figure 6.15: Path Elevation for Cell ID 27761

From Figure 6.14 and Figure 6.15 the relative vertical angle loss as well as the horizontal angle loss for these two cell ID's can be determined. The angle loss, is then given as the total angle loss, sum of vertical angle loss and horizontal angle loss, for this specific case.

$$\text{Angle Loss}_{(27761)} = 11.5dB$$

$$\text{Angle Loss}_{(34408)} = 23.2dB$$

Next, the influence of multipath propagation needs to be taken into account. The simulation of this effect, can be seen in the next two figures.

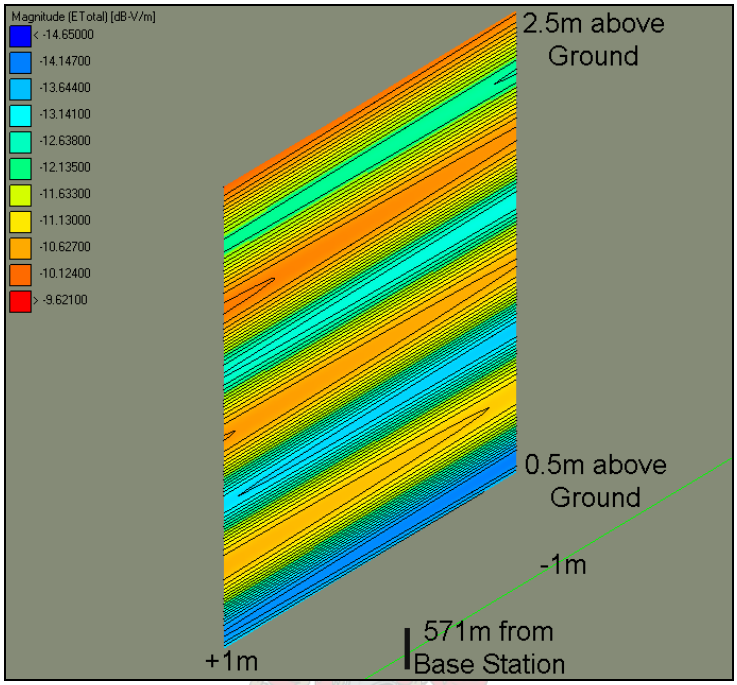

Figure 6.16: Multipath Effect for ID 27761

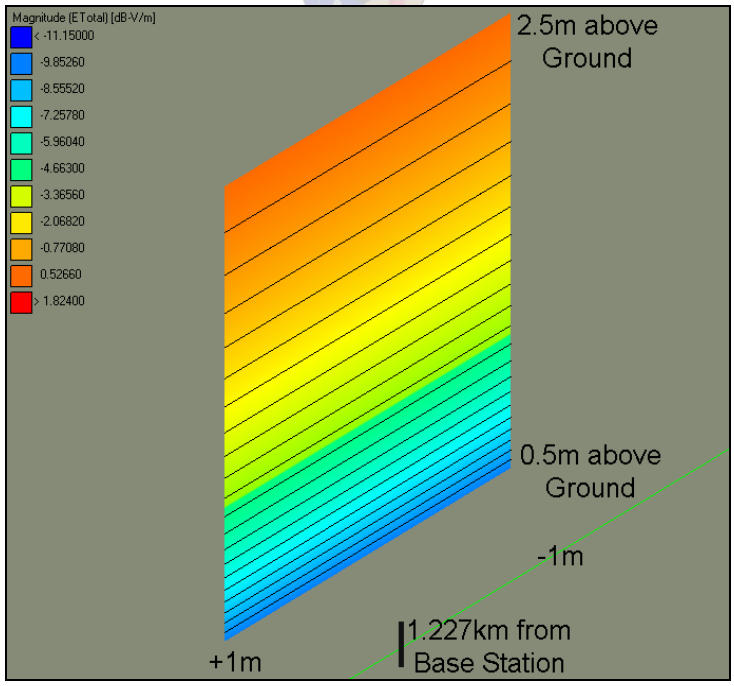

Figure 6.17: Multipath Effect for ID 34408

From this, it can be seen that the multipath effect for cell ID 27761 is $-15.5dB$ and for the 34408 ID the effect is $-2dB$. Again, at an assumed receiver antenna height of 1.5m, the multipath loss in this case is not

correct. But when the error is taken into account for this specific position, it correlates and shows that for both measurements taken, the receiver antenna height is at round about 1.9m. This relation between the two can be seen in the next two figures.

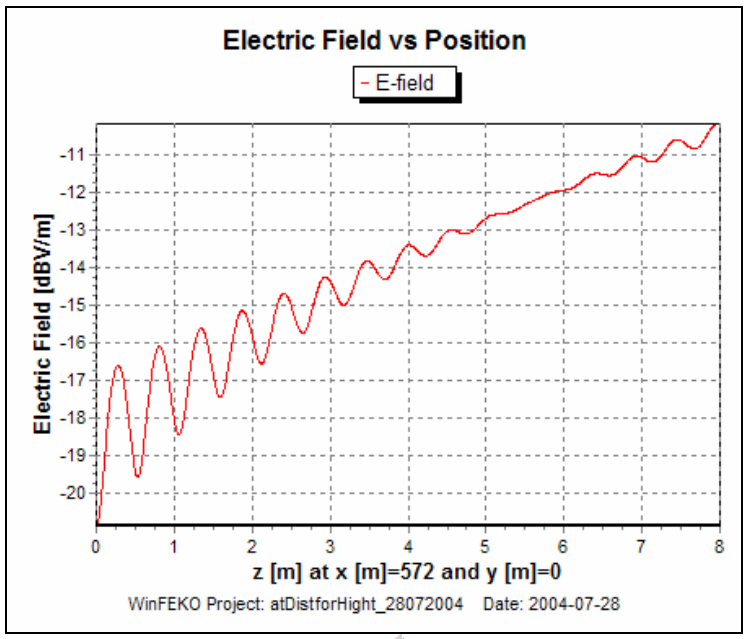

Figure 6.18: Multipath Error for ID 27761

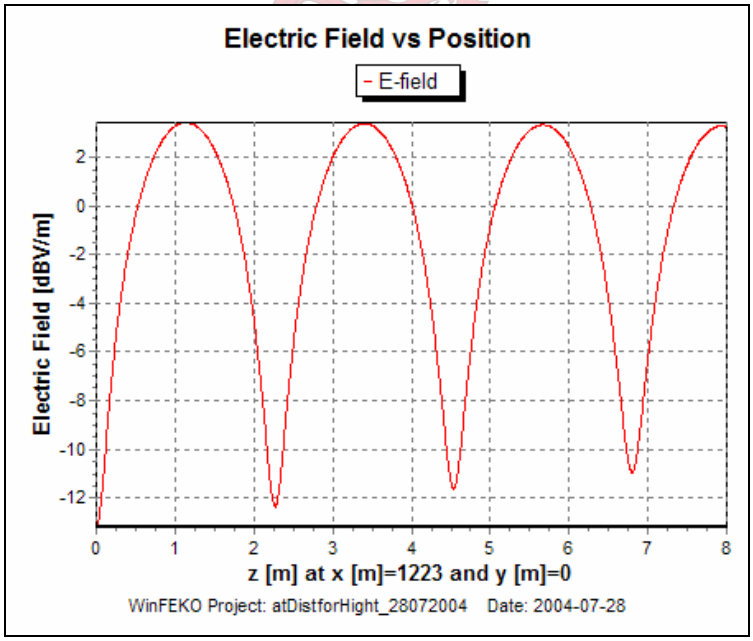

Figure 6.19: Multipath Error for ID 34408

From Figure6.13 it can be seen that there is a tree obstructing the line-of-sight between the mobile phone and the base station. With reference to work done in chapter 4.5, it is found that the attenuation of a propagated signal due to the presence of the vegetative obstruction can be calculated by:

$$A_{et} = d\gamma$$
$$= 0.38 \times 4$$
$$= -1.52dB$$

With all the most important variables now known, the link budget can be done. This is shown for each cell ID in the next table.

	dB (27761)	dB (34408)
Power Transmit	53.5	54.86
Free Space Propagation Loss	-92.94	-99.58
Angle Loss	-11.5	-23.2
Multipath Loss/Gain	-15.5	-2
Loss due to Vegetation	-1.52	0
Cable Loss	-1.63	-1.63

Table 6.3: Link Budget for cell ID's 27761 and 34408

From Table 6.3 the predicted signal levels from each cell ID can be determined. These predicted signal levels are now given together with the logged signal levels in the next figure.

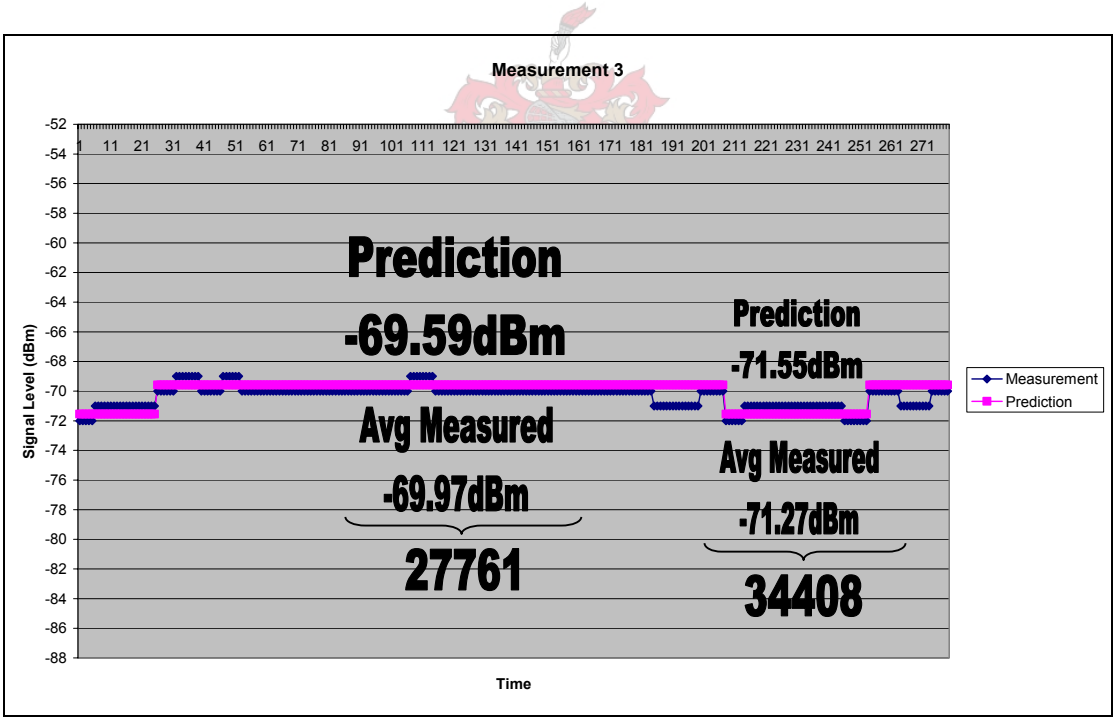

Figure 6.20: Prediction vs. Measurement for both cell ID's

From Figure 6.20 it can be seen that the received signal level compares well with the predicted signal level. Again, a certain amount of small scale fading can be seen, but this is expected. From this measurement it is clear that the accuracy of the terrain model is very important when making an accurate prediction.

6.1.4. Measurement 1.4:

The next measurement is reasonable line-of-sight, but the influence of some of the surrounding vegetation will be seen. The propagation channel view from the mobile phone to the base station can be seen in Figure 6.21.

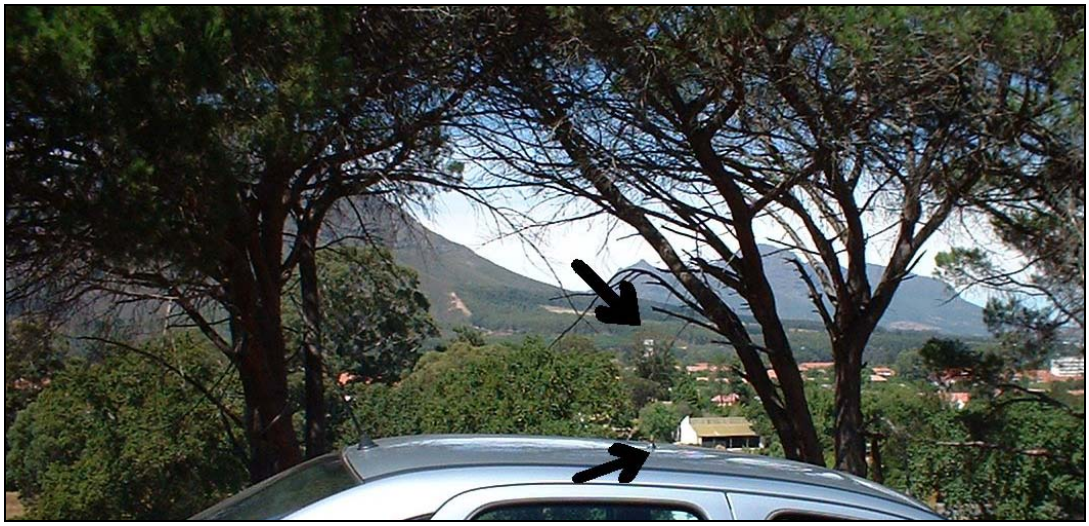

Figure 6.21: Propagation Channel for Measurement 1.4.

The distance between the mobile phone and the base station is calculated to be $1.128km$. From this, the free space propagation loss can be calculated and it is found to be $98.733dB$. Next, the elevation between the mobile phone and the base station, needs to be taken into account.

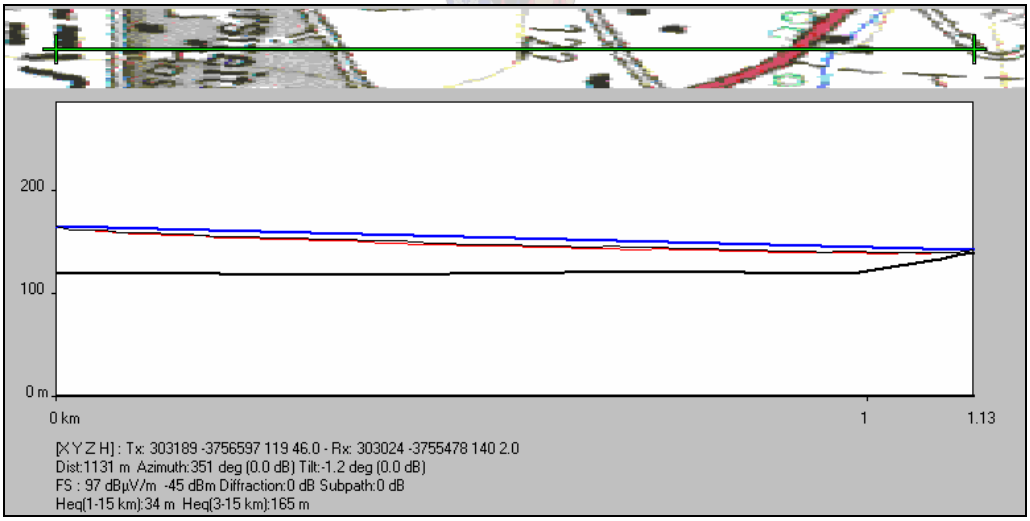

Figure 6.22: Path Elevation between Base Station and Mobile Phone

From Figure 6.22 it can be seen that the azimuth difference between the mobile phone and the base station is $21°$ and the tilt is $1.2°$. Using these known values, the vertical angle loss as well as the horizontal angle loss can be determined.

$$\text{Vertical Angle Loss} = 1.2dB$$

$$\text{Horizontal Angle Loss} = 1dB$$

The next important factor to take into account is the effect of multipath propagation. Using a FEKO simulation, this variable can be modelled and taken into account when the link budget is done. The result from the FEKO simulation is shown in the next figure.

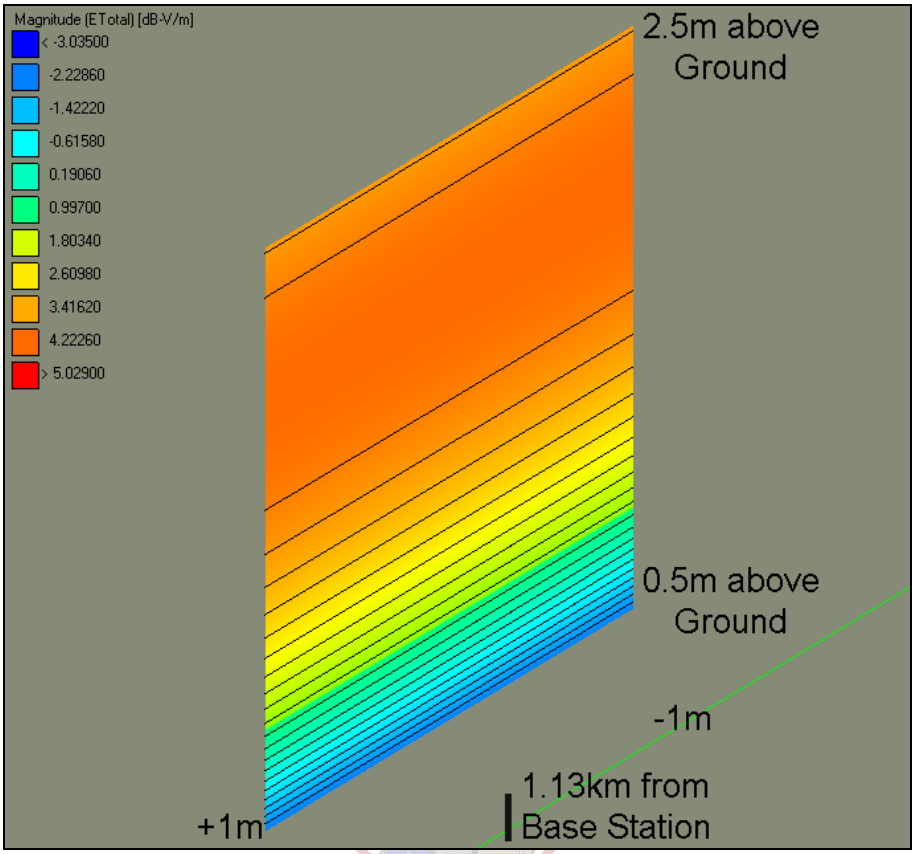

Figure 6.23: Multipath loss/gain at the Mobile Receiver

Again, the local terrain plays an enormous role in the influence of the multipath signal. The multipath loss/gain as a function of antenna height, can be seen in the next figure.

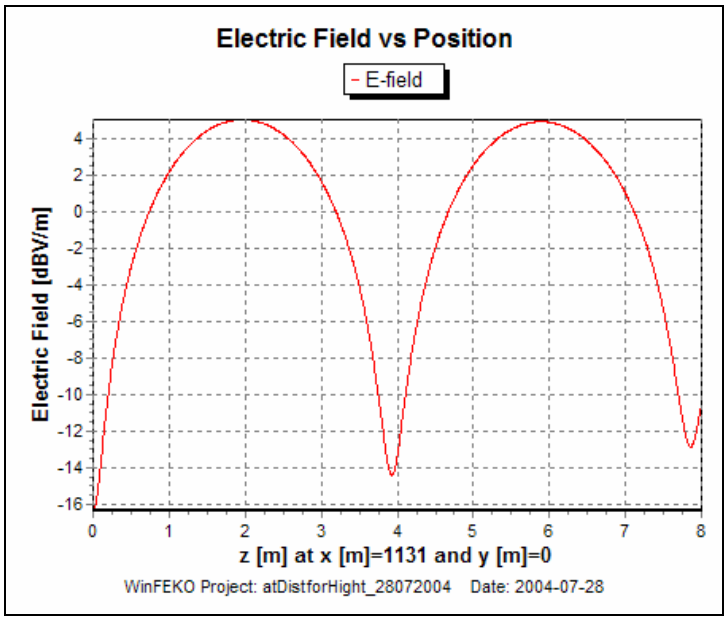

Figure 6.24: Multipath error as a function of Height above Ground Level

From Figure 6.24. it can be seen that the influence due to multipath propagation can be taken as $-5dB$, with an error of 1m in receiver antenna height.

The next factor that needs to be taken into account is the tree canopy through which the received signal has to propagate. From the surroundings, it can be assumed that the distance over which the signal must propagate through trees, is more or less five percent of the total path length. Using this, the attenuation due to vegetation is found to be $21.14dB$. When this is used in the link budget, it is found that the amount of vegetation in the propagation medium is assumed to be too much. The percentage obstruction is brought down from five percent to four percent. Now the attenuation due to vegetation is brought down to $16.9dB$.

The link budget for this measurement is shown in the next table.

	dB
Power Transmit	54.86
Free Space Propagation Loss	-98.73
Vertical Angle Loss	-1.2
Horizontal Angle Loss	-1
Multipath Loss/Gain	-5
Loss due to Vegetation	-16.9
Cable Loss	-1.63

Table 6.4: Link Budget for Measurement 1.4.

$$dBm_{prediction} = dB_{send} - dB_{FreeSpaceLoss} - dB_{RadPattern} - dB_{mobAnt} - dB_{Multipath} - dB_{Vegetation}$$
$$= 54.86 - 98.73 - 1.2 - 1 - 5 - 1.63 - 16.9$$
$$= -69.6dBm$$

The predicted signal level, together with the measured signal level can be seen in the next figure.

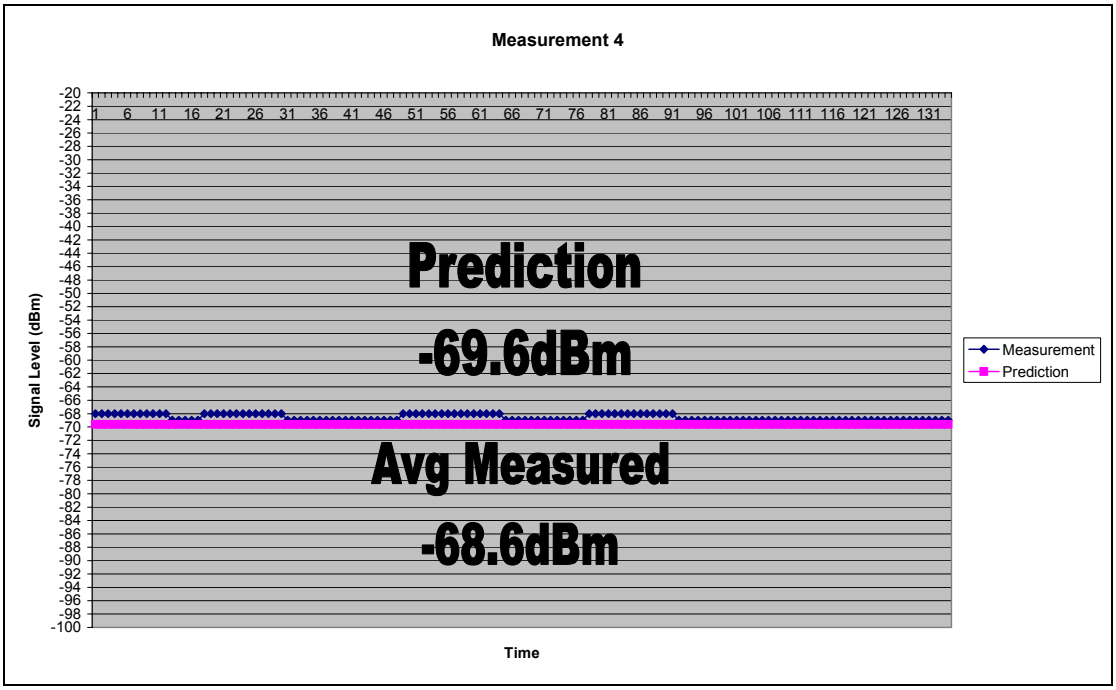

Figure 6.25: Prediction vs. Measurement

From this measurement, it is clear that the amount of tree cover influencing the amount of attenuation to a propagated signal have a significant effect on the predicted signal level. This is a factor that needs to be taken into account when predicting the amount of attenuation due to vegetation.

6.1.5. Measurement 1.5:

This is another clear line-of-sight measurement. The difference is that the mobile phone is now very close to the base station.

Figure 6.26: Measurement 1.5 – clear line-of-sight close range

The distance between the mobile phone and the base station is calculated to be $200m$. From this, the free space propagation loss is calculated to be $83.822dB$. The next step would be to take into account the elevation difference between the mobile phone and the base station. From the figure below it can be seen that the mobile phone and base station is at the same ground level. The only variable to take into account when looking at this measurement, is the difference in antenna height.

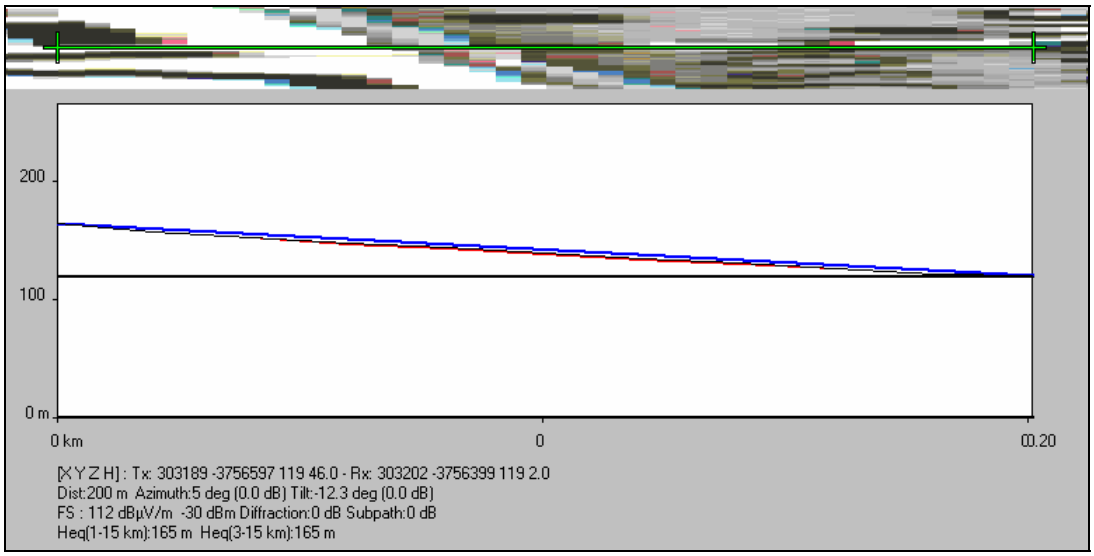

Figure 6.27: Path elevation between Mobile Phone and Base Station

From the above figure, it can be seen that the difference in azimuth is $5°$ and the tilt is $12.3°$. From this, the loss due to the position of the mobile phone relative to the base station, is determined to be:

$$\text{Vertical Angle Loss} = 9dB$$

$$\text{Horizontal Angle Loss} = 0dB$$

The next step is to determine the influence of multipath propagation on the received signal level. This done by simulation using FEKO software. The result from the simulation can be seen in the next figure.

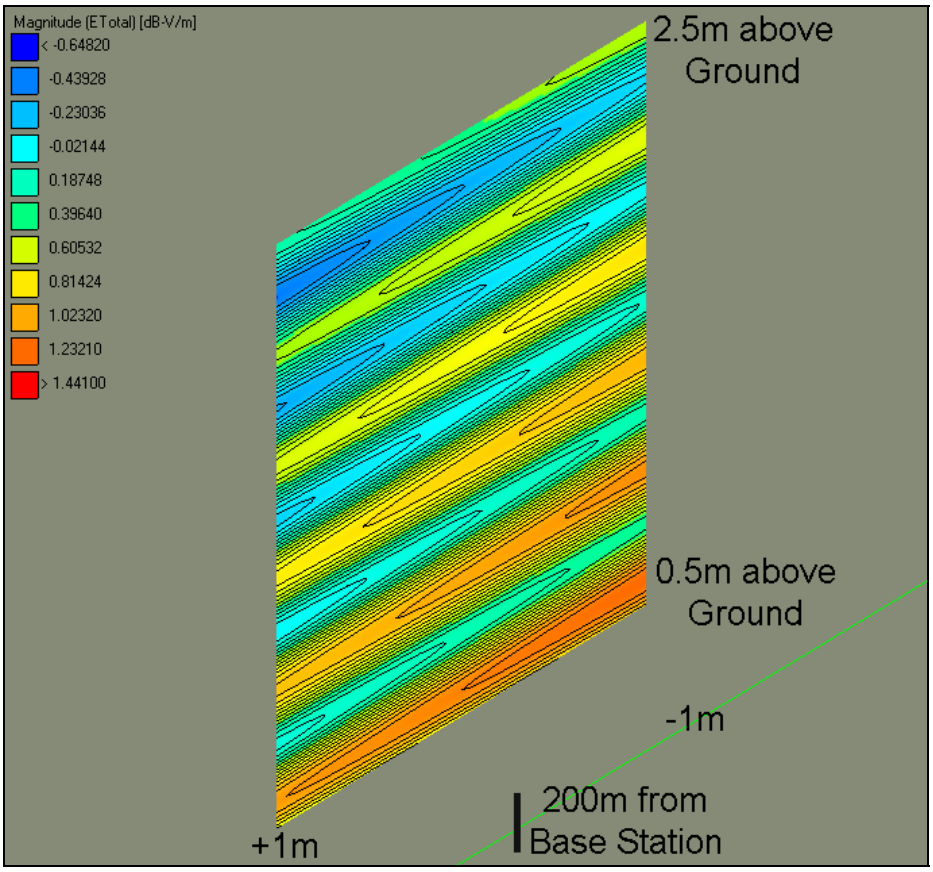

Figure 6.28: Multipath loss/gain at the Mobile Receiver

From the above figure, it can be seen that for this case, the gain due to multipath propagation is $1dB$. From all this known data, the link budget can be done as seen in the next table.

	dB
Power Transmit	54.86
Free Space Propagation Loss	-83.822
Vertical Angle Loss	-9
Horizontal Angle Loss	0
Multipath Loss/Gain	+1
Loss due to Vegetation	0
Cable Loss	-1.63

Table 6 5: Link Budget for Measurement 1.5.

For this measurement, the predicted signal is calculated to be:

$$dBm_{prediction} = dB_{send} - dB_{FreeSpaceLoss} - dB_{RadPattern} - dB_{mobAnt} + dB_{Multipath}$$
$$= 54.86 - 83.822 - 9 + 1 - 1.63$$
$$= -38.59dBm$$

In the next figure the measured signal level is compared with the predicted signal level. From the figure below, it can be seen that the prediction compares well with measured signal level.

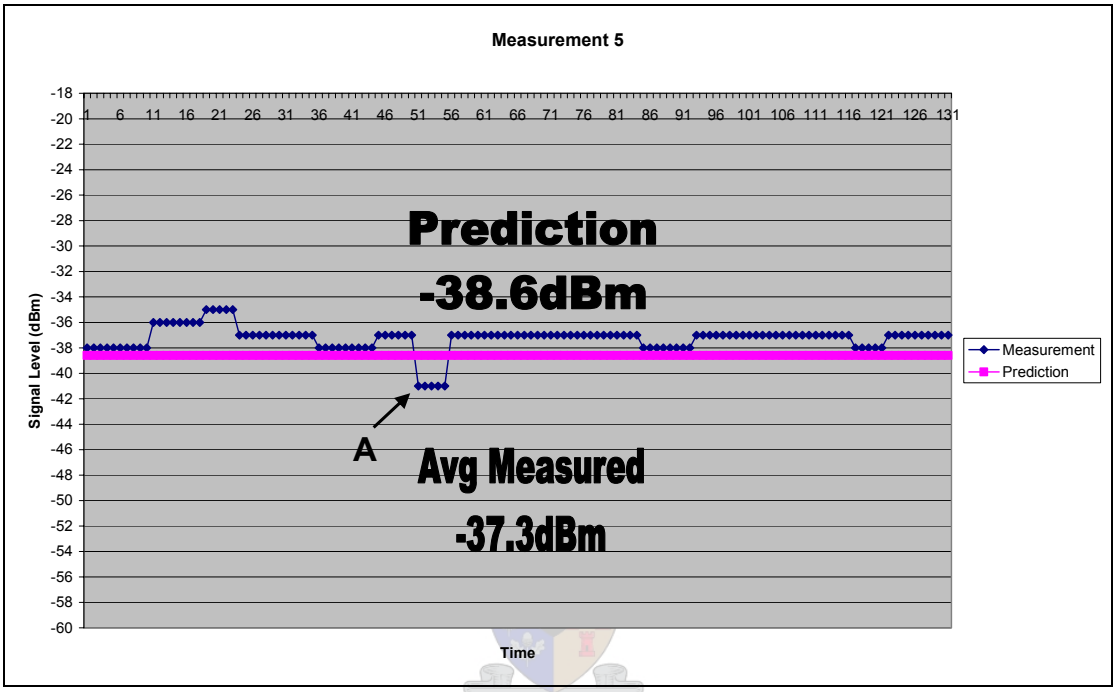

Figure 6.29: Prediction vs. Measurement

Again, the small-scale fading is clearly noticeable. Marked Point A on the data was when a vehicle drove by while the signal was being logged. The movement of the vehicle in the close vicinity of the mobile receiver, changed the propagation medium and altered the signal level that was being logged. Other than this, the prediction compares well with the measured signal level.

6.1.6. Measurement 1.6:

For this measurement, line-of-sight conditions are not totally satisfied because of the metal fence that obstructs the line-of-sight view. This obstruction will be looked at in more detail later in this section.

Figure 6.30: Partial line-of-sight for Measurement 1.6.

First the distance between the mobile phone and the base station need to be determined. From GPS measurements taken, the distance is calculated to be $588m$ and from this, the free space propagation loss can be determined. The free space propagation loss is calculated to be $93.19dB$.

The next important variable that needs to be taken into account, is the elevation between the mobile phone and the base station. This can be seen in the next figure.

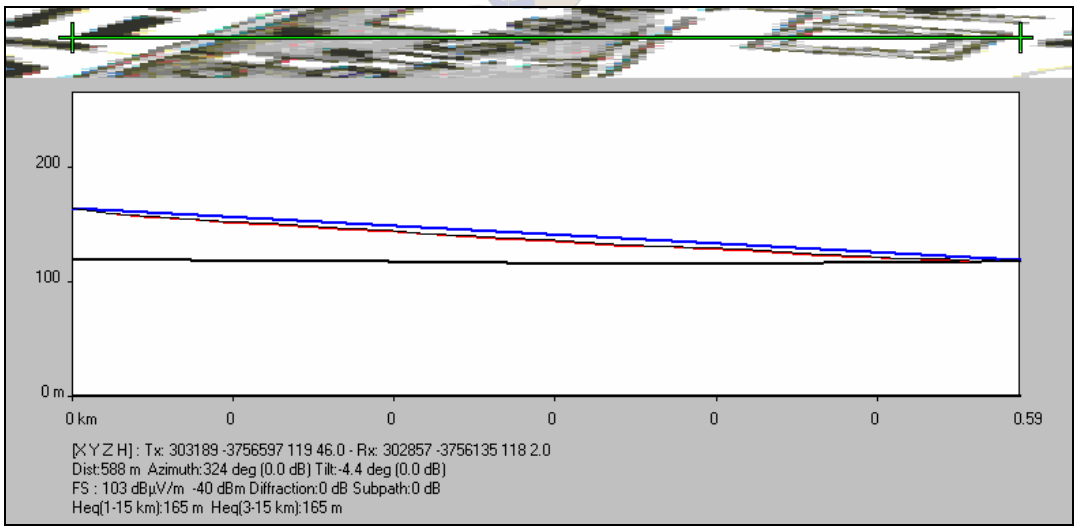

Figure 6.31: Path Elevation for Measurement 1.6.

In the above figure, it can be seen that the azimuth between that mobile phone and base station is determined to be $46°$ and the tilt is $4.4°$. From this, the vertical angle loss is $1.2dB$ and the horizontal angle loss is $5.9dB$.

Next the influence of multipath propagation needs to be taken into account. The simulation is done using FEKO software and the result can be seen in the next figure.

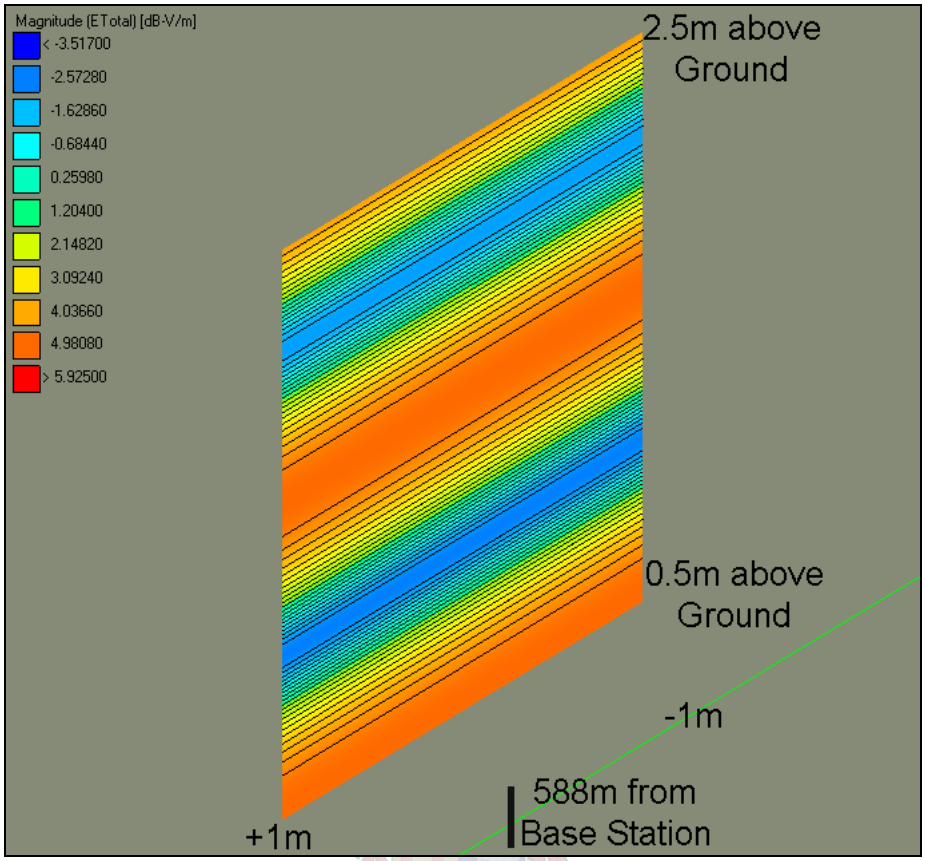

Figure 6.32: Multipath loss/gain for Measurement 1.6.

From the above figure it can be seen that gain in this case, due to multipath propagation is $5dB$.

The next important factor is metal fence partially obstructing the line-of-sight view between the mobile phone and the base station. Referring back to chapter 4.6, the loss due to this obstruction can be calculated using the approximation for single knife-edge diffraction. Therefore the loss is:

$$\upsilon = \theta \sqrt{\frac{2}{\lambda\left(\frac{1}{d_1}+\frac{1}{d_2}\right)}}$$

$$J(\upsilon) = 6.9 + 20\log\left(\sqrt{(\upsilon-0.1)^2+1}+\upsilon-0.1\right)$$

With $\theta = 0.0349rad(2°)$, $d_1 = 30m$ and $d_2 = 458m$ the loss due to knife-edge diffraction over the fence is found to be $11.399dB$. λ being the wavelength of the carrier frequency. Using the known variables, the loss due to diffraction over the obstacle is calculated to be:

$$L_{diff} = 11.3995dB$$

The link budget for this link can now be done and is shown in the next table.

	dB
Power Transmit	54.86
Free Space Propagation Loss	-93.19
Vertical Angle Loss	-1.2
Horizontal Angle Loss	-5.9
Multipath Loss/Gain	+5
Diffraction Loss	-11.399
Cable Loss	-1.63

Table 6.6: Link Budget for Measurement 1.6.

The predicted signal level is therefore given as:

$$dBm_{prediction} = dB_{send} - dB_{FreeSpaceLoss} - dB_{RadPattern} - dB_{mobAnt} + dB_{Multipath} - dB_{diff}$$
$$= 54.86 - 93.19 - 1.2 - 5.9 - 1.63 + 5 - 11.399$$
$$= -53.45dBm$$

The measured signal level, together with the predicted signal level is shown in the next figure.

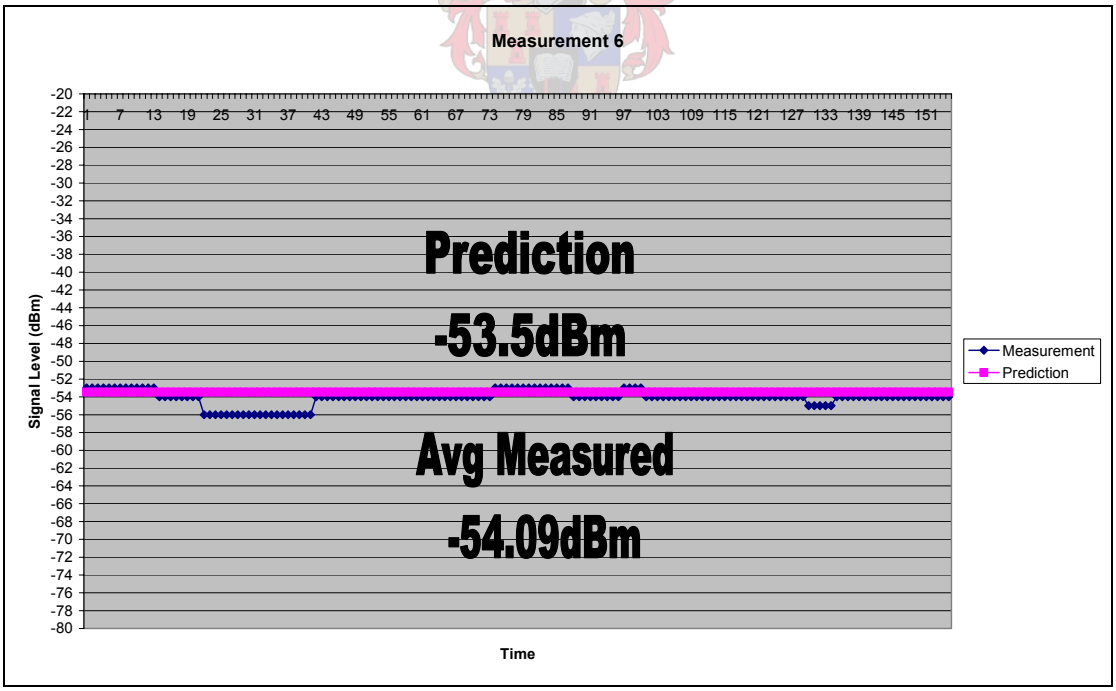

Figure 6.33: Prediction vs. Measurement

From the above figure it can be seen that the predicted signal level compares well with the measured signal level. Small-scale fading can be seen which can be attributed to movement of objects within the propagation medium.

6.1.7. Measurement 1.7:

This measurement is used to show how a vegetative obstruction influences the propagated signal. The view from the mobile phone can be seen in the next figure. It can be seen that it is clear line-of-sight, if not for the trees.

Figure 6.34: Tree obstruction for Measurement 1.7.

First the distance between the mobile phone and the base station is determined, this is found to be $1.39km$. Using this, the free space propagation loss can be determined.

$$L_{FSP} = 32.4 + 20\log_{10}(d_{km}) + 20\log_{10}(f_{MHz})$$

$$L_{FSP} = 100.72dB$$

The next step is to take into account the elevation difference between the mobile phone and the base station. The position of the mobile phone relative to the base station, can be seen in the next figure.

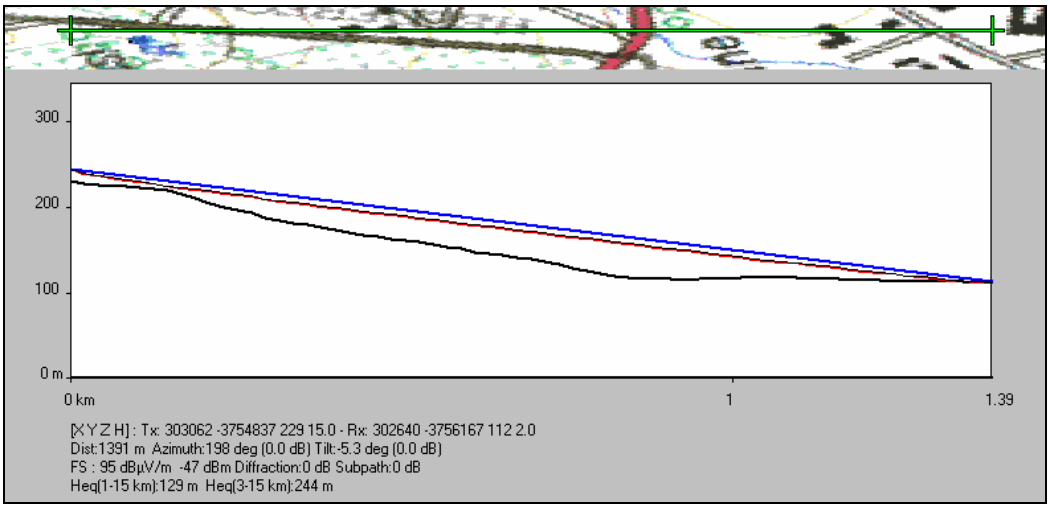

Figure 6.35: Path Elevation between the Mobile Phone and Base Station

From the above figure, the azimuth is found to be $18°$ and the tilt is $5.3°$. The loss due to the position of the mobile phone, relative to the base station, is determined to be:

$$\text{Vertical Angle Loss} = 1.2dB$$
$$\text{Horizontal Angle Loss} = 0.1dB$$

The next step is to simulate the influence of multipath propagation on the specific measurement. This is done using FEKO and the result can be seen in the next figure. The multipath loss/gain is found to be:

$$\text{Multipath Loss} = 11dB$$

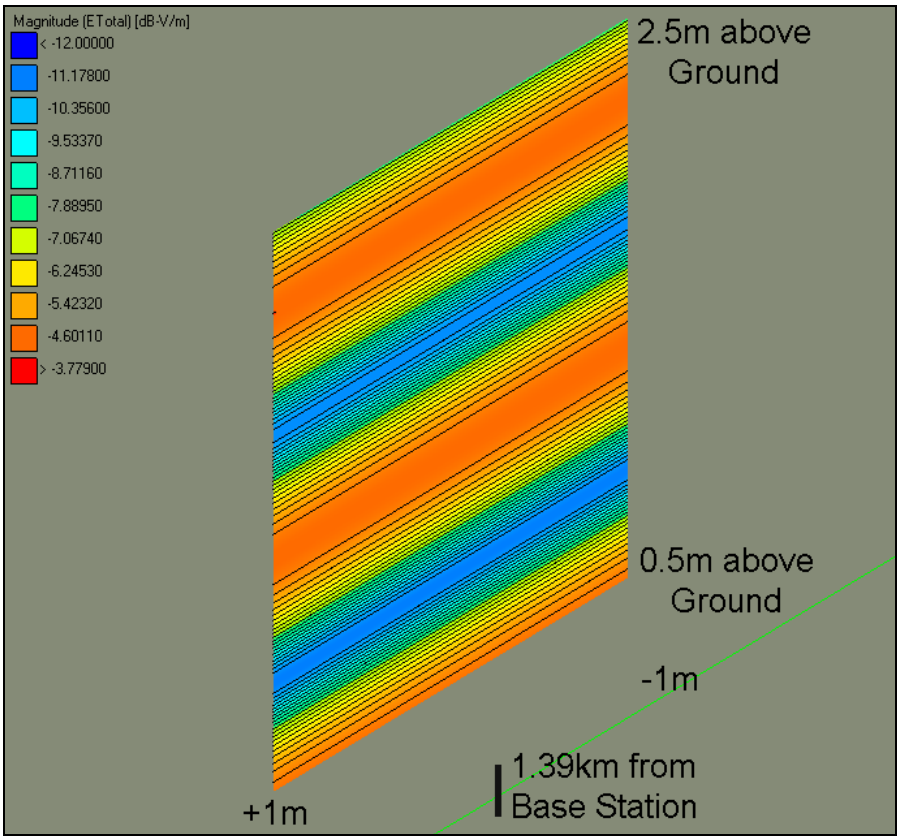

Figure 6.36: Multipath loss/gain at the Mobile Phone

The next part of the link budget that need to be looked at, is the line of trees that block the clear line-of-sight from the base station to the mobile phone. From chapter 4.5 it is found to be $1.9dB$.

With all this data now known, the link budget for this measurement can now be done, this is shown in the next table.

	dB
Power Transmit	53.5
Free Space Propagation Loss	-100.72
Vertical Angle Loss	-1.2
Horizontal Angle Loss	-0.1
Multipath Loss/Gain	-11
Attenuation due to Vegetation	-1.9
Cable Loss	-1.63

Table 6.7: Link Budget for Measurement 1.7.

$$dBm_{prediction} = dB_{send} - dB_{FreeSpaceLoss} - dB_{RadPattern} - dB_{mobAnt} - dB_{Multipath} - dB_{AttVeg}$$
$$= 53.5 - 100.72 - 1.2 - 0.1 - 1.63 - 11 - 1.9$$
$$= -63.05 dBm$$

The predicted signal level is now plotted together with the measured signal level and is shown in the next figure.

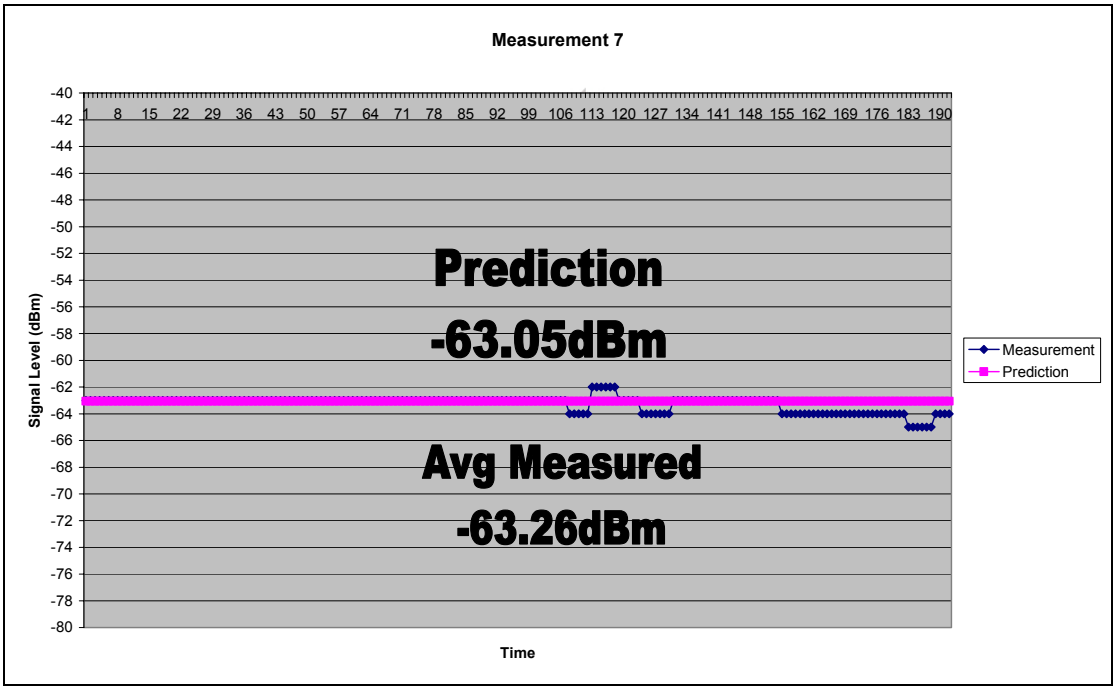

Figure 6.37: Prediction vs. Measurement

From the above figure, it can be seen that the prediction compares well with the measurement that is taken.

6.2. Measurements (Group 2)

In the next figure, the layout and positions of these measurements can be seen. Most of these measurements are taken in an informal settlement just outside Stellenbosch, Kayamandi. The area is populated with metal shacks, consisting mostly of metal and it is expected that there will be a lot of reflections because of this.

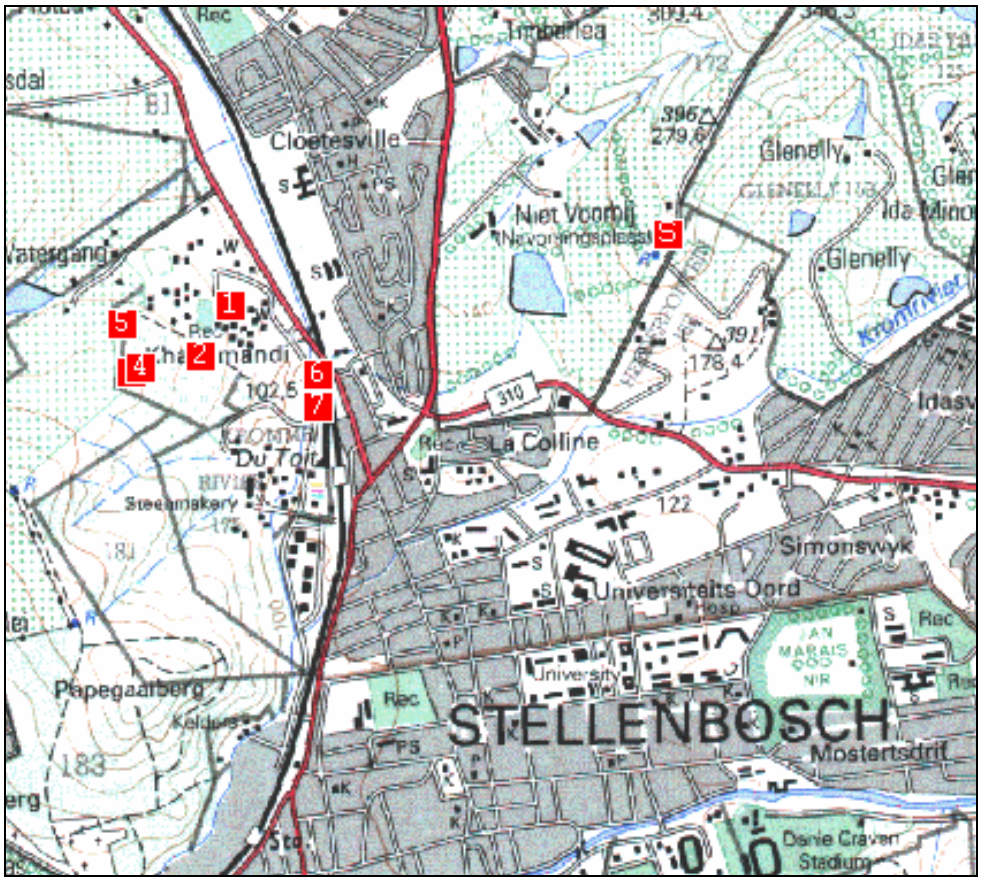

Figure 6.38: Setup for Measurements – Group 2

Only one base station is used for these measurements. Sentech is marked (S) on the above figure as well as the position of each of the mobile phone measurements. The distance over which these measurements are taken, vary between 1.8km and 2.8km.

Measurement 2.1:

The first measurement is taken in the informal settlement with a clear line-of-sight between the transmitter and the mobile receiver. This can be seen in Picture 6.39. The distance between the mobile phone and the base station is almost $2km$.

Figure 6.39: Line-of-sight view for Measurement 2.1.

The exact distance between the mobile phone and the base station is found to be $1.919km$. Using this, the free space propagation loss can be calculated and it is found to be:

$$L_{FSP} = 32.4 + 20\log_{10}(d_{km}) + 20\log_{10}(f_{MHz})$$
$$L_{FSP} = 103.463dB$$

The next step is to take into account the elevation between the mobile phone and the base station. The elevation as well as the terrain profile between the mobile phone and the base station can be seen in the next figure.

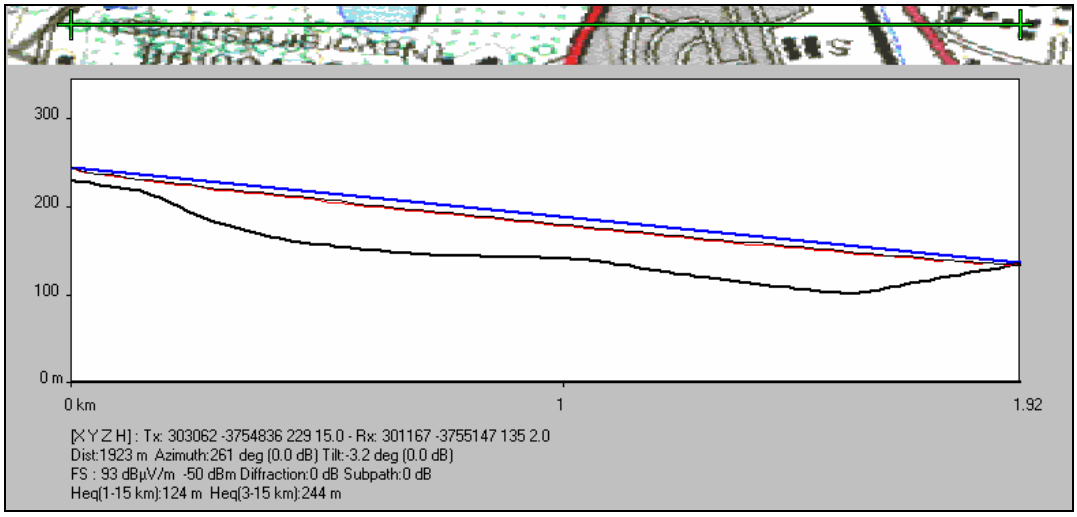

Figure 6.40: Path Elevation between the Mobile Phone and the Base Station

Using the above figure, the loss due to relative position can be determined. The info needed to determine this is the azimuth between the mobile phone and the base station, found to be $19°$, and the tilt is $3.2°$. The losses are:

$$\text{Vertical Angle Loss} = 0.3dB$$

$$\text{Horizontal Angle Loss} = 1dB$$

The next step will be to simulate the influence of multipath propagation on the received signal level. This is now where the problem starts. Because most of the ground in the vicinity of the mobile phone receiver is covered with metal shacks, the reflection is difficult to predict. But for purposes of this measurement, the ground will be assumed to be perfectly electrically conducting ground to simulate the influence of the metal shacks. The results of the simulation can be seen in the next figure

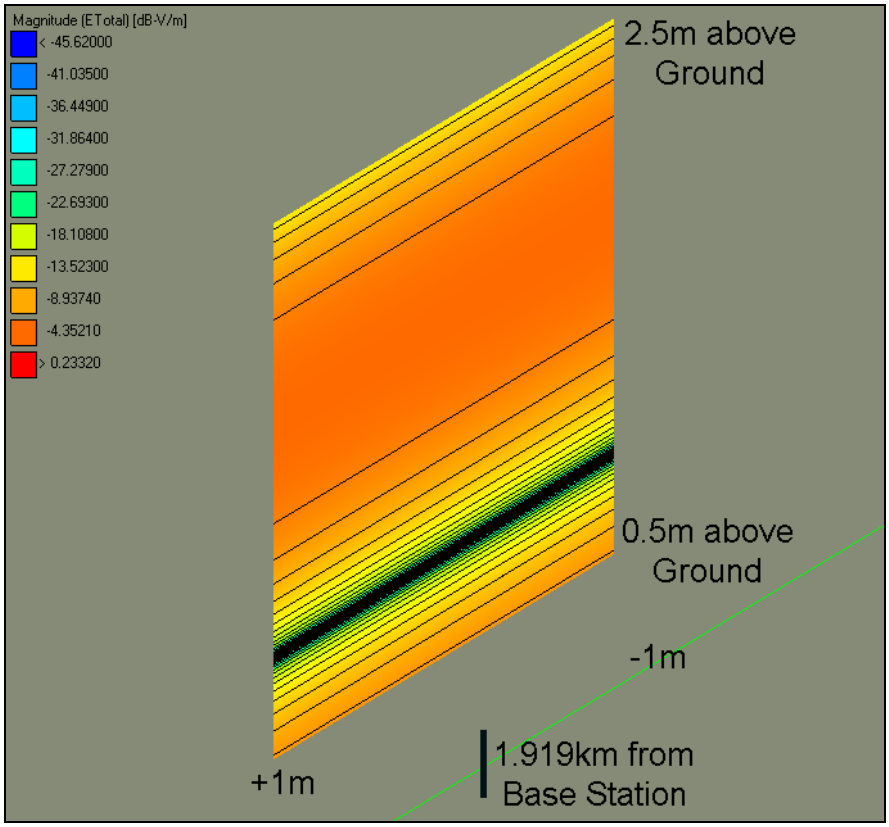

Figure 6.41: Multipath loss/gain at the Mobile Receiver

From the above figure, it can be seen that the loss due to multipath propagation in the vicinity of the mobile phone will be between $0dB$ and $8dB$. This then for when the ground cover in the vicinity of the mobile receiver is modelled as being perfectly conducting.

With all this data now known, the link budget can be done, using all the data supplied in the next table.

	dB
Power Transmit	53.5
Free Space Propagation Loss	-103.46
Vertical Angle Loss	-0.3
Horizontal Angle Loss	-1
Multipath Loss/Gain	-3
Attenuation due to Vegetation	0
Cable Loss	-1.63

Table 6.8: Link Budget for Measurement 2.1.

From the above table, it can be calculated that the predicted signal level at the mobile phone is:

$$dBm_{prediction} = dB_{send} - dB_{FreeSpaceLoss} - dB_{RadPattern} - dB_{mobAnt} - dB_{Multipath}$$

$$= 53.5 - 103.46 - 0.3 - 1 - 1.63 - 3$$

$$= -55.89dBm$$

The predicted signal level, together with the measured signal level, is now shown in the next figure.

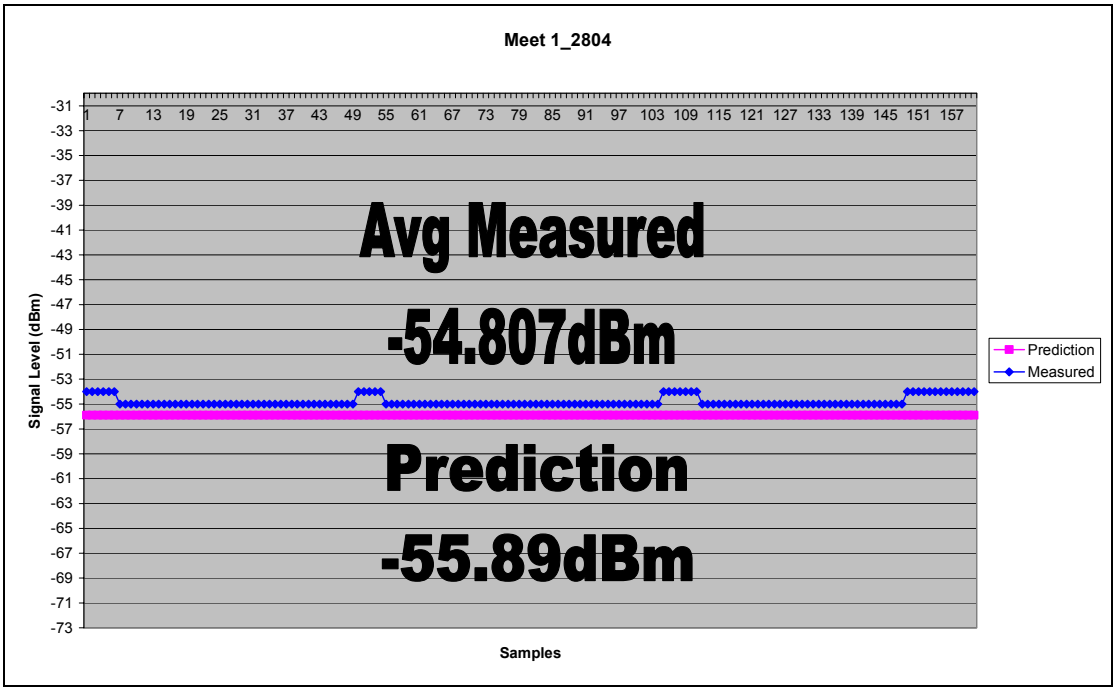

Figure 6.42: Prediction vs. Measurement

From the above figure, it can be seen that the predicted signal level compares well with the measured signal level. It isn't exactly the same, but this can be attributed to the fact that there are many shacks in close vicinity of the mobile receiver. These shacks are the source of more reflections and therefore more difficult to model.

6.2.2. Measurement 2.2:

The next measurement is also a line-of-sight link. Again the ground in the vicinity of the mobile phone is covered by metal shacks as shown in Picture 6.43.

Figure 6.43: Line-of-sight view for Measurement 2.2.

The distance between the mobile phone and the base station is found to be $2.105km$. Using this, the free space propagation loss can be calculated and it is found to be:

$$L_{FSP} = 32.4 + 20\log_{10}(d_{km}) + 20\log_{10}(f_{MHz})$$
$$L_{FSP} = 104.267dB$$

The next step is to take into account the elevation between the mobile phone and the base station. The elevation as well as the terrain profile between the mobile phone and the base station can be seen in the next figure.

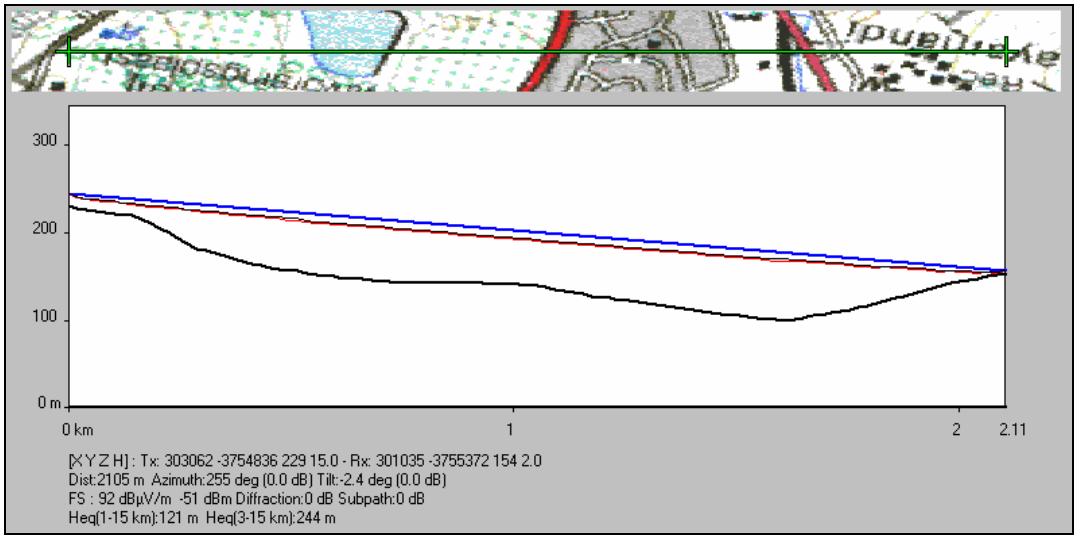

Figure 6.44: Path Elevation between the Mobile Phone and the Base Station

Using the information gathered from the above figure, the loss in received signal strength due to the relative position of the mobile phone to the base station can be determined. The information gathered, is the azimuth relative to each other, found to be $25°$, and the tilt is $2.4°$. The losses are then determined to be:

$$\text{Vertical Angle Loss} = 0.3dB$$
$$\text{Horizontal Angle Loss} = 1.7dB$$

The next step is now to simulate the effect of multipath propagation on the received signal level using FEKO software. Again, the ground cover in the vicinity of the mobile phone is mainly metal shacks. Therefore, for simulation purposes, the ground is set to be perfectly electrically conducting. The results from this simulation can be seen in the next figure.

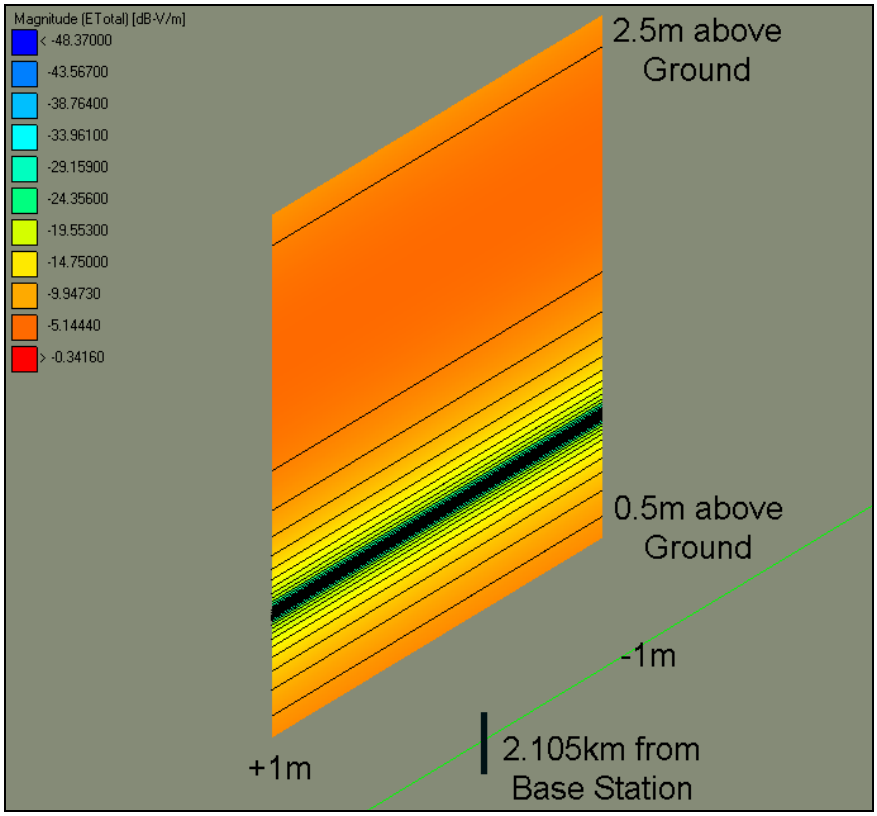

Figure 6.45: Multipath loss/gain at the Mobile Receiver

From the above figure, it can be seen that the loss due to multipath propagation will vary between $0dB$ and $5dB$. This will be taken into account when the link budget is done.

With all the data now known, the link budget can be done. A table showing all the calculated value, is given next.

	dB
Power Transmit	53.5
Free Space Propagation Loss	-104.267
Vertical Angle Loss	-0.3
Horizontal Angle Loss	-1.7
Multipath Loss/Gain	-2
Attenuation due to Vegetation	0
Cable Loss	-1.63

Table 6.9: Link Budget for Measurement 2.2.

From the above table, it can be calculated that the predicted signal level at the mobile phone is:

$$dBm_{prediction} = dB_{send} - dB_{FreeSpaceLoss} - dB_{RadPattern} - dB_{mobAnt} - dB_{Multipath}$$

$$= 53.5 - 104.267 - 0.3 - 1.7 - 1.63 - 2$$

$$= -56.39dBm$$

The predicted signal level, together with the measured signal level, is now shown in the next figure.

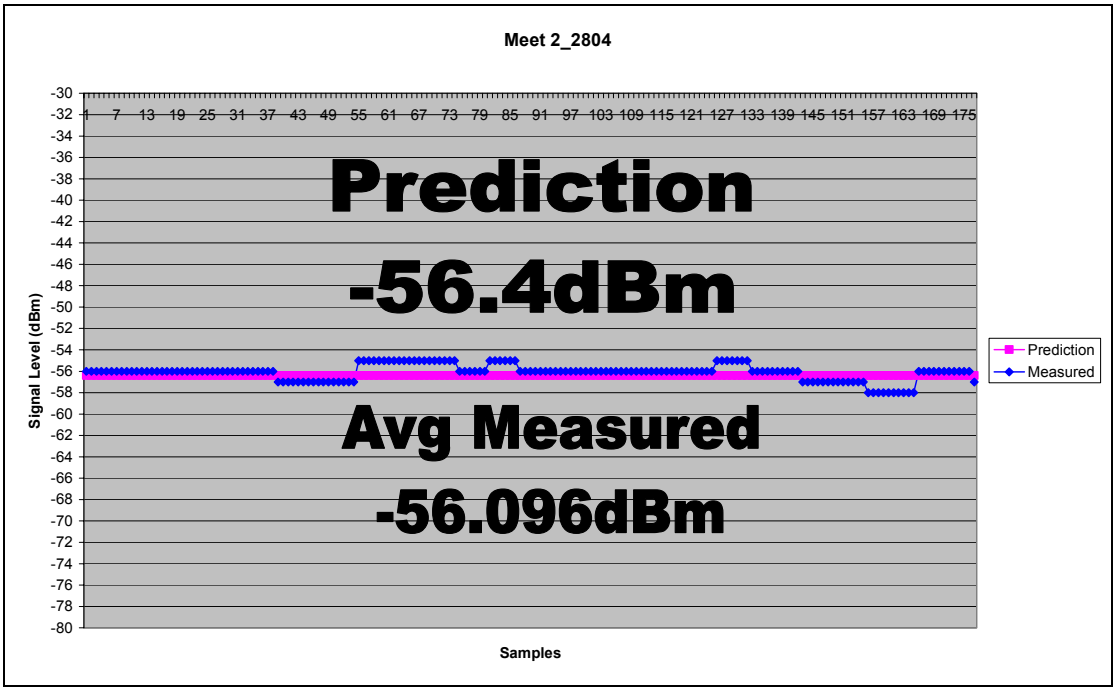

Figure 6.46: Prediction vs. Measurement

From the above figure, it can be seen that the predicted signal level compares well with the measured signal level.

6.2.3. Measurement 2.3:

This measurement is also taken in the rural area, the only difference is that the area in the vicinity of the mobile phone, is clear of any metal shacks.

Figure 6.47: Line-of-sight view for Measurement 2.3.

The distance between the mobile phone and the base station is found to be $2.415km$. Using this, the free space propagation loss can be calculated as:

$$L_{FSP} = 32.4 + 20\log_{10}(d_{km}) + 20\log_{10}(f_{MHz})$$
$$L_{FSP} = 105.4603dB$$

The next step, is to take into account the elevation between the mobile phone and the base station. The elevation as well as the terrain profile between the mobile phone and the base station can be seen in the next figure.

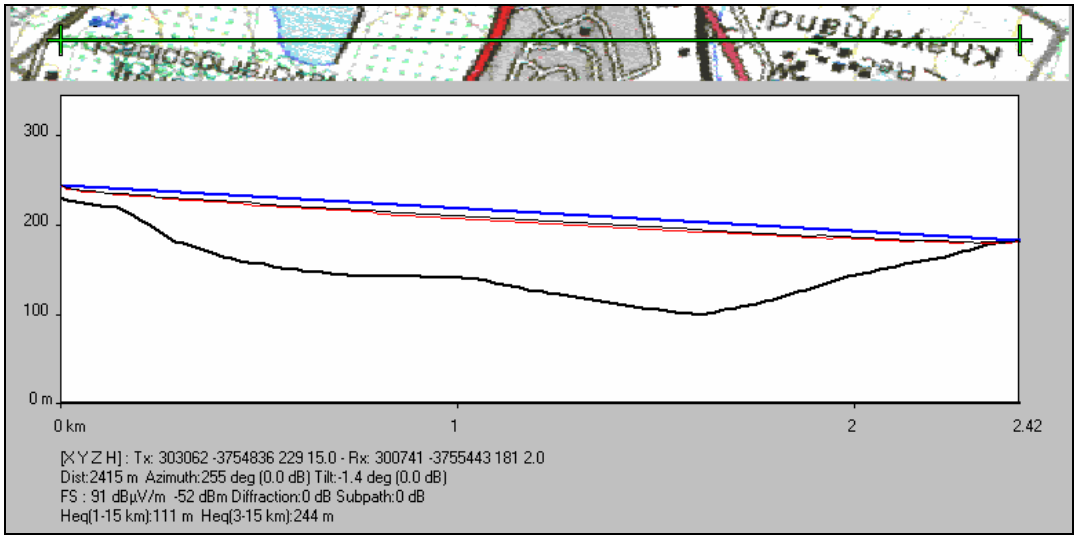

Figure 6.48: Path Elevation between the Mobile Phone and the Base Station

Using the information gathered from the above figure, the loss in the received signal strength due to the relative position of the mobile phone to the base station, can be determined. The information gathered, is the azimuth relative to each other, found to be $25°$, and the tilt is $1.4°$. The losses are then determined to be:

$$\text{Vertical Angle Loss} = 0.3dB$$
$$\text{Horizontal Angle Loss} = 1.7dB$$

The next step is now to simulate the effect of multipath propagation on the received signal level using FEKO software. As noted earlier in this section, there are no metal shacks in the vicinity of the mobile phone. Therefore the ground cover is simulated to be general ground. The result from this simulations can be seen in the next figure.

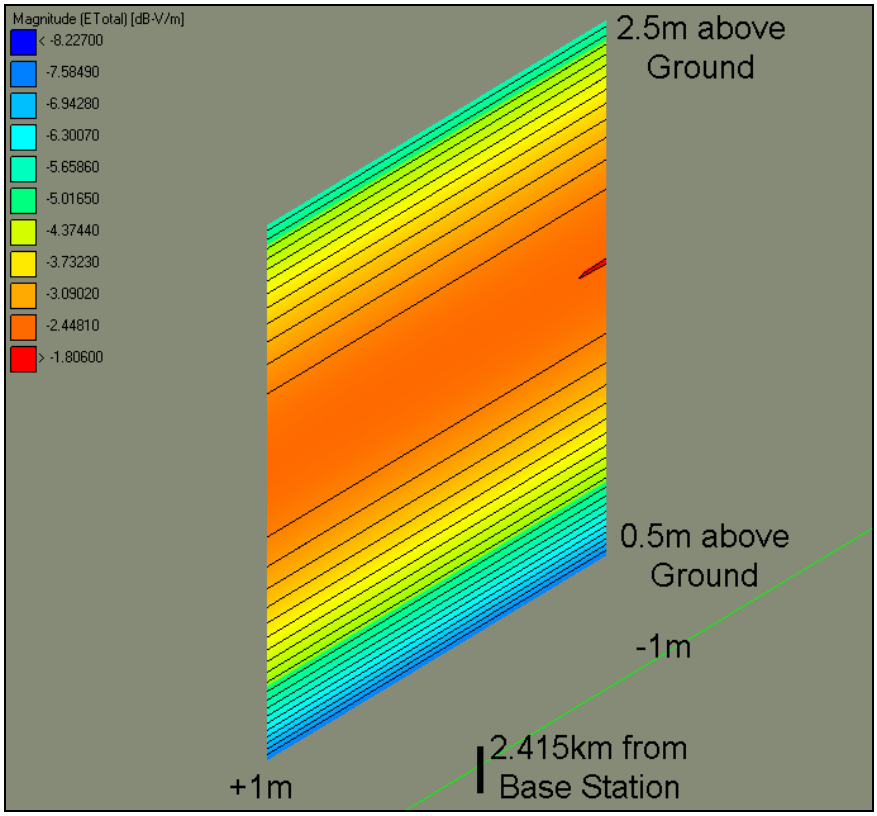

Figure 6.49: Multipath loss/gain at the Mobile Phone

From the above figure it can be seen that the loss due to multipath propagation is found to be $5dB$. This loss value will be taken into account when the link budget is done.

With all the data now known, the link budget is done.

	dB
Power Transmit	53.5
Free Space Propagation Loss	-105.4603
Vertical Angle Loss	-0.3
Horizontal Angle Loss	-1.7
Multipath Loss/Gain	-5
Attenuation due to Vegetation	0
Cable Loss	-1.63

Table 6.10: Link Budget for Measurement 2.3.

From the above table, it can be calculated that the predicted signal level at the mobile phone is:

$$dBm_{prediction} = dB_{send} - dB_{FreeSpaceLoss} - dB_{RadPattern} - dB_{mobAnt} - dB_{Multipath}$$

$$= 53.5 - 105.4603 - 0.3 - 1.7 - 1.63 - 5$$

$$= -60.59dBm$$

The predicted signal level, together with the measured signal level, is shown in the next figure.

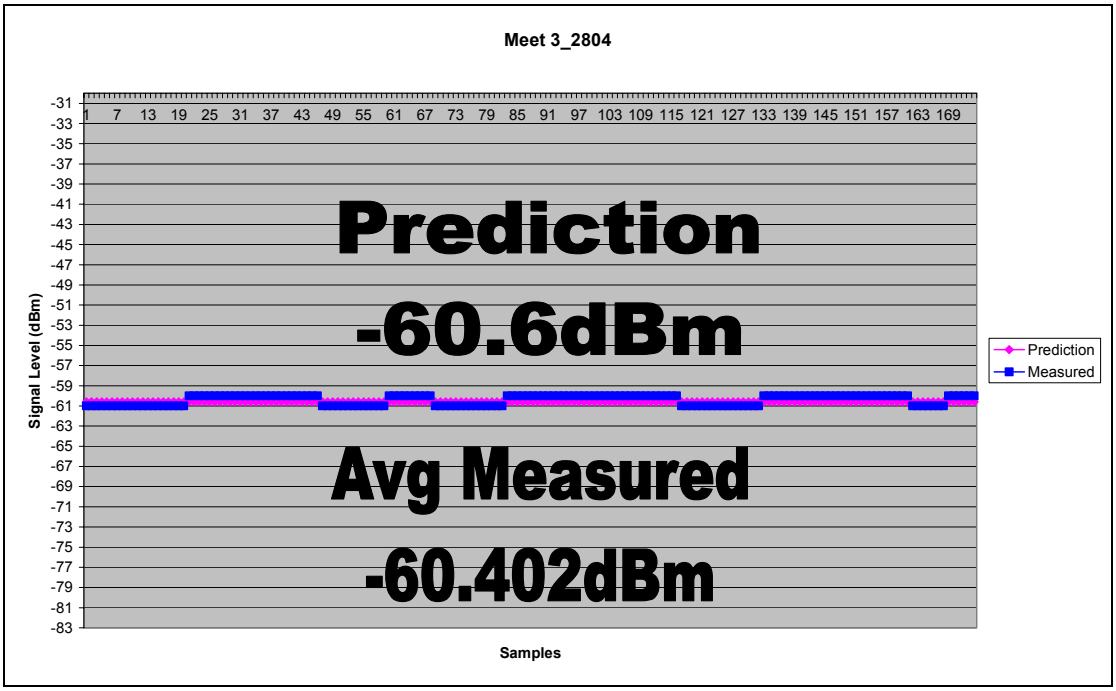

Figure 6.50: Prediction vs. Measurement

From the above figure it can be seen that the predicted signal level compares well with the measured signal level. Fading in the signal level is also less because of the absence of metal shacks in close vicinity.

6.2.4. Measurement 2.4:

In this measurement, there is a house the obstructs the clear line-of-sight view between the mobile phone and the base station.

Figure 6.51: No Line-of-sight for Measurement 2.4.

The distance between the mobile phone and the base station is found to be $2.372km$. Using this, the free space propagation loss can be calculated and it is found to be:

$$L_{FSP} = 32.4 + 20\log_{10}(d_{km}) + 20\log_{10}(f_{MHz})$$
$$L_{FSP} = 105.304dB$$

The next step is to take into account the elevation between the mobile phone and the base station. The elevation as well as the terrain profile between the mobile phone and the base station can be seen in the next figure.

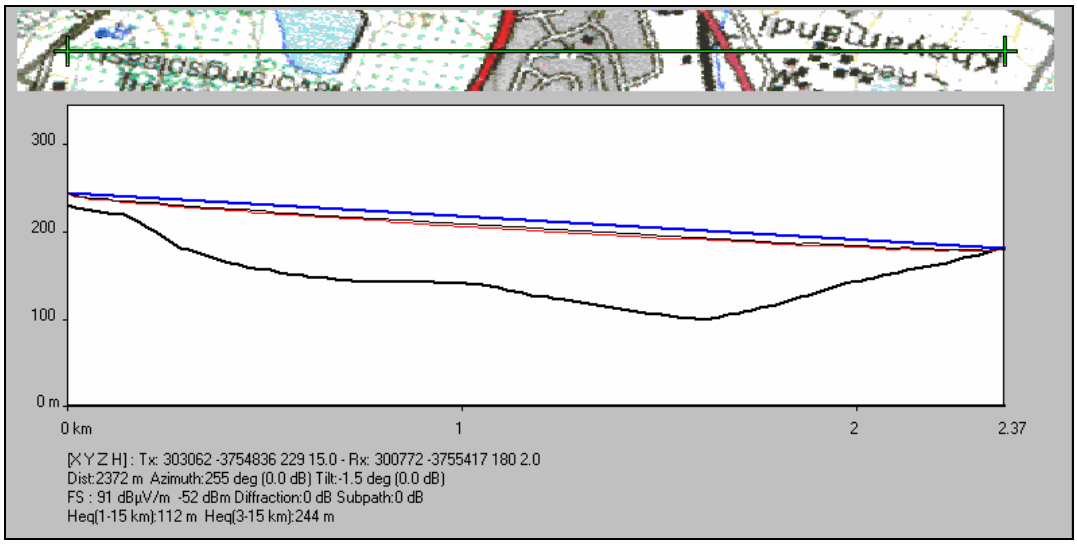

Figure 6.52: Path Elevation between the Mobile Phone and the Base Station

Using the information gathered from the above figure, the loss in the received signal strength due to the relative position of the mobile phone to the base station, can be determined. The information gathered, is the azimuth relative to each other, found to be $25°$, and the tilt is $1.5°$. The losses are then calculated to be:

$$\text{Vertical Angle Loss} = 0.3dB$$
$$\text{Horizontal Angle Loss} = 1.7dB$$

The next step is to calculate the effect of multipath propagation on the received signal level. This is done using a FEKO simulation. The result from the simulation is shown in the next figure.

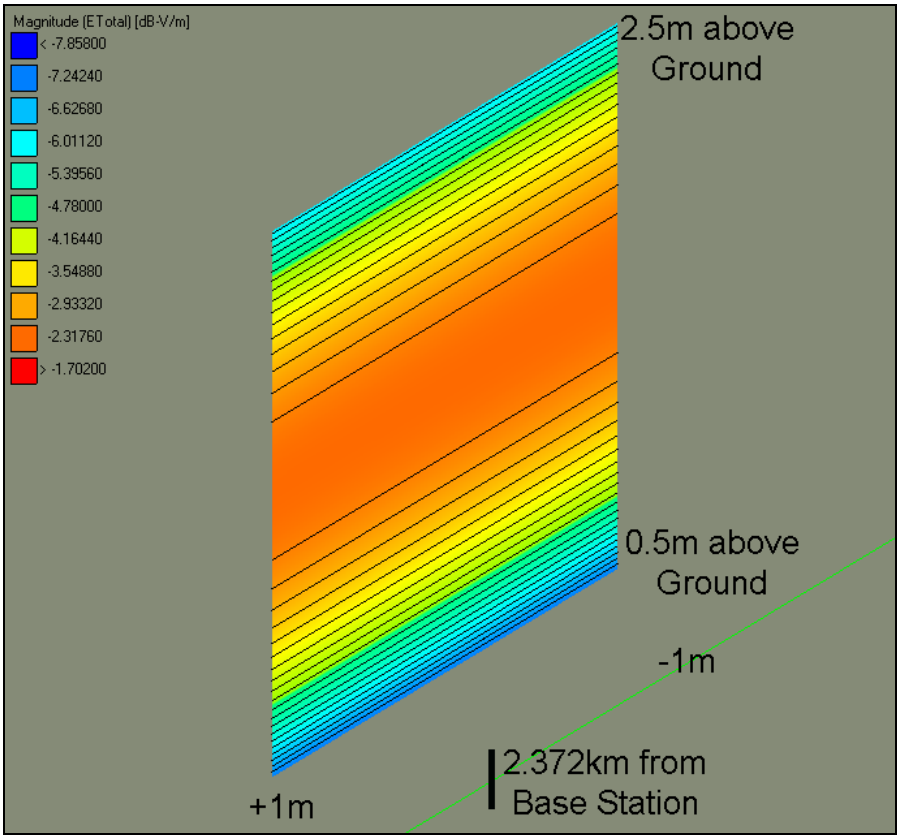

Figure 6.53: Multipath loss/gain at the Mobile Receiver

From the above figure, it can be seen that the loss due to multipath propagation is $2dB$. This will be taken into account when doing the link budget for this measurement.

As seen earlier, the direct line-of-sight path between the mobile phone and the base station is being obstructed by a house. This obstruction will be modelled as a single knife-edge diffraction covered in detail in chapter 4.4.1.

$$\upsilon = h\sqrt{\frac{2}{\lambda}\left(\frac{1}{d_1}+\frac{1}{d_2}\right)}$$

$$J(\upsilon) = 6.9 + 20\log\left(\sqrt{(\upsilon-0.1)^2+1}+\upsilon-0.1\right)$$

With $d_1 = 25m$, $d_2 = 2362m$, $h = 2m$ and $\lambda = 0.16667m$. Using these known values, the diffraction loss due to the single knife-edge is calculated to be $20.6688dB$.

With all the data now known, the link budget is done.

	dB
Power Transmit	53.5
Free Space Propagation Loss	-105.304
Vertical Angle Loss	-0.3
Horizontal Angle Loss	-1.7
Multipath Loss/Gain	-2
Diffraction Loss	-20.6688
Cable Loss	-1.63

Table 6.11: Link Budget for Measurement 2.4.

From the above table, it can be calculated that the predicted signal level at the mobile phone is:

$$dBm_{prediction} = dB_{send} - dB_{FreeSpaceLoss} - dB_{RadPattern} - dB_{mobAnt} - dB_{Multipath} - dB_{diff}$$
$$= 53.5 - 105.304 - 0.3 - 1.7 - 1.63 - 2 - 20.6688$$
$$= -78.1dBm$$

The predicted signal level, together with the measured signal level, is now shown in the next figure.

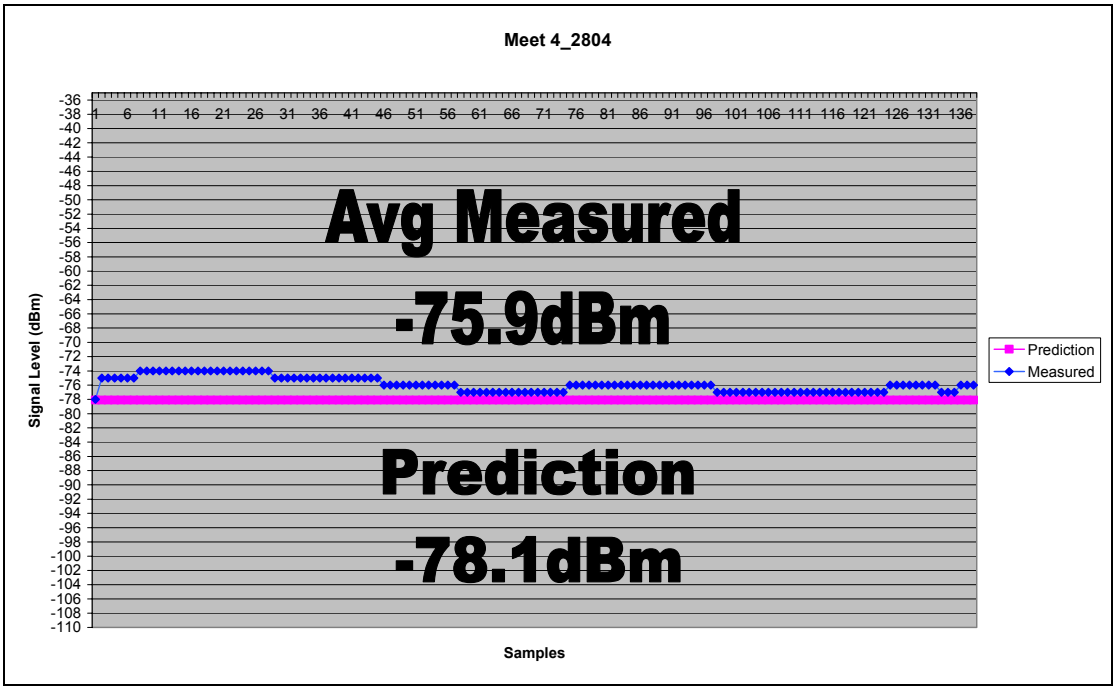

Figure 6.54: Prediction vs. Measurement

From the above figure, it can be seen that the prediction compares well with the measured signal level. It can also be seen that the amount of small-scale fading is more visible then in previous measurements. This is due to the fact the there is no line-of-sight component present, still the fading is small because the mobile receiver is stationary at all times.

6.2.5. Measurement 2.5:

For this measurement, the mobile phone has no clear line-of-sight available and the logged signal level also travels partly through a tree. The ground in the vicinity is also mostly covered with metal from the shacks.

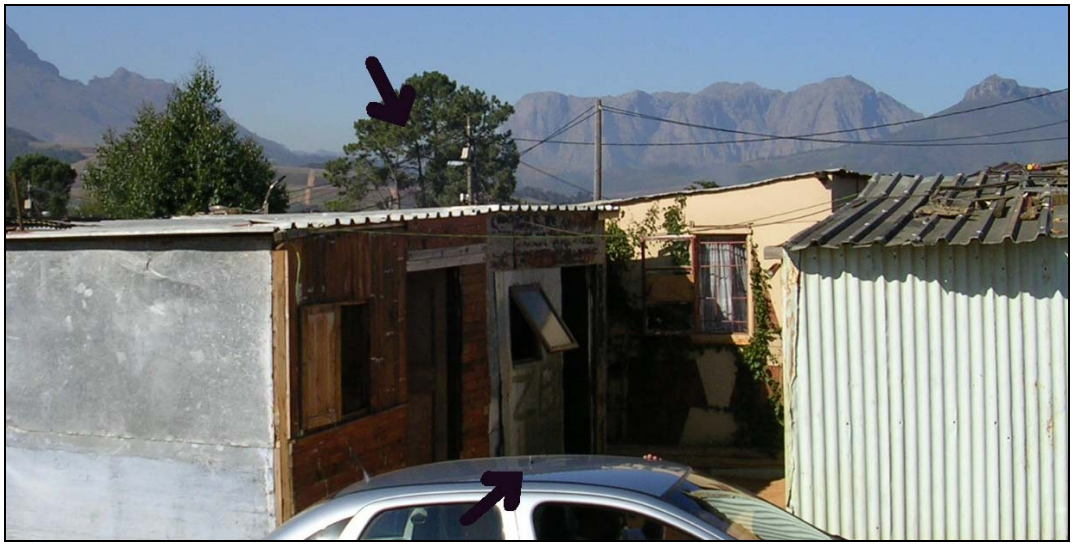

Figure 6.55: No clear Line-of-sight for Measurement 2.5.

The distance between the mobile phone and the base station is found to be $2.41km$. From this, the free space propagation loss is calculated to be:

$$L_{FSP} = 32.4 + 20\log_{10}(d_{km}) + 20\log_{10}(f_{MHz})$$

$$L_{FSP} = 105.4423dB$$

The next step, is to take into account the elevation between the mobile phone and the base station. The elevation as well as the terrain profile between the mobile phone and the base station can be seen in the next figure.

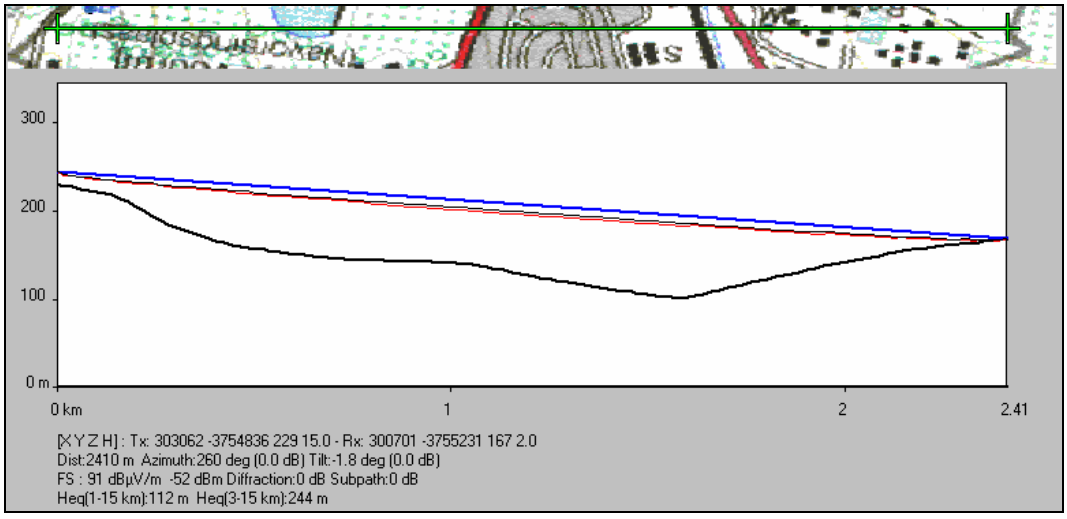

Figure 6.56: Path Elevation between the Mobile Phone and the Base Station

Using the information gathered from the above figure, the loss in the received signal strength due to the relative position of the mobile phone to the base station, can be determined. The information gathered, is the azimuth relative to each other, found to be $20°$, and the tilt is $1.8°$. The losses are then calculated to be:

$$\text{Vertical Angle Loss} = 0.3dB$$
$$\text{Horizontal Angle Loss} = 1.1dB$$

The next step is to simulate the effect of multipath propagation on the received signal level. This is done by using FEKO software. The ground cover in the vicinity of the mobile phone is metal shacks, therefore the ground properties are simulated as electrically perfectly conducting. The result from the simulation can be seen in the next figure.

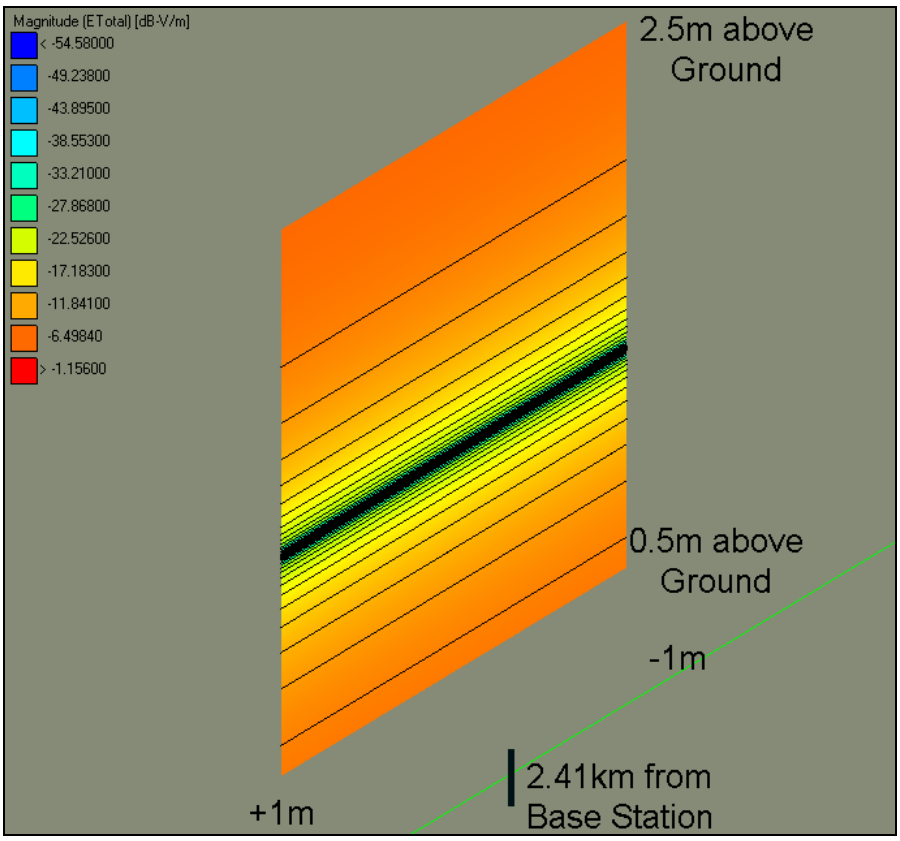

Figure 6.57: Multipath loss/gain at the Mobile Receiver

From the above figure, it can be seen that the loss due to multipath propagation is $2.5dB$. This loss will be taken into account when the link budget is done.

One of the obstacles in the line-of-sight path is a piece of vegetation. As covered in chapter 4.5, the attenuation due to this part of the path passing through vegetation, can be determined by:

$$A_{et} = d\gamma$$

With $d = 4m$ and $\gamma = 0.38dB/m$ the loss due to vegetation is equal to $1.52dB$.

The other important obstacle, is the metal shack that is right in front of the mobile phone. This obstruction is modelled using single knife-edge diffraction and is calculated using:

$$\upsilon = h\sqrt{\frac{2}{\lambda}\left(\frac{1}{d_1}+\frac{1}{d_2}\right)}$$

$$J(\upsilon) = 6.9 + 20\log\left(\sqrt{(\upsilon-0.1)^2+1}+\upsilon-0.1\right)$$

With $d_1 = 8m$, $d_2 = 2402m$, $h = 2.5m$ and $\lambda = 0.1667m$ the loss due to the obstruction in the line-of-sight path is calculated to be $-22.6035dB$. With all the variables now known, the link budget can be done. A table showing all the calculated values are given below.

	dB
Power Transmit	53.5
Free Space Propagation Loss	-105.4423
Vertical Angle Loss	-0.3
Horizontal Angle Loss	-1.1
Multipath Loss/Gain	-2.5
Diffraction Loss	-22.6035
Attenuation due to Vegetation	-1.52
Cable Loss	-1.63

Table 6.12: Link Budget for Measurement 2.5.

From the above table, it can be calculated that the predicted signal level at the mobile phone is:

$$dBm_{prediction} = dB_{send} - dB_{FreeSpaceLoss} - dB_{RadPattern} - dB_{mobAnt} - dB_{Multipath} - dB_{diff} - dB_{Veg}$$
$$= 53.5 - 105.4423 - 0.3 - 1.1 - 1.63 - 2.5 - 22.6035 - 1.52$$
$$= -81.59dBm$$

The predicted signal level, together with the measured signal level, is shown in the next figure.

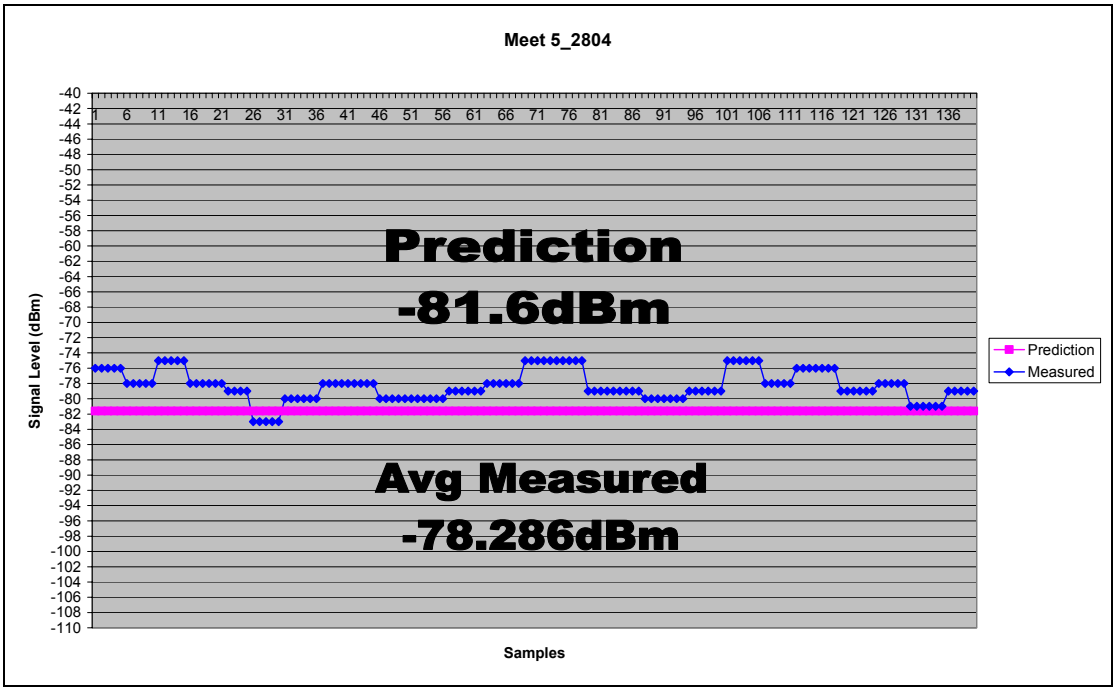

Figure 6.58: Prediction vs. Measurement

From the above figure, it is clear that if there is no line-of-sight present, the received signal seem to vary quite a bit. This is the expected small-scale fading because the measured signal consists only of reflected and diffracted components. The amount of fading is much clearer in this comparison, this is due to the fact that there is no clear line-of-sight and the density of shacks around the mobile receiver is much more. In general, the predicted signal level compares well with the measured signal level.

6.2.6. Measurement 2.6:

For the next measurement, the line-of-sight is obstructed by a piece of hilly terrain and a tree growing on top of the hill.

Figure 6.59: No clear line-of-sight for Measurement 2.6.

The distance between the mobile phone and the base station is calculated to be $1.648km$. From this, the free space propagation loss is calculated to be:

$$L_{FSP} = 32.4 + 20\log_{10}(d_{km}) + 20\log_{10}(f_{MHz})$$
$$L_{FSP} = 102.1405dB$$

The next step, is to take into account the elevation between the mobile phone and the base station. The elevation as well as the terrain profile between the mobile phone and the base station can be seen in the next figure.

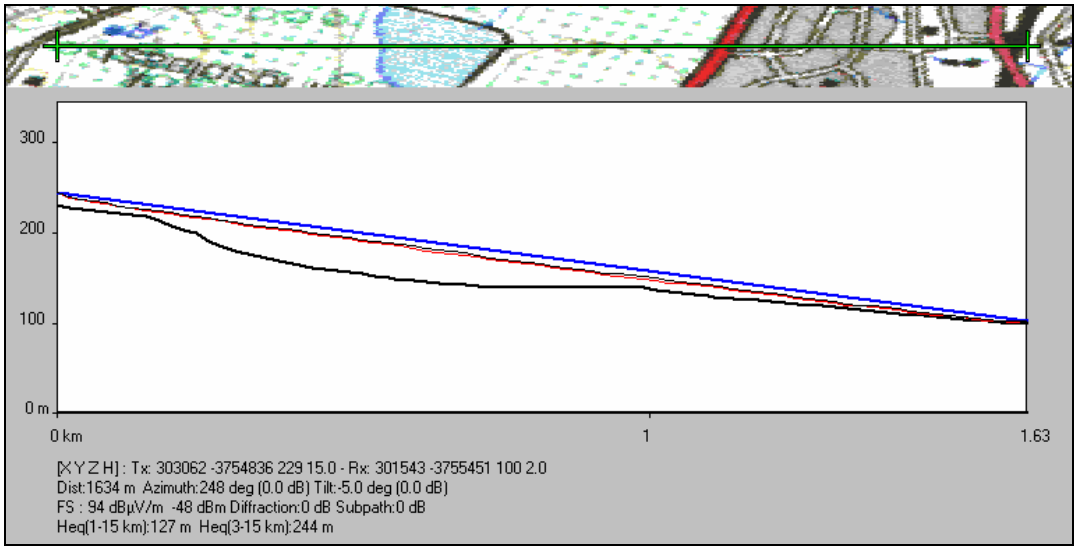

Figure 6.60: Path Elevation between the Mobile Phone and the Base Station

Using the information gathered from the above figure, the loss in the received signal strength due to the relative position of the mobile phone to the base station, can be determined. The information gathered, is the azimuth relative to each other, found to be $32°$, and the tilt is $5°$. The losses are then calculated to be:

$$\text{Vertical Angle Loss} = 0.3dB$$

$$\text{Horizontal Angle Loss} = 2.9dB$$

The next step, is to simulate the effect of multipath propagation on the received signal level. This is done by using FEKO software. The ground cover in the vicinity of the mobile phone is assumed to be normal, no shacks nearby that can have an effect on the signal. The result from the simulation can be seen in the next figure.

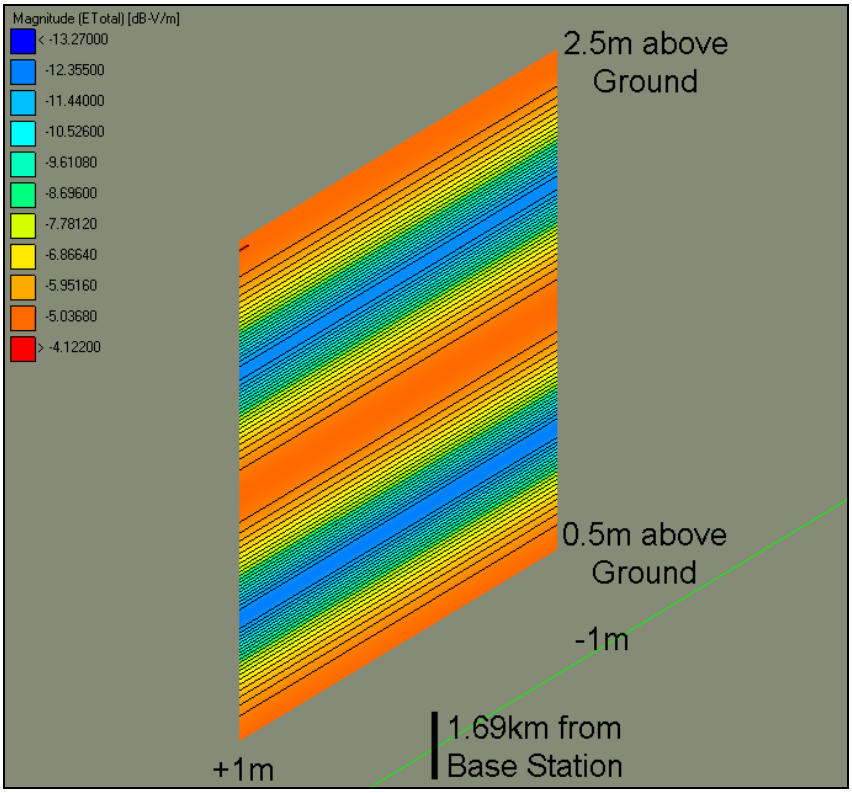

Figure 6.61: Multipath loss/gain at the Mobile Receiver

From the above figure, it can be seen that the loss due to multipath propagation is $4.5dB$. This loss will be taken into account when the link budget is done.

The other obstacle in the line-of-sight path is a tree. As covered in chapter 4.5, the attenuation due to this piece of vegetation can be determined by:

$$A_{et} = d\gamma$$

With $d = 6m$ and $\gamma = 0.38dB/m$ the loss due to the vegetation is equal to $2.28dB$.

The other important obstacle, is the elevated road that runs through the line-of-sight view. This piece of obstruction will be modelled using a single knife-edge diffraction approximation, as covered in chapter 4.6. The loss is given by:

$$\upsilon = h\sqrt{\frac{2}{\lambda}\left(\frac{1}{d_1}+\frac{1}{d_2}\right)}$$

$$J(\upsilon) = 6.9 + 20\log\left(\sqrt{(\upsilon-0.1)^2+1}+\upsilon-0.1\right)$$

With $h = 2m$, $d_1 = 100m$ and $d_2 = 1570m$ the diffraction loss due to the obstruction in the line-of-sight view is calculated to be $11.9487dB$. With all the variables now known, the link budget can be done. A table showing all the calculated values are given below.

	dB
Power Transmit	53.5
Free Space Propagation Loss	-102.1405
Vertical Angle Loss	-0.3
Horizontal Angle Loss	-2.9
Multipath Loss/Gain	-4.5
Diffraction Loss	-11.9487
Attenuation due to Vegetation	-2.28
Cable Loss	-1.63

Table 6.13: Link Budget for Measurement 2.6.

From the above table, it can be calculated that the predicted signal level at the mobile phone is:

$$dBm_{prediction} = dB_{send} - dB_{FreeSpaceL\ oss} - dB_{RadPattern} - dB_{mobAnt} - dB_{Multipath} - dB_{diff} - dB_{Veg}$$
$$= 53.5 - 102.1405 - 0.3 - 2.9 - 1.63 - 4.5 - 11.9487 - 2.28$$
$$= -72.1992dBm$$

The predicted signal level, together with the measured signal level, is shown in the next figure.

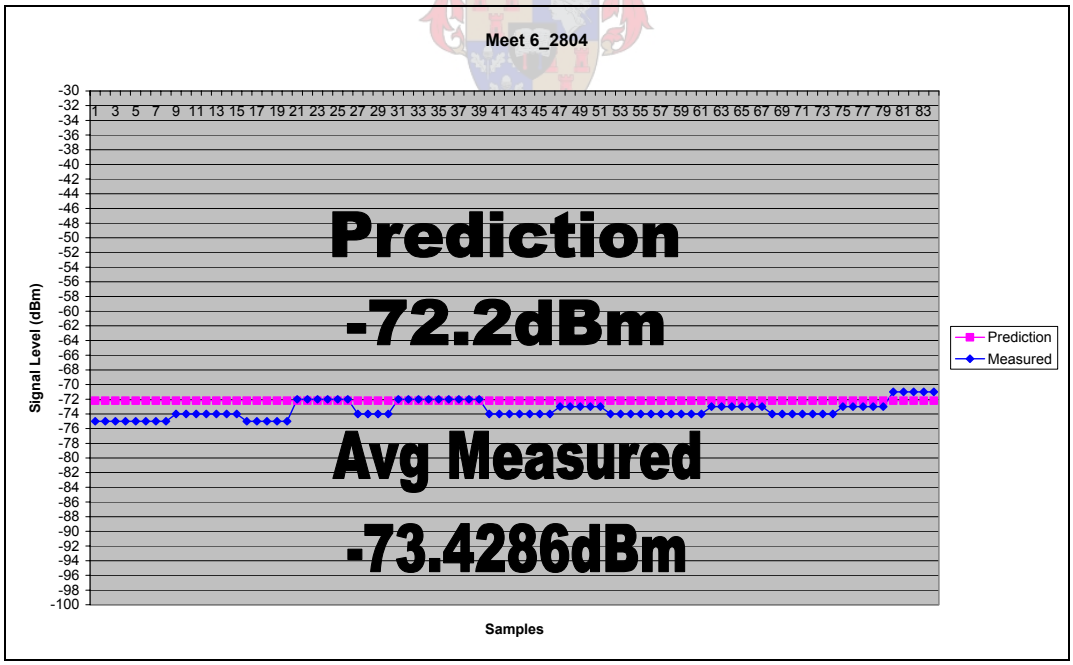

Figure 6.62: Prediction vs. Measurement

From the above figure, it is clear that there is no line-of-sight present. This can be seen in the amount of small-scale fading visible in the measurements. In general, the predicted signal level compares well with the measured signal level.

6.2.7. Measurement 2.7:

This measurement is taken behind a metal building. The mobile receiver is close to the building, therefore the diffraction loss is expected to be high.

Figure 6.63: No line-of-sight available for Measurement 2.7.

The distance between the mobile phone and the base station is calculated to be $1.69km$. From this, the free space propagation loss is calculated to be:

$$L_{FSP} = 32.4 + 20\log_{10}(d_{km}) + 20\log_{10}(f_{MHz})$$
$$L_{FSP} = 102.3899dB$$

The next step, is to take into account the elevation between the mobile phone and the base station. The elevation as well as the terrain profile between the mobile phone and the base station can be seen in the next figure.

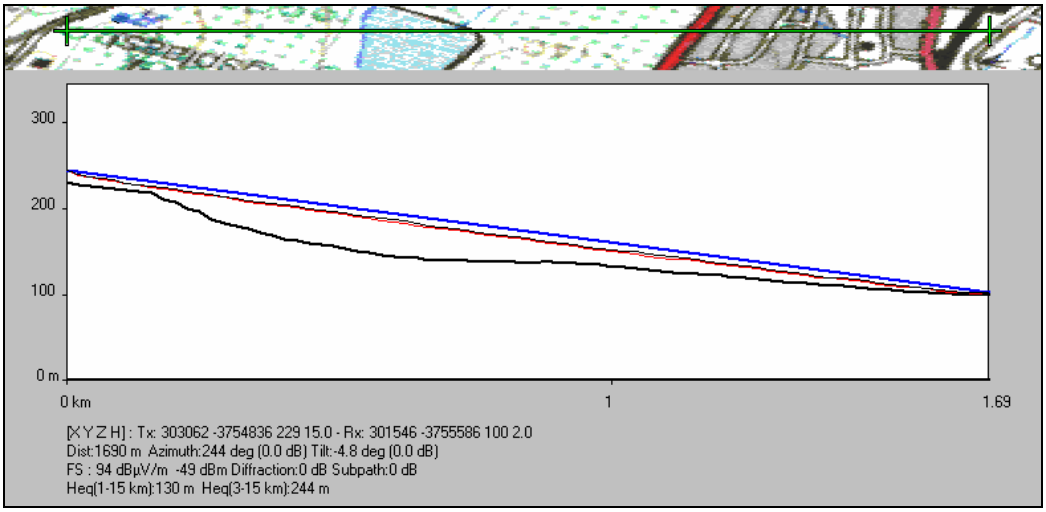

Figure 6.64: Path Elevation between Mobile Phone and Base Station

Using the information gathered from the above figure, the loss in the received signal strength due to the relative position of the mobile phone to the base station, can be determined. The information gathered, is the azimuth relative to each other, found to be $36°$, and the tilt is $4.8°$. The losses are then calculated to be:

$$\text{Vertical Angle Loss} = 0.3dB$$
$$\text{Horizontal Angle Loss} = 3.6dB$$

The next step, is to simulate the effect of multipath propagation on the received signal level. This is done using FEKO software. The ground in the vicinity of the mobile receiver is assumed to be normal ground. The result of the simulation can be seen in the next figure.

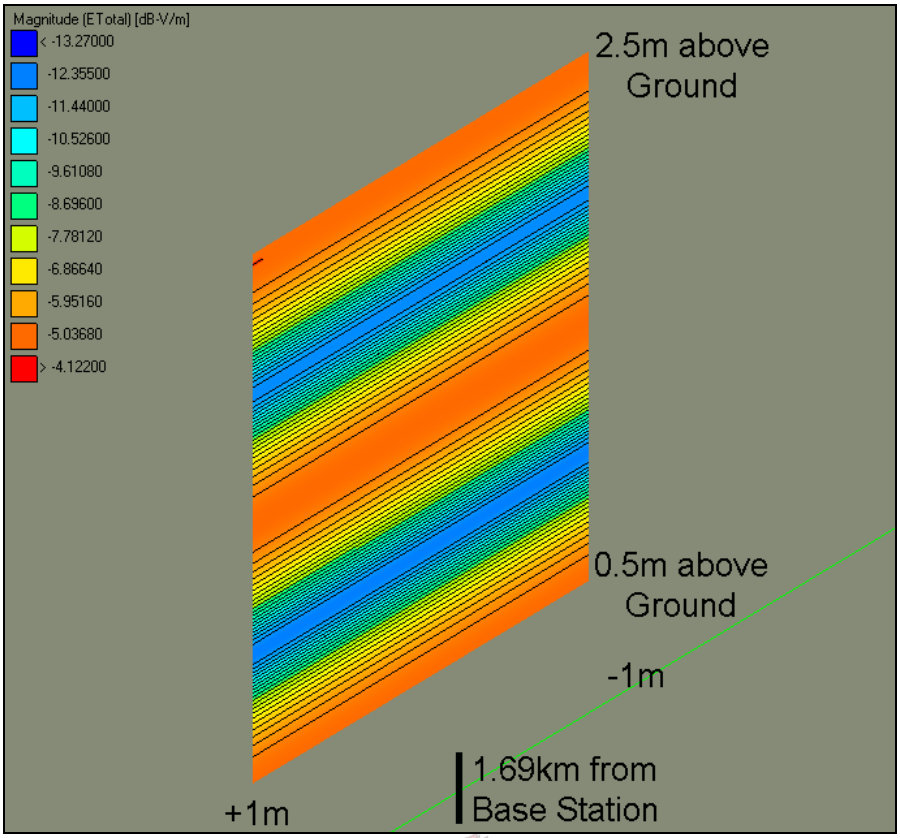

Figure 6.65: Multipath loss/gain at the Mobile Receiver

From the above figure, it can be seen that the loss due to multipath propagation is $4dB$. This loss will be taken into account when the link budget is done.

The obstacle that blocks the line-of-sight view between the mobile phone and the base station now needs to be looked at. The diffraction around the top corner of the building towards the mobile receiver is modelled as single knife-edge diffraction. Therefore it can be assumed that:

$$\upsilon = h\sqrt{\frac{2}{\lambda}\left(\frac{1}{d_1}+\frac{1}{d_2}\right)}$$

$$J(\upsilon) = 6.9 + 20\log\left(\sqrt{(\upsilon-0.1)^2+1}+\upsilon-0.1\right)$$

With $h = 8m$, $d_1 = 15m$ and $d_2 = 1500m$. From this, the loss due to diffraction is calculated to be $29.9777dB$. With all the variable now known, the link budget can be done. A table showing all the calculated values are given below.

	dB
Power Transmit	53.5
Free Space Propagation Loss	-102.3899
Vertical Angle Loss	-0.3
Horizontal Angle Loss	-3.6
Multipath Loss/Gain	-4
Diffraction Loss	-29.9777
Attenuation due to Vegetation	0
Cable Loss	-1.63

Table 6.14: Link Budget for Measurement 2.7.

From the above table, it can be calculated that the predicted signal level at the mobile phone is:

$$dBm_{prediction} = dB_{send} - dB_{FreeSpaceL\ oss} - dB_{RadPattern} - dB_{mobAnt} - dB_{Multipath} - dB_{diff}$$
$$= 53.5 - 102.3899 - 0.3 - 3.6 - 1.63 - 4 - 29.9777$$
$$= -88.3976 dBm$$

The predicted signal level, together with the measured signal level, is shown in the next figure.

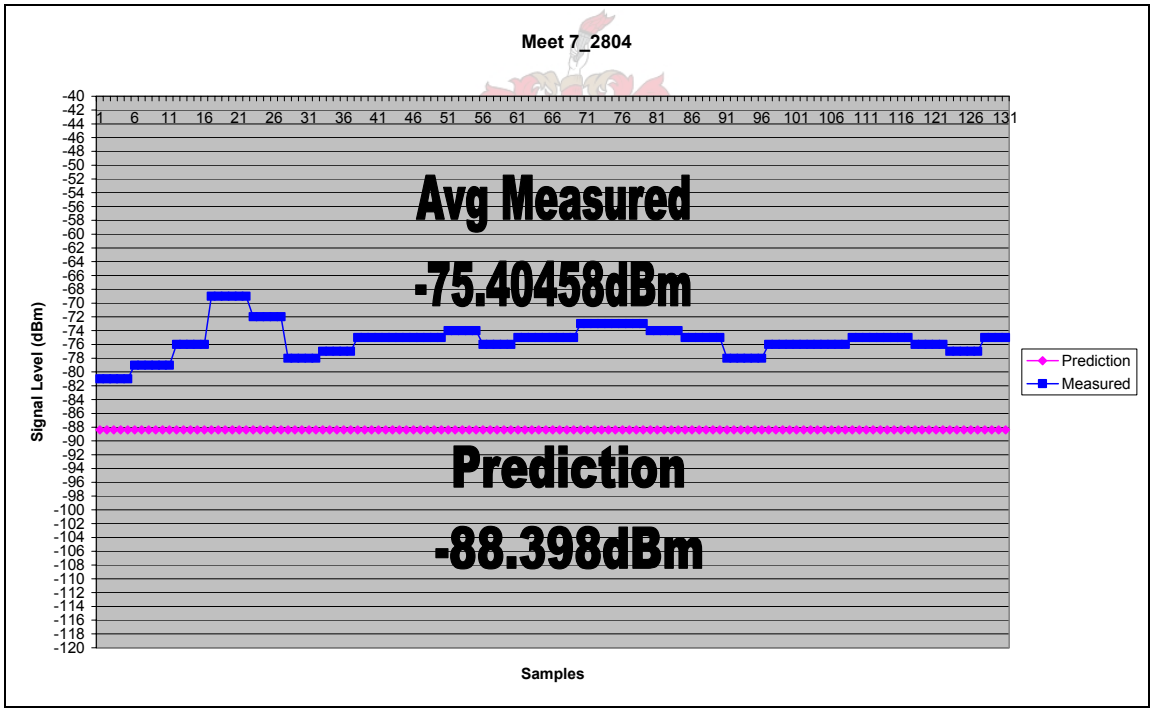

Figure 6.66: Prediction vs. Measurement

From the above figure, it can be seen that the predicted signal level is much lower then that what is measured. This can be attributed to the fact that the mobile phone is very close to the obstructing building and this is very difficult to model accurately. What is clear from this measurement is that this measuring device does not work well when there is no clear line-of-sight present. Taking this fact into consideration, it still seems that that prediction compares well with the measured signal level.

6.3. Conclusions

In total fourteen different measurements were looked at. A summary of these measurements and there results is given in Table 6.15.

Measurement	Area	Obstructions	Results	Comments
1.1.	open area	none	excellent	clear line-of-sight measurement
1.2.	elevated above tree canopy	none	excellent	clear line-of-sight measurement
1.3.1	elevated above tree canopy	none	excellent	clear line-of-sight measurement
1.3.2	open area	vegetation	excellent	vegetative obstruction
1.4.	lots of vegetation	vegetation	excellent	vegetative obstruction
1.5.	residential	none	excellent	fading more prominent in residential area
1.6.	residential	metal fence	excellent	diffraction over metal fence
1.7.	open area	vegetation	excellent	single line of trees obstructing line-of-sight view
2.1.	informal settlements	none	excellent	clear line-of-sight measurement
2.2.	informal settlements	none	excellent	fading more prominent due to reflections from metal shacks
2.3.	open area	none	excellent	min. fading; no metal shacks in vicinity of receiver
2.4.	residential area	building	good	no line-of-sight; difficult to model accurately
2.5.	informal settlements	metal shacks; vegetation	good	no line-of-sight; metal shacks increase fading; difficult to model accurately
2.6.	open area	elevated road; vegetation	good	no line-of-sight; loss due to vegetation; diffraction over elevated road
2.7.	behind building	metal shed	poor	no line-of-sight; difficult to model diffraction; varying signal level

Table 6.15: Summary of Measurements

From Table 6.15. it can be seen that the measurement system works well when there is a line-of-sight between the transmitter and receiver present. The influence of vegetation on the signal level can also be seen. It is also noticed that when there is no line-of-sight present and the signal is diffracted over a building or other object, the logged signal level varies quite a bit. This is due to the delay in arrival of different diffracted components. This varying signal level can also be seen when the receiver is in the vicinity of metal shacks. Again this is due to the multiple reflections arriving at the receiver at different times.

The data capturing system do not work well for non line-of-sight measurements, because it is difficult to model the different components arriving at the mobile receiver. A median value for the received signal level can however be predicted when obstacles are modelled as perfect knife-edges.

This data capturing device could how ever be useful for capturing data that can be used in training artificial neural networks.

CONCLUSIONS

The aim of this thesis, was to design and develop a data capturing device using a Nokia mobile phone and GPS connected to a laptop computer. To proof that this data capturing device work, the measured data had to be verified against known propagation models and other propagation phenomenon.

The data capturing device that was designed works well. The device is very flexible and many of the parameters can be changed to accommodate different data capturing setups. The external antenna to the mobile phone can be changed to discriminate between 900MHz and 1800MHz carrier frequencies thus broadening the field over which propagation studies can be done. The rate at which the signal level is sampled from the phone can also be changed according to the user's preferences. The Microsoft Visual Basic Programming that is used to interface with the mobile phone, has got numerous other functions that can also be used in a data capturing system.

The data capturing device works well for line-of-sight measurements especially when the line-of-sight component of the measured signal is dominant. When there is no line-of-sight component present, the measured signal level varies considerably, depending on the clutter in the vicinity of the mobile receiver. The more the mobile receiver is taken out of line-of-sight conditions, the further the prediction is from the measured signal level. When the clutter in the vicinity of the mobile receiver is metal shacks, rate of fading increase and this is expected because the amount of reflections reaching the mobile receiver in this case is much more than for previous measurements.

At 1800MHz it is also clear to see that the effect of vegetation is not that big, but rather the amount of diffraction and reflections between the mobile phone receiver and the base station transmitter. The most unpredictable component of the link budget is the attenuation due to multipath propagation. Multipath propagation is modelled using FEKO software and the modulations are found to be satisfactory. The ground cover in the vicinity of the mobile receiver is taken into consideration when these simulations are done.

This project is successful in many ways. It is shown that the data capturing device works very well for line-of-sight measurements. The influence of obstacles obstructing the line-of-sight view between the transmitter and receiver were also covered extensively and modelled to satisfactory results. The attenuation due the vegetation in the propagation medium was also investigated and satisfactory results were drawn. Other elements such as water vapour and dry air attenuation were also covered and it was seen that these

could be ignored for the 1800MHz frequency band. In general this project covered a wide variety of propagation theory and the data capturing device was proven to be accurate.

Further work proposed regarding the data capturing system will now be discussed. One of these is trying to find an alternative for the GPS connected to the laptop. The GPS is another component and the challenge will be to gather data from the mobile phone in order to eliminate the need for the GPS. The method in which this can be accomplished, it to use the time of arrival (TOA) or time difference of arrival (TDOA) data measured from the phone. The accuracy of this method for determining positions relative to the base station must be looked at first.

The author also proposes that the data capturing device be used for outdoor-to-indoor propagation modelling. The device can be used to determine the effect of different building materials on the propagating signal. The results from tests such as this can be used for planning purposes of other wireless networks, such as finding an optimum position for a remote receiver proving service in rural areas of urban areas.

The author also proposes that this data capturing system be used for capturing artificial neural network (ANN) training data. The device is easy to use. Different ground cover and areas can be covered easily without constructing special transmitters and receivers.

The effect of multipath, as said earlier, is difficult to model and can be used to the service providers advantage. By making use of the fact that antenna height can improve the received signal level. The author propose some work to be done, using the data capturing system, to measure how the signal level changes as the position of the mobile antenna changes as a function of height above ground level. The flip side of multipath propagation is that it is unwanted in many cases and for this reason there are multipath mitigation techniques as discussed in ITU-R F1093. These mitigation techniques can also be looked at and tested in practical measurements.

For this project, both the transmitting antenna as well as the receiver antenna was vertically polarized. The effect of polarization and can also be tested and investigated using the data capturing system. The polarization of the receiver antenna can easily be changed by just fitting a different antenna when needed.

REFERENCES

[1] **Rice, P.L., Longley, A.G., Norton, K.A., Barsis, A.P.**, *"Transmission Loss Predictions for Tropospheric Communication Circuits"*, NBS Tech Note 101, January 1967

[2] **Rappaport, T.S.**, *"Wireless Communications, Principles and Practice"*, Prentice Hall PTR, Upper Saddle River, New Jersey 07458, ISBN: 0-133-75536-3, 1996

[3] **Longley, A.G.**, *"Radio Propagation in Urban Areas"*, OT Report, pp. 78-144, April 1978

[4] **Edwards, R., Durkin, J.**, *"Computer Prediction of Service Area for VHF Mobile Radio Networks"*, Proceedings of the IEE, Vol. 116, pp. 1493-1500, 1969

[5] **Neskovic, A., Neskovic, N., Paunovic, G.**, *"Modern Approaches in Modeling of Mobile Radio Systems Propagation Environment"*, IEEE Communication Surveys, http://www.comsoc.org/pubs/surveys, pp. 3-4, Third Quarter, 2000

[6] **Rappaport, T.S.**, *"Wireless Communications, Principles and Practice"*, Prentice Hall PTR, Upper Saddle River, New Jersey 07458, ISBN: 0-133-75536-3, pp. 119-120, 1996

[7] **European Cooperation in the Field of Scientific and Technical Research EURO-COST 231**, *"Urban Transmission Loss Models for Mobile Radio in the 900 and 1800MHz Bands"*, Revision 2, The Hague, September 1991

[8] *"DIGITAL MOBILE RADIO TOWARDS FUTURE GENERATION SYSTEMS, Propagation Prediction Models"*, **COST 231 Final Report**, Chapter 4, pp. 135-139

[9] **Neskovic A., Neskovic N., Paunovic D.**, *"A Field Strength Prediction Model Based on Artificial Neural Networks"*, Proc. 9th IEEE Mediterranean Electrotechnical Conference, MELECON 98, Tel Aviv, Israel, 1998

[10] **Chen, D.S., Jain, R.C.**, *"A Robust Back Propagation Learning Algorithm for Function Approximation"*, IEEE Transactions on Neural Networks, Vol. 5, No. 3, pp. 467-479, May 1994

[11] **Neskovic, A., Neskovic, N., Paunovic, D.**, *"Macrocell Electric Field Strength Prediction Model Based Upon Artificial Neural Networks"*, IEEE Journal on Selected Areas in Communications, Vol. 20, No. 6, pp. 1170-1177, August 2002

[12] **Kuznetsov, G.G., Walden, C.J., Holt, A.R.**, *"Attenuation of Microwaves in Sleet"*, Final Report to Radiocommunications Agency on Contract AY 3564 (51000279), Colchester, August 2000

[13] *"Propagation Data and Prediction Methods Required for the Design of Terrestrial Line-of-Sight Systems"*, **Recommendation ITU-R P.530**, 2001

[14] **Myers, W.**, *"Comparison of Propagation Models"*, IEEE P802.16 Broadband Wireless Access Working Group, August 1999

[15] **International Telecommunication Union**, *"Terrestrial Land Mobile Radiowave Propagation in the VHF/UHF Bands"*, ITU Handbook, page 73, 2002

[16] **Erceg, V., Hari, K.V.S., Smith, M.S., Sheikh, K.P., Tappenden, C., Costa, J.M., Baum, D.S., Bushue, C.**, *"Channel Models for Fixed Wireless Applications"*, IEEE 802.16 Broadband Wireless Access Working Group, January 2001

[17] **Raja, K., Buchanan, W.J., Munoz, J.**, *"Location Tracking"*, IEE Communications Engineer Magazine, Vol. 2, Issue 3, June/July 2004, pp. 34-39

[18] **Balanis, C.A.**, *"Antenna Theory, Analysis and Design"*, Second Edition, John Wiley and Sons, Inc., ISBN: 0-471-59268-4, 1997

[19] **McLean, J., Sutton, R., Hoffman, R.**, *"Interpreting Antenna Performance Parameters for EMC"*, Part 2, TDK RF Solutions, pp. 7-17

[20] **Stutzman, W.L., Thiele, G.A.**, *"Antenna Theory and Design"*, Second Edition, John Wiley and Sons, Inc., ISBN: 0-471-02590-9, 1998

[21] **Naffall Herscovici and Christos Christodouloc ,** *"Wideband monopole antennas for multi-band wireless systems"* IEEE Antennas and Propagation Magazine , Vol. 45, No.2, April 2003.

[22] **Yazdandoost, K.Y., Kohno, R.**, *"Ultra Wideband Antenna"*, IEEE Radio Communications Magazine, Vol. 42, No. 6, June 2004, pp. S29-S32

[23] **Hall, M.P.M., Barclay, L.W., Hewitt, M.T.,** *"Propagation of Radiowaves"*, The Institution of Electrical Engineers, Short Run Press Ltd, ISBN: 0-852-96819-1, 1996

[24] *"Multipath Propagation and Parameterization of its Characteristics"*, **Recommendation ITU-R P.1407**, 1999

[25] **Andersen, J.B., Rappaport, T.S., Yoshida, S.**, *"Propagation Measurements and Models for Wireless Communications Channels"*, IEEE Communications Magazine, Vol 33, No. 1, pp. 42-49, January 1995

[26] *"Propagation Data and Prediction Methods Required for the Design of Terrestrial Line-of-Sight Systems"*, **Recommendation ITU-R P.530**, pp. 30-32, 2001

[27] *"Electrical Characteristics of the Surface of the Earth"*, **Recommendation ITU-R P.527**, 1992

[28] **Von Hippel, R.**, *"Dielectric Materials and Applications"*, The M.I.T. Press, Cambridge, Massachusetts, ISBN: 0-262-72002-7, 1966

[29] *"Propagation by Diffraction"*, **Recommendation ITU-R P.526**, pp. 10-22, 2003.

[30] **Solheim, F.S., Vivekanandan, J., Ware, R.H., Rocken, C.**, *"Propagation delays induced in GPS signals by dry air, water vapour, hydrometeors and other particulates"*, Journal of Geophysical Research, Vol 104, No. D8, pp. 9663-9670, April 27, 1999

[31] *"Attenuation in Vegetation"*, **Recommendation ITU-R P.833**, 2003

[32] **Bőlcskei, H., Paulraj, A.J., Hari, K.V.S., Nabar, R.U., Lu, W.W.**, *"Fixed Broadband Wireless Access: State of the Art, Challenges, and Future Directions"*, IEEE Communications Magazine, pp. 100-108, January 2001

[33] **Greenstein, L.J., Ghassemzadeh, S., Erceg, V., Michelson, D.G.**, *"Ricean K-Factors in Narrowband Fixed Wireless Channels"*, WPMC '99 Conference Proceedings, Amsterdam, September 1999

[34] **Erceg, V.**, *"Channel Models for Broadband Fixed Wireless Systems"*, IEEE 802.16 Broadband Wireless Access Working Group, IEEE 802.16.3c-00/47, October 2000

[35] **Rappaport, T.S.**, *"Wireless Communications, Principles and Practice"*, Prentice Hall PTR, Upper Saddle River, New Jersey 07458, ISBN: 0-133-75536-3, 1996

[36] **Suzuki, H.**, *"A Statistical Model for Urban Radio Propagation"*, IEEE Transactions on Communications, Vol. 25, pp. 673-680, July 1977

[37] **Gans, M.J.**, *"A Power-spectral Theory of Propagation in the Mobile Radio Environment"*, IEEE Transactions on Vehicular Technology, Vol. VT-21, pp. 27-38, February 1972

[38] **Durgin, G.D., Rappaport, T.S.**, *"Theory of Multipath Shape Factors for Small-Scale Fading Wireless Channels"*, IEEE Transactions on Antennas and Propagation, Vol. 48, No. 5, pp. 682-693, May 2000

[39] **Jakes, W.C.**, *"Microwave Mobile Communications"*, New York, IEEE Press, 1974